Title

Microbial Metamorphosis: How microbes influence pollen and pollinator development

Author

Christensen, Shawn M

Publication Date

2024

Peer reviewed|Thesis/dissertation

Microbial Metamorphosis: How microbes influence pollen and pollinator development

By

SHAWN MASON CHRISTENSEN
DISSERTATION

Submitted in partial satisfaction of the requirements for the degree of

DOCTOR OF PHILOSOPHY

in

Microbiology

in the

OFFICE OF GRADUATE STUDIES

of the

UNIVERSITY OF CALIFORNIA

DAVIS

Approved:

_____
Rachel Vannette, Chair

_____
Alison Berry

_____
Tiffany Lowe-Power

Committee in Charge

2024

Table of Contents

Abstract

Host-microbe interactions underlie the development and fitness of many macroorganisms; microbial symbionts can facilitate digestion, mitigate pathogens, and even produce essential developmental cues. My dissertation focuses on the impacts of microbes within the plant-pollinator system, investigating the crucial and complex interactions between bees, plants, and microbes- with a focus on how microbes use specialized tools to influence pollen processes, bee development, and the wider microbial community. Through use of classical natural history observations combined with entirely novel experimental and sampling approaches, I have been able to discover unique phenomena in microbial ecology that not only have important implications for pollinator systems but have changed broader perception and understanding of ecology and evolution. Chapter 1 explores the role of nectar-associated bacteria, particularly *Acinetobacter pollinis*, in facilitating pollen digestion. By inducing pollen germination and bursting, these bacteria access critical nutrients, with implications for pollinator nutrition and the role of flower associated microbes in pollinator systems. Chapter 2 examines the developmental microbiome of a solitary bee, revealing that immature stages of *Anthophora bomboides standfordiana* host a distinct core microbiome dominated by Actinobacteria and a yeast-like fungus, *Moniliella spathulata.* Data from microbial community profiling, qPCR, and functional experiments support the hypothesis that the bee's microbial community may provide critical fitness advantages, such as pathogen protection (*Streptomyces*) and enhanced cold tolerance (*M. spathulata*) during the bees' diapausing larval stage- suggesting that microbes play a vital role in the bees' overwintering success and long-term survival. Chapter 3 builds on these findings by describing two novel species, *Streptomyces solapis* sp. nov. and *Streptomyces nidicoloris* sp. nov., isolated from the brood of *A. bomboides*. These new bee- associated species display unique biosynthetic gene clusters that correlate with antifungal activity, underscoring the potential of leveraging the diversity of microbial symbionts to support discovery of new bioactive compounds. Collectively, this dissertation highlights the profound influence of microbes on macroorganisms, offering broader insights into the dynamics of pollination ecology, host-microbe symbioses, and the unique evolutionary strategies of microbes in these environments.

Acknowledgements

This dissertation would not have been possible without the support and encouragement of a vast number of people. First among these is my advisor, Rachel Vannette- thank you for being my co-conspirator, mentor and advocate, and for always, without exception, being on my team. For my other committee members, Tiffany Lowe-Power and Alison Berry- I sincerely appreciate your dedication, understanding, and sincere investment throughout this journey. I also thank each of the many teachers, professors, and mentors who taught me, guided me, met with me, and otherwise shaped my work and mind. For my lab mates throughout my time in the Vannette Lab- I am deeply grateful to you all for making the lab a warm, fun, and welcoming place, and especially for the countless lunchtime crossword puzzles. I am grateful for the solidarity of my union siblings in UAW 4811, the Microbiology Graduate Student Association, and Microbiology Graduate Group Diversity Equity and Inclusion Committee in working to support and empower student workers. I could not have completed this degree without the help of my therapists and healthcare providers; special thanks to Jessica Wilson, for her fierce persistence and unwavering belief in me. For my friends, family, and chosen family, thank you for being gentle when I was stressed and for keeping things in perspective when I got in too deep. Ben- thank you for being there for me at every step, and for all of things I've forgotten to thank you for since embarking on this PhD. Abby- your unconditional support, consistency, and love are in every day and every page of this dissertation.

Main Introduction

Microorganisms are among the most diverse and ubiquitous forms of life on Earth, playing pivotal roles in the functioning of the global ecosystem[1]. From nutrient conversion to disease resistance, these microscopic entities can interact with macroorganisms in complex ways, many of which are only recently starting to be recognized[2–4]. Among these, symbiotic host-microbe interactions have received much attention, and can be essential for the health and survival of many organisms[5–8]. In particular, the interactions between microbes, plants, and pollinators form a critical nexus in the maintenance of global biodiversity and ecosystem stability[9–13]. Despite their importance, many of the mechanisms by which symbiotic microbes influence these interactions remain poorly understood.

Bees are essential for the reproduction of a vast number of flowering plants, contributing to the production of fruits and seeds that are fundamental to both human agriculture and natural ecosystems[14,15]. However, the global decline in bee populations has led to rising concerns and prompted the expansion of pollination biology as a field, to learn how to best protect and conserve bees and other pollinators[12]. The central divergence of bees from within the wasp lineage was a dietary shift; bees began eating pollen instead of preying on other insects or arachnids[16]. Pollen provides bees with all their protein, lipids, and trace nutrients, but as pollen is the male reproductive gamete of plants, it is well defended and difficult to digest[17]. The mechanisms by which pollen consumers access these nutrients has been uncertain, but as microbes are known to exploit and break down recalcitrant materials, it follows that they may play a role in this central enigma of bee biology[3,17–21].

Previous work has shown that microbial partners can play critical roles in bee health, some of which are known (complex sugar breakdown, competitive exclusion of pathogens), but many are not[21–23]. While much attention has been given to social bees, like honeybees, solitary bees represent the vast majority of bee species and play critical roles in pollination[24]. Unlike social bees, solitary bees do not have a communal hive structure and instead, each female constructs and provisions her own nest[24]. These solitary lifestyles, coupled with unique life cycles that include extended periods of dormancy (diapause),

and the isolation of the bee and its food from the outer environment for most of the year, make solitary bees particularly interesting subjects for studying host-microbe interactions[25–27]. Understanding the microbiomes of solitary bees is essential, not only for conserving these important pollinators but also for uncovering broader ecological principles that govern host-microbe symbioses.

This dissertation aims to unravel some of the mysteries surrounding the microbial influences on pollen and solitary bee development. By exploring the diverse and dynamic relationships between microbes, plants, and bees, this research seeks to provide a deeper understanding of how these interactions affect not only the health and survival of pollinators but also the broader ecological and evolutionary dynamics within this system. Through a combination of natural history observations, experimental approaches, and novel sampling techniques, this work uncovers unique phenomena in microbial ecology with significant implications for pollinator systems and beyond. Natural history observations have guided hypothesis generation, sampling design, and interpretation of molecular data, leading to discoveries that might have otherwise been overlooked.

The research presented here is divided into three main chapters, each addressing different aspects of microbe-pollinator interactions. The first chapter investigates how nectar-associated bacteria stimulate pollen germination and bursting, enhancing microbial fitness in ways that challenge our understanding of pollen development and pollinator nutrition. The second chapter shifts focus to the developmental microbiome of a solitary bee species, revealing how specific bacteria and fungi contribute to the overwintering survival and overall fitness of these pollinators. The third chapter more deeply explores the microbial isolates found in chapter two by characterizing the genomes of six *Streptomyces* strains associated with the developing brood. By integrating microbial ecology with entomology, pollination biology, and natural history, this dissertation not only contributes to the growing body of knowledge on pollination ecology but also offers broader insights into the dynamics of host-microbe symbioses and the unique evolutionary strategies of microbes.

Chapter I:

Nectar bacteria stimulate pollen germination and bursting to enhance microbial fitness[1]

[1] Chapter I was published in *Current Biology* in 2021: *31*(19), 4373-4380.e6.
https://doi.org/10.1016/j.cub.2021.07.016.
Authors: Shawn M. Christensen 1, Ivan Munkres 1, Rachel L. Vannette 1
Affiliations: 1. Department of Entomology and Nematology, University of California Davis, Davis, CA, USA.

Contributions: S.M.C. and R.L.V. conceived of the study. S.M.C. performed investigation, formal analysis, and visualization, and wrote the original manuscript. I.M. performed PGA assays and contributed to review and editing. R.L.V. contributed to review and editing, supervision, and final approval for publication.

Abstract

Many organisms consume pollen, yet mechanisms of its digestion remain a fundamental enigma in pollination biology[1–3], as pollen is protected by a recalcitrant outer shell[4–8]. Pollen is commonly found in floral nectar[9,10], as are nectar microbes, which are nearly ubiquitous among flowers[11–13]. Nectar specialist bacteria, like *Acinetobacter,* can reach high densities (up to 10^9 cells/mL), despite the fact that floral nectar is nitrogen poor[14–17]. Here, we show evidence that the genus *Acinetobacter*, prevalent nectar- and bee-associated bacteria[12,18–20], can induce pollen germination and bursting, gain access to protoplasm nutrients, and thereby grow to higher densities. Although induced germination had been suggested as a potential method in macroscopic pollen consumers[2,21–23], and fungal inhibition of pollen germination has been shown[24–27], direct biological induction of germination has not been empirically documented outside of plants[28–32]. *Acinetobacter pollinis* SCC477[19] induced over 5x greater pollen germination and 20x greater pollen bursting than that of uninoculated pollen by 45 minutes. When provided with germinable pollen, *A. pollinis* stimulates protein release and grows to nearly twice the density compared to growth with ungerminable pollen, indicating that stimulation of germination benefits bacterial fitness. In contrast, a common nectar-inhabiting yeast (*Metschnikowia*)[33] neither induced nor benefited from pollen germination. We conclude that *Acinetobacter* both specifically causes and benefits from inducing pollen germination and bursting. Further study of microbe-pollen interactions may inform many aspects of pollination ecology, including floral microbial ecology[34,35], pollinator nutrient acquisition from pollen[2,3,21,36], and cues of pollen germination for plant reproduction[37–39].

Introduction

Pollen is a nutrient dense food source, but the nutrients are difficult to access, as they are surrounded by a protective outer shell which preserves the male gametophyte during transport to the female pistil (angiosperms)[1-4]. Once on the pistil, pollen germinates, carrying the sperm cells via the pollen tube to fertilize the ovule[5]. The protective shell is known as the exine, which is made of sporopollenin, a highly crosslinked polymer and one of the most highly resistant and enzymatically inert polymers found in nature[3-7]. Directly beneath the exine shell is the intine layer, comprised of mostly pectins and cellulose in a multilayered structure; this layer swells and emerges through the exine during germination to form the pollen tube[5]. Most of the pollen nutrition is in the cytoplasm, contained within the exine and intine, although the lipid-rich pollenkitt, a waxy layer covering the exine of some pollens, may also contain nutrients[3,8].

Pollen is an essential food source for many insects, birds, mammals and microbes[3]. Pollen's chemical and physical characteristics render it highly resistant to degradation and can make it difficult for consumers of pollen to access the nutrients inside[3-4]. As a result, specialized adaptations are required to access nutrients within pollen. Five general mechanisms have been suggested: mechanical disruption, piercing, enzymatically or chemically penetrating, osmotically shocking, and inducing germination[3]. However, mechanisms of pollen nutrient acquisition have received little empirical attention and remain a fundamental enigma in pollination biology[3,5].

In flowers, bacteria and fungi are thought to be nutrient-limited, having access to high carbon but low nitrogen, and pollen has been shown to increase microbial growth[9-10]. Yeasts have also been observed aggregating on compromised pollen grains in nectar, suggesting that nectar inhabiting microbes may utilize pollen as a nutrient source, but mechanisms of nutrient acquisition remain unknown[9-10]. Nectar-inhabiting *Acinetobacter* spp are ubiquitous nectar-specialists and are known to reach very high (up to 10^9 cells/ml) densities in nectar despite the nectar's nutrient imbalance[11-14]. Initial observations that *Acinetobacter* grow poorly in traditional media and exhibit specific interactions with pollen grains led us to the current investigation.

Overall, there is weak consensus on general methods of pollen digestion by either macro- or microscopic consumers. Here, we suggest that the nectar specialist bacteria *Acinetobacter* uses induced germination, a previously proposed mechanism, to access pollen nutrients. To examine if this effect is common among within the nectar inhabiting members of this genus, we examined the interactions between multiple species of the floral-associated *Acinetobacter* and pollen. We also included a nectar-inhabiting yeast and a pectinase producing bacterium as it has been hypothesized that pectinases are involved in pollen degradation[45]. We also hypothesized that *Acinetobacter* growth would benefit from pollen addition, and specifically from germination of the added pollen. Finally, we used enzyme assays to assess if pectinase activity was associated with microbial effects on pollen. Our experiments demonstrate that microbial species and strains differ in their effects on pollen and that the *Acinetobacter* strain that most strongly induces germination also benefits from this phenotype.

Methods

Strains used

We chose to examine the nectar *Acinetobacter* clade and their impact on pollen after initial observations of *Acinetobacter* induced pollen germination. We chose 3 nectar-specialist *Acinetobacter* species representing the species most commonly isolated from nectar *(A. boissieri* and *A. nectaris*[18]*)*, and an additional species in the clade that was isolated from the honeybee gut (*A. apis*[20]). We recently isolated and described *A. pollinis*[19], of which we used two strains. *Acinetobacter pollinis* SCC477 is available through American Type Culture Collection (ATCC), type strain deposit number TSD-214. *Metschnikowia reukaufii* is a commonly isolated nectar-dwelling yeast and is a member of an assemblage of nectar microbes in *Asclepias* that has been observed to negatively impact germination of *Asclepias* pollinia and has also been observed to aggregate around the pollen of *Helleborus foetidus*[9,33,42]. We included the pectin degrader and plant pathogen *Pectobacterium carotovorum* as a control for Microbial Associated

Molecular Patterns (MAMPs: which can trigger plant immune system); it also has high pectinase activity and is a plant associated bacteria that is not associated with nectar or pollen[43].

Plants

We used pollen from the California native poppy *Eschscholzia californica* (Papaveraceae). Flowers were obtained from the native plant prairie at the University of California Davis Arboretum, where they receive occasional watering. Flowers were collected in the morning, before 10:00AM, 2-3 days prior to use in assays, which occurred from 2019 to 2021. *E. californica* produces a large amount of pollen, is easily obtainable near our laboratory to allow for minimal effects of storage, and flowers are covered by a cap that is pushed off just before its first opening with the sun; this allowed us to collect flowers before insect or wind activity introduces contaminating microbes (Appendix I, Figure S4). *E. californica* does not have nectar, reducing the likelihood of contaminating nectar microbes. Pollen of Papaveraceae has ectoapertures[78,79] meaning that the outermost layer of the exine shell is missing from the aperture region but there are still other sporopollenin layers surrounding the intine[80].

Microbial impact on pollen

To test whether microbial inoculation impacts pollen germination and bursting, we collected newly opened *Eschscholzia californica* flowers the morning of the assay to minimize the chances that flowers had been visited by insects or otherwise "contaminated" with microorganisms or other pollen grains. Many attempts were made to sterilize the pollen prior to the assays (low heat sterilization, autoclaving, chlorine gas fumigation, 50%-70% (v/v) ethanol submersion, 1%-10% (v/v) bleach submersion), but all rendered the pollen unable to form visible pollen tubes at all or were ineffective at sterilizing pollen, so newly collected pollen from pre-collected flowers was used. Newly collected pollen had low levels of microbial growth (Figure 1.4).

For all microbial growth assays, bacterial strains were plated from freezer stocks onto Tryptic Soy Agar (TSA; 1.5% tryptone, 0.5% soytone, 0.5% NaCl, 5% fructose, 1.5% agar – all (w/v), + cycloheximide) and yeast (*Metschikowia reukaufii)* onto Yeast extract Media (YM; + chloramphenicol),

then colonies were inoculated into Tryptic Soy Broth (same as TSA but -cycloheximide, - agar) and incubated at 25 °C for 1-3 days. Suspensions were normalized to an $OD_{600\ nm}$ =0.1 or 0.05 (depending on the microbe with the lowest OD, and consistent within each assay). Suspensions were centrifuged for 5 minutes at 12,000 rpm to pellet the cells, and supernatant was poured off to remove the growth media along with any released metabolites and proteins, then cells resuspended in phosphate buffered saline (PBS). After resuspension by repeated pipetting, the suspension was vortexed for 30 seconds and then sonicated for 3 minutes. To ensure no carryover of metabolites from microbial growth media, these washing steps (from centrifugation through sonication) were performed twice for the first five assays, and three times for the last four assays. The final resuspension was in Brewbaker and Kwack (BK) pollen germination media[49] (10% w/v sucrose, 100 mg/L boric acid, 300 mg/L calcium nitrate, 200 mg/L magnesium sulfate, 100 mg/L potassium nitrate) instead of PBS. 50 µl of each washed microbial BK suspension (or the control sterile BK) was added to respective wells (3-5 replicate wells per microbe per assay) in a sterile, flat bottom, clear 96 well plate.

Immediately before beginning each assay, the pollen solution was prepared. Briefly, pollen from 1-3 flowers was vacuumed or shaken directly from anthers into a sterile 5 mL Eppendorf tube and 2 mL of BK solution was added. Immediately after pollen grains were in solution, 50 µl of the pollen solution was added to each well of the sterile 96-well plate, mixing pollen stock solution every 5-7 wells to ensure even pollen deposition in each well. Control (uninoculated) wells also received 50 µl of pollen, but instead of 50 µl of microbe solution, they received 50 µl of sterile BK. The plate was covered with a lid and wrapped in a layer of aluminum foil to limit evaporation, contamination, and light exposure. Each treatment was replicated in at least three wells per assay. Each well of the plate was then imaged on an EVOS M5000 imaging system at 15, 45, and 90 minutes after mixing. Final pollen concentrations were on average 20 grains/µl in each well, SD= 11 (based on pollen grains/image and extrapolating to volume of well), well within normal range of pollen in nectar[9].

Image analysis

Images were analyzed in FIJI2 (v2.0.0)[81], using a custom Macro script (below) to count total pollen grains in each image. The numbers of germinated, burst, and tip burst grains were then counted by hand in FIJI2 using CellCounter[82]. This was used to count pollen grains within each of three classifications (Figure 1.1). Any pollen grain touching the edge of the image was excluded in both the total and subset counts. A grain was counted as "germinated" if the pollen intine was clearly emerging from the exine (Figure 1.1C), as "burst" if the pollen grain was surrounded in loose cytoplasm, but without any visible protrusions (Figure 1.1B), and as "tip burst" if the pollen grain had germinated, and then the pollen tube had burst and released cytoplasm (Figure 1.1D). For all assays, pollen grains were classified twice; once just after assay completion, and all assays were recounted by the same observer within a week prior to combined final analysis to ensure consistency of each category between assays. These final counts were used for analysis. Eleven total assays were done, and two were eliminated from further analysis. One assay was eliminated due to data loss of images-making recount and validation of pollen ratios impossible, and the other was eliminated due to contamination of the initial growth media. An average of 4,564 (+/- 1501.6) pollen grains were counted per assay, with a total of 41,079 pollen grains overall (for microbial comparison assays).

We validated this macro script to be accurate with a paired t-test comparing macro script counts with hand counts of the same images (90 minute timepoint from three assays). The macro counts and hand counts were not significantly different (N=53, p= 0.3353). The 90 minute timepoint was selected because the pollen tubes and burst grains present at 90 minutes (in some images) were initially an obstacle for accurate macro counting. This script was used for Figure 1.2 and Appendix I- Figure S1 to count total pollen grains. All images for each timepoint were analyzed in a batch using "Process"-> "Batch"-> "Macro" with the following script:

```
run("8-bit");
setAutoThreshold("Default dark no-reset");
//run("Threshold...");
//setThreshold(176, 255);
run("Make Binary", "thresholded remaining black");
```

```
run("Convert to Mask");
run("Fill Holes");
run("Watershed");
run("Analyze Particles...", "size=900-3500 circularity=0.30-1.00 show=Overlay display exclude
summarize");
```

Note: The size and circularity ranges can be changed for use with different pollen sizes and shapes. This is especially important in the later time points (with germination) as the circularity measure can be altered by protruding pollen tubes, or even bulging pollen tube tips.

Germination data processing

For analysis, the pollen grain counts in each category (described above in main assay description) were converted into percentages of the total number of pollen grains in each image. “Germinated” and “tip burst” were combined in the category of “all germination”, because the “tip burst” pollen had also germinated. Likewise, “burst” and “tip burst” were combined to form the category “all burst” because the pollen grains in both initial categories expelled their protoplasm into the solution. Dataset and code are available in Appendix I- Table S2.

Density-dependence

To test whether pollen responds differently to differing amounts of *Acinetobacter,* we repeated the above methods, but inoculated pollen with dilution series of *A. pollinis* SCC477 suspensions (1, 1:2, 1:3, 1:5, 1:20, 1:100) as well as sterile BK (no microbes). We started with a solution at an $OD_{600\ nm}$=0.1 (10^7 cells/ml) and diluted to the above ratios, with the first being “full concentration” and the last consisting of only sterile BK. We then imaged the wells at 15, 45, 90 minutes, and 3, 4, 6, 12, and 24 hours. The images were analyzed, and pollen grains counted and categorized as described for the previous assay. In addition, we measured and recorded the lengths of each pollen tube in all of the images using FIJI2. We measured the tubes using the basic FIJI tool, used the image scale bar to set the scale, then used ROI manager (“Analyze”->“Tools”->”ROI Manager”) with Freehand drawing tool to trace and keep track of pollen tubes (check “Show all”) “add [t]” each line to the manager, then highlight all and “Measure”. Dataset and code are available in Appendix I- Table S2.

Microbial growth benefit

To test whether *Acinetobacter* benefits from pollen addition and specifically from pollen germination, we monitored growth responses of *A. pollinis* SCC477 in the presence of live pollen, pollen rendered unable to germinate, and without pollen. We created washed suspensions of $OD_{600\ nm}$= 0.1 *A. pollinis* SCC477 as above (pellet cells, remove media, replace with BK, vortex, sonicate- repeated 3x). *A. pollinis* SCC477 was selected because its addition resulted in the greatest induction of germination and bursting of the species and strains that we tested. The initial cell number of *A. pollinis* SCC477 cell suspension was immediately counted on a hemocytometer and adjusted to $5x10^7$ cells/mL.

Pollen was collected as above and was weighed out into each of two 5mL tubes. The first was microwaved for 3 minutes to prevent germination by submerging the pollen in BK media, opening the lid and placing in a glass beaker to hold tube upright, then immediately microwaving on high for 3 minutes. The second tube remained untreated. Just before combining at time 0, BK media was added to the fresh, germinable tube of pollen. Assays had consistent concentrations of pollen solution (4.2 mg/mL, ~40 grains/µl) which was made by weighing out pollen to nearest hundred-thousandth of a gram and adding enough media to adjust concentration to exactly 4.2 mg/mL.

In 1.7 mL Eppendorf tubes, 50 µl of *A. pollinis* SCC477 solution was mixed with 50 µl of the microwaved pollen solution, the live (untreated) pollen, or the no-pollen (BK) control, and 400 µl of sterile BK (N=3 for each pollen type, final pollen concentration ~4 grains/µl). We added the same amount (50 µl) sterile BK instead of *A. pollinis* SCC477 to 3 tubes each of both untreated and ungerminable (microwaved) pollen as a control for the microbes already present on the pollen. The initial concentration of microbes in each tube was determined by hemocytometer cell count. The tubes were sealed with headspace and left at room temperature for 24 hours. At 24 hours each tube was sonicated to separate cells for visual enumeration, as nectar-dwelling *Acinetobacter* can form dense biofilms, then vortexed, diluted 1:10 in PBS, and counted on the hemocytometer. The pollen grains in the tubes that pollen was added to were checked to ensure that the microwaved pollen did not germinate, and that the fresh pollen could. 100 µl of each tube was also plated on TSA at 24 hours to verify that bacterial colony morphology

and characteristics matched the inoculum. Individual colonies from these plates were correctly identified by MALDI-TOF and Compass Explorer as described below. To assess if pollen germinability affects the growth of microbes that do not induce germination, we repeated this assay with *M. reukaufii,* a common nectar yeast. Instead of beginning with $5x10^7$ cells/mL, we began with $5x10^6$ cells/mL, to control for microbial biomass. Dataset and code are available in Appendix I- Table S2.

Confirmation of phenotype in alternate media

To confirm that the phenotype of SCC477 induced germination and bursting can occur in ecologically relevant conditions, we used essentially the same setup format as the germination assay (Figure 1.2), but in artificial nectar media (30% sucrose, 0.125% tryptone, 0.025% soytone- all w/v). This media was selected because it is more ecologically relevant (no boron or calcium, higher sugar content) and allows *Acinetobacter* to grow without the presence of pollen so that we could include controls for just *Acinetobacter* growth and potential resulting protein release. SCC477 was grown for 24 hours in artificial nectar then $OD_{600\ nm}$ was measured ($OD_{600\ nm}$ = 0.1 to 0.2). The microbes were washed in PBS once (centrifuged at 14,000 rpm for 5 minutes, decanted supernatant, resuspended in PBS, repeated once with final resuspension in sterile artificial nectar). Pollen solutions for germinable and ungerminable pollen treatments were created as described for growth assays (above) but in artificial nectar instead of BK media (4.2 mg/mL). 50 µl of microbe solution and 50 µl of pollen solution were added to each well of a 96 well plate with treatments of germinable pollen, ungerminable pollen or no pollen (sterile artificial nectar; final pollen concentration ~20 grains/µl) with SCC477 or without microbial inoculation (sterile artificial nectar).

Pollen germination and bursting were quantified at 15 minutes, 12 hours, and 24 hours using the same criteria as germination assay above (germination: visibly protruding intine, busting: visible release of protoplasm) but on a different microscope due to unavailability of the EVOS M5000 (ECLIPSE Ts2 with Levenhuk M300 Base series microscope camera and Levenhuk Lite software for macOS v 1.016). The resulting images were not compatible for counting with the FIJI Macro script (Supplementary methods 1), therefore we used an iOS app "CountThings"[83] (Template ID: 386 v. 004) to count total

pollen in each image, and validated that the counts were not significantly different from hand counting. Dataset and code are available in Appendix I- Table S2.

We validated this method to be accurate with a paired t-test comparing automated CountThings app counts with hand counts of the same images (24 hour timepoint from one assay). The macro counts and hand counts were not significantly different (N=20, p= 0.86). The 24 hour timepoint was selected because the pollen tubes and burst grains present at 24 hour (in some images) were can pose an obstacle for accurate automated counting. This script was used for Appendix I, Figure S3 to count total pollen grains. Germinated and burst grains were counted by hand in FIJI as described above.

Protein release and validation in ecologically relevant media

To test whether pollen releases protein into solution when exposed to SCC477, we used a Pierce Modified Lowry Assay Kit (ThermoFisher) to quantify protein release into solution from the assay described above in *Confirmation of phenotype in alternate media.* Immediately after mixing of pollen and microbe treatments and at 24 hours, 15 µl was removed with a multichannel pipette and combined with 45 µl sterile water (for a 1:4 dilution). This was then filtered through a 96 well filter plate (0.2 micron, spun at 1,400 rpm for 4 minutes) to remove both microbes and pollen. 40 µl of this solution was then used to quantify protein concentration as per kit instructions; we included a dilution series of known concentration albumin standards in each plate. After reading the plate at 750 nm on a plate reader, the blank (water) value was subtracted from all other values. The albumin dilution series was used to create a standard curve for each plate, which was used to translate 750 nm reading to protein concentration (µg/mL). Dataset and code are available in Appendix I- Table S2.

Microbial identification via MALDI-TOF

Because effective sterilization of the pollen could not be done without compromising germinability, we wanted to confirm that added microbes remained as the primary species/strain in their wells, and to identify pollen-borne microbes in the control wells. We therefore validated microbial identity with MALDI-TOF for some of the assays[84]. Within 1 day after select assays (2x microbial impact

on pollen assays, 1x dose dependence assay), used wells (50 µl) were plated onto separate plates of TSA and allowed to grow for 48-72 hours. For each morphotype present, (if more than one) material from one or two representative colonies was selected and spotted in duplicate onto an MTP 384 Ground Steel Target Plate (Bruker Daltonics), overlaid with 1 µl 70% (v/v) formic acid, and allowed to air dry. 1 µl of alpha-cyano-4-hydroxycinnamic acid (HCCA) matrix dissolved in a 50:45:5 (v/v) solution of acetonitrile, water, and trifluoroacetic acid was added and allowed to dry [same prep as in [85]]. Spectra were obtained twice per spot, in succession, using an ultrafleXtreme MALDI-TOF instrument (Bruker Daltonics, Billerica, MA, United States). Spectra for each isolate were then compared with a custom in-house library of main spectral profiles (MSPs) and the Bruker libraries (Bacteria, Eukaryotes) using MBT Compass Explorer software (Bruker Daltonics, Billerica, MA, United States). Log scores between 1 and 3 were generated for each isolate's top 10 best matches. Scores ≥2.0 are considered close matches; lower scores indicate that the exact species may not have been present or matched closely enough to the library spectra. Genus-level identification was used for those with scores above 1.6. Sometimes, there is no spectra generated from a spot (eg. HCCA crystals do not form correctly, the spotting is too thick, the laser strikes areas where either of these causes lack of ionization). Spots/wells that failed to generate spectra were removed from the compiled 'MALDI_identifications.csv'.

Pectinase assay

Microbial strains described above were grown on either Reasoner's 2 Agar (R2A) or YM plates. For pectin degradation experiments, microbial strains were spotted onto polygalacturonic acid (PGA) plates containing 0.5% PGA in 0.1 M Tris-HCl pH 8.6, with 1.5% agar and 0.5% yeast extract- all (w/v). Plates were incubated for 48-72 hours at 25 ºC and stained with 1% (w/v) cetyltrimethylammonium bromide (CTAB) for 20 minutes to visualize clearance zones. Each microbe spot was replicated 9 times (Appendix I, Table S1).

To determine whether exposure to pollen would increase or trigger polygalacturonase activity, we grew *A. pollinis* SCC477, *Pectobacterium carotovorum* (positive control) and *Metchnikowia reukaufii* (negative control) on PGA plates. We then mixed one colony of each with prepared fresh *E. californica*

pollen in BK germination media, in PCR tubes, to provide initial exposure. As a control for polygalacturonase activity from pollen germination itself, we included another tube into which we added a crushed stigma of *E. californica,* as well as a tube with only pollen in BK media. After one hour of co-incubation at room temperature, we checked each treatment for germination and spotted each of these treatments onto fresh PGA plates in triplicate. We also spotted, in triplicate, the microbes themselves directly from the PGA plates that they had been grown on. After incubation for 72 hours at 25 °C, CTAB solution (1% w/v) was added for 20m to visualize clearance zones (Appendix I, Figure S2, Table S1).

Examination of flower sterility and identification of common contaminants

We verified that flowers collected prior to opening that opened naturally in lab were relatively free of contaminants. We plated the anthers by removing them with sterilized tweezers, rubbing across surface of plate to spread microbes and pollen, and leaving them on the plate. We did this for both lab-opened and outside-opened flowers onto multiple media types (3 types: R2A, TSA, and YM. We then picked and identified morphotypes as described above (Appendix I, Figure S4).

Quantification and statistical analysis

All statistical analyses were done in RStudio 1.2.1335 [86] using R 3.6.2 [87]. Details for each test can be found in figure legends, including the statistical tests used, exact value and definition of n, definitions of boxplot parameters (eg. median, IQR). Significance markings (stars) are defined in Figure 1.2, significance lettering defined and used in Figures 3 and 4, with baseline threshold for significance $p<0.05$. Further information can be obtained by running the code for each figure.

To compare if pollen germination and bursting differed among microbes, Kruskal-Wallis tests were run (base R) with microbe treatment as predictor of pollen germination or bursting, respectively. Separate tests were performed for each timepoint. To test for differences in pollen germination (and separately, pollen bursting) between microbes, pairwise comparisons between microbes were calculated using the "FSA" package[88] to run a Dunn test with Benjamin-Hochberg p-value adjustment (28 tests). Eleven total assays were done, and two were eliminated from further analysis. One assay was eliminated

due to data loss of images-making recount and validation of pollen ratios impossible, and the other was eliminated due to contamination of the initial growth media. For germination and bursting comparison across dilutions of *A. pollinis* SCC477 (density-dependence), one-way ANOVA was calculated at each timepoint and the "emmeans" package[89] was used for pairwise comparisons and calculation of p-values, with Tukey adjustment (21 tests). For comparison of 24 hour cell counts of both *A. pollinis* and *M. reukaufii (*separately) with different pollen treatments, one-way ANOVA was calculated, then the "emmeans" package[89] was used for pairwise comparisons and calculation of p-values, with Tukey adjustment (10 tests). To compare protein release over pollen and microbe treatments, a Kruskal-Wallis test was run (base R), with treatment (combined pollen treatment and microbe treatment) as predictor of protein in solution. Pairwise comparisons were calculated using the "FSA" package[88]- using a Dunn test with Benjamin-Hochberg p-value adjustment (15 tests). To compare germination and (separately) bursting of pollen in artificial nectar, a Kruskal-Wallis test was run (base R), with treatment (combined pollen treatment and microbe treatment) as predictor of germination or bursting. Pairwise comparisons were calculated using the "FSA" package[88]- using a Dunn test with Benjamin-Hochberg p-value adjustment (6 tests).

Results

Microbial species and strains differ in effects on E. californica *pollen germination and bursting*

Nectar microbes may gain access to pollen nutrients by causing them to prematurely germinate[40,41]. To assess microbial effects on *Eschscholzia californica* pollen germination, we inoculated pollen solutions with seven microbial species (detailed in Methods) and imaged them at 15, 45, and 90 minutes (N=27-36 per species). Nectar- and bee-associated *Acinetobacter* species and strains were selected following initial observations with pollen and because they are both common in nectar [9–12,18–20]. *Metschnikowia reukaufii,* a common nectar yeast, frequently co-occurs with[9,10] and benefits from pollen[35], but is associated with inhibitory effects on pollinia germination[42]. *Pectobacterium carotovorum* was included to control for bacterial presence (Microbial Associated Molecular Patterns may trigger plant

immune response) and to test the potential mechanism of pectinase activity[43], which can stimulate pollen germination and bursting[44], and is associated with pollen degradation[45–47]. In the assays, a pollen grain was classified as germinated if intine was visibly bulging out of the exine, regardless of whether the pollen tube had also burst (Figure 1.1C,D). The germination percentage for each replicate was calculated by dividing grains which had germinated by total grains and multiplying by 100.

By 15 minutes, pollen in wells inoculated with *Acinetobacter pollinis* SCC477 or *A. boissieri* had on average at least 3x higher germination than the control uninoculated pollen (6.4%, 8% and <2%, respectively) and germination was significantly higher than pollen inoculated with *P. carotovorum* (<1%) or *M. reukaufii* (<1%) (Kruskal-Wallis $\chi2 = 46.366$, df = 7, $p<0.0001$; pairwise comparisons $p<0.001$; Figure 1.2A,C,D). Across all microbial treatments, pollen germination increased over time, but wells treated with *A. pollinis* SCC477 and *A. boissieri* had, respectively, 4.4x and 3.7x higher average pollen germination than the uninoculated pollen at 90 minutes (36.9%, 31.3%, and 8.4%, respectively; Kruskal-Wallis $\chi2 = 53.702$, df = 7, $p<0.0001$; pairwise comparisons $p<0.001$; Figure 1.2A,C,D). In contrast, neither the yeast *M. reukaufii* nor pectinase producer *P. carotovorum* affected pollen germination differently from the uninoculated control at any timepoint ($p>0.05$). All *Acinetobacter* strains induced significantly higher germination compared to the control by 90 minutes except for *A. nectaris,* which had variable effects on pollen germination (Figure 1.2A).

To assess microbial induction of pollen bursting, which releases nutrient-dense protoplasm[3], we also monitored pollen tube and whole pollen bursting visually in the same assays referenced above for pollen germination. A pollen grain was classified as burst if it released protoplasm either from the pollen tube (tip bursting) or directly from the pollen grain (Figure 1.1B, D). Both *A. pollinis* SCC477 and *A. boissieri*-inoculated pollen showed significantly higher pollen bursting than the no microbe control, *M. reukaufii* ($p<0.001$), or *P. carotovorum* ($p<0.05$) by 45 minutes (Kruskal-Wallis $\chi2 = 47.557$, df = 7, $p<0.0001$; Figure 1.2B). The average percentages of burst pollen grains for *A. pollinis* SCC477 and *A. boissieri* were 75x and 45x higher than the no-microbe control at 45 minutes, respectively. At 90 minutes, pollen inoculated with *A. boissieri*, *A. apis*, *A. pollinis* SCC477, and *A. pollinis* SCC474 were burst to a

greater extent than in the no microbe control (Kruskal-Wallis $\chi 2 = 74.454$, df = 7, $p < 0.0001$; pairwise comparisons $p<0.001$; Figure 1.2B), but *A. nectaris, M. reukaufii,* and *P. carotovorum* did not differ significantly from the no microbe control at any timepoint (Figure 1.2B).

In a separate assay, we used a dilution series of SCC477 to determine if concentration of SCC477 had an effect of pollen germination and bursting over 24 hours. We found that bacterial effects on germination, bursting, and pollen tube length vary with bacterial titer. Pollen inoculated with the highest densities of SCC477 germinated and burst more quickly than those with lower bacterial densities (Appendix I, Figure S1 A-C). Pollen tubes also grew to shorter lengths when inoculated with higher concentrations of SCC477 (Appendix I, Figure S1 D).

Acinetobacter pollinis *SCC477, but not* M. reukaufii*, gains additional benefit from germinability of pollen*

To assess the effects of pollen presence and germination on microbial growth, we assessed the growth of two species that differed in their ability to germinate pollen- *A. pollinis* SCC477, which readily germinates and bursts pollen, and the yeast *M. reukaufii* which did not germinate or burst pollen in our assays (Figure 1.2). We made microbial suspensions that were within the normal range of microbial densities in nectar[12,14] then added: no pollen, germinable pollen (GP) or pollen rendered unable to germinate (UP, confirmed visually at 24 hours). Compared to microbial growth with no pollen, *A. pollinis* SCC477 and *M. reukaufii* displayed significantly higher cell density after 24 hours with either pollen (ANOVA *A. pollinis,* $F_{4,40} = 56.17$, $p = <0.0001$; ANOVA *M. reukaufii,* $F_{4,40} = 21.15$, $p < 0.0001$; pairwise comparisons $p<0.0001$; Figure 1.3). However, only *A. pollinis* SCC477 growth differed with pollen germinability: its cell density after 24 hours was almost twice as high with germinable pollen (1.9x higher than UP, 7.4x higher than no pollen control) than it was with ungerminable pollen (3.8x higher than no pollen control) (ANOVA $F_{4,40} = 56.17$, df = 4, $p = <0.0001$; pairwise comparisons $p<0.0001$; Figure 1.3A). In the absence of pollen, both microbes barely grew from the starting concentration during the 24 hour window (Figure 1.3), indicating significant reliance on pollen-derived nutrients. *M. reukaufii* grew equally well with both pollen treatments, indicating comparable nutrient content for GP and UP (Figure

1.3B). Uninoculated pollen had low levels of contamination, likely from the pollen itself (Appendix I, Figure S4).

Acinetobacter pollinis *SCC477 effects on pollen are robust in alternative media*

To validate that *Acinetobacter pollinis* SCC477 effects on pollen are not dependent on specific components of BK media used in assays above, and to examine potential mechanisms of microbial growth germination, we performed additional assays in a second media type. We used 30% sucrose media more closely mimicking nectar composition, as BK germination medium is lower in sucrose and contains calcium (Ca) and boron (B), typically not found in nectar[48,49]. To validate microbial effects on pollen, we imaged and quantified pollen germination and bursting at time 0, 12 hours and 24 hours. In media lacking Ca and B, SCC477 induced initial stages of pollen germination and pollen bursting by 12 hours (Appendix I, Figure S3). Germination was over 10x higher with SCC477 inoculated than in the control (35.6% and 3.4% respectively, Figure 1.4A) and bursting with SCC477 inoculation was nearly 3x higher than the control (1.7% and 0.6% respectively, Figure 1.4B).

Acinetobacter pollinis *SCC477 stimulates protein release from germinable pollen*

In the same assays as described above, we examined the potential cause of the observed growth benefit from germinable pollen by quantifying protein levels in solution after exposure of germinable and ungerminable pollen to SCC477. Using Modified Lowry Protein Assays, we found that germinable pollen exposed to SCC477 released over twice as much protein into solution than uninoculated germinable pollen over 24 hours, while the addition of SCC477 only marginally increased protein release for ungerminable pollen (Kruskal-Wallis $\chi 2 = 40.768$, df = 5, $p < 0.0001$; Figure 1.4C). Further, germinable and ungerminable pollen released near-equivalent amounts of protein when not exposed to SCC477.

Discussion

For many flower-associated organisms, pollen is the primary source of protein and trace nutrients[3] but mechanisms by which consumers breach pollen's recalcitrant outer shell remain poorly documented. Here, we show that the nectar specialist bacteria *Acinetobacter* can induce pollen

germination, bursting and protein release into solution, resulting in higher microbial density when grown with germinable pollen. While pollen benefits the growth of most nectar microbes[9,10], the results here demonstrate that microbial species differentially induce changes in pollen physiology that affects nutrient release and obtain differential growth benefit from pollen in a habitat that is often nutrient-limited[15,17,50].

*Acinetobacter'*s ability to access additional pollen nutrients likely contributes to its ecology. The nectar environment is a highly specialized niche, requiring microbial inhabitants to tolerate high osmolarity, plant secondary metabolites or toxins, reactive oxygen species (ROS), and low nutrient levels- all within an ephemeral habitat[34,51,52]. Here, rapid growth—fueled by pollen nutrients-- is likely to strongly affect microbial fitness and allow transfer to the next suitable habitat[34,35,53,54]. The ability to induce pollen germination and bursting could contribute to the prevalence and abundance of *Acinetobacter* species in floral nectars[11,12,14] and other environments frequently containing pollen, such as bee pollen provisions and potentially stigmas[55–58]. The fact that ungerminable pollen still releases protein and benefits growth could be due to leaching of internal nutrients or from the pollenkitt on the pollen exterior. The difference between microbial species' effects on pollen may allow for niche partitioning among nutrient sources. Indeed, the common nectar yeast *M. reukaufii* neither induced germination nor derived additional benefit from germination, suggesting that *Acinetobacter* may have a key fitness advantage in the floral landscape. Alternatively, bacterial effects may facilitate yeast growth[50,59]. Though we predict that the observed benefit from pollen is due to the observed increased availability of protein (Figure 1.4), pollen germination or bursting could also release other components including lipids, sterols, trace elements[3] or growth hormones[60,61]. Additionally, the ungerminable pollen may have been altered in other ways that we were unable to characterize, which may also affect microbial growth. The mechanism by which pollen benefits nectar microbes merits further study.

Although the mechanism behind the induced germination phenotype described here has yet to be determined, microbe-pollen interactions could prove a useful system in identifying chemical cues required for pollen germination. Pollen germination is tightly controlled, being influenced by hydration rate of the desiccated grain[62], pectin modifications[63], pistil-pollen crosstalk[64], calcium[49], and other

molecules[65] as well as aperture number, exine thickness and nutrient composition[39,66]. Pollen tube growth requires continuous spatial and temporal adjustments to create and maintain polarity for directed growth; interference can result in tube defects such as branching and premature bursting[67–70], similar to the phenotype observed here (Figure 1.1). It is worth noting that pollen tube tips have mechanisms for tip bursting to allow bursting sperm release when induced by the female gametophyte during regular fertilization[71], but are also known to burst *in vitro* due to: osmotic changes, polysaccharides (modification, cycling), pH, ROS signaling, and pectinase activity[72,73]. While we did not identify the mechanism responsible for tube bursting documented here, the published genomes of nectar *Acinetobacter* contain multiple assigned pectinase genes (Appendix I, Table S1), which are known to impact germination and bursting[73]. Evidence presented here–including minimal effects of *Pectobacterium*, a known pectinase producer, and a lack of detected pectinase activity by *Acinetobacter* suggest that pectinases alone are not responsible for the germination or bursting phenotype (Appendix I, Figure S2, Table S1). It is generally observed that pollen germination *in vitro* takes longer than stigmatic germination, presumably due to missing factors or less-than-ideal conditions[64]. *Acinetobacter* effects may be a promising system to either identify species-specific cues if effects are restricted to *E. californica* pollen or universal cues of pollen germination if *Acinetobacter* can also affect pollen of other plant species. Moreover, the variability within and among strains of *Acinetobacter* (Figure 1.2) could reflect species specificity in interaction or reliance on pollen[50], recent evolution of the phenotype, or variability in pollen state (e.g. desiccation, outdoor temperature, low abundance microbes, or endophytes that could affect pollen viability). We anticipate that further work on this system will shed light on the specificity and mechanisms involved in interactions between pollen and *Acinetobacter*, as well the potential for other flower-dwelling microbes to alter pollen physiology to access nutrients.

There are ecological implications of microbial effects on pollen that remain to be explored. Since many pollen consumers also consume floral nectar, *Acinetobacter*-induced pollen germination and bursting could illuminate a previously undocumented mechanism for macroscopic species to access pollen nutrients via microbial partners. While pollen germination has been considered and studied as a

potential mechanism of digestion for macroscopic consumers[2,22,23], microbial involvement in this mechanism has not been studied. *Acinetobacter* spp. are common in floral nectar, and are also found in the nectar and pollen provisions that bees provide their offspring[57,58,74]. Our study suggests that the role of floral microbes in pollen germination and bee nutrition warrants further study.

Microbial stimulation of pollen germination may also affect plant fitness. Previous work has shown that nectar microbes can alter pollinator preference for flowers by altering nectar composition and volatiles[10,75], directly impacting plant reproduction as these microbes grow to greater density by using pollen nutrients. Effects on pollen nutrient availability to pollinators could also potentially influence pollinator foraging and pollination. Direct effects of microbes on plant reproduction are also possible. *Acinetobacter* is common on many floral surfaces, including stigmas[76] and its presence in nectar is correlated with presence in seed microbiomes[55]. Whether *Acinetobacter* growth on stigmas or seeds affects pollen or seed germination or success in the context of fertilization will also require further study.

As we have demonstrated, floral microbes can significantly affect pollen physiology- this in turn may have important consequences for plants and pollinators[10,34,75,77]. Further investigation of microbe-pollen interactions could shed light on the specific biochemical triggers of pollen germination and the ecological effects of microbe-pollen interactions on plants and pollinators.

Acknowledgements

We would like to thank the UC Davis Arboretum for allowing us to collect flower samples; Sergio Álvarez-Pérez, Robert Gilbertson, Griffin Hall and Megan Morris for strain collection and donation, Abby Ray, Marshall McMunn, Jacob Francis, Tobias Mueller, Danielle Rutkowski, Amber Crowley-Gall, Alexandria Igwe and Tory Hendry for offering project advice and comments on the manuscript; Antoine Abrieux for assistance with microscopy; William Jewel and UC Davis Campus Mass Spectrometry Facilities for assistance and access to the MALDI-TOF. This work was supported by the National Science Foundation DEB #1929516 to RLV, Davis Botanical Society Student Research Award to SMC and Microbiology Graduate Group Diversity Equity and Inclusion Award to SMC.

Figures

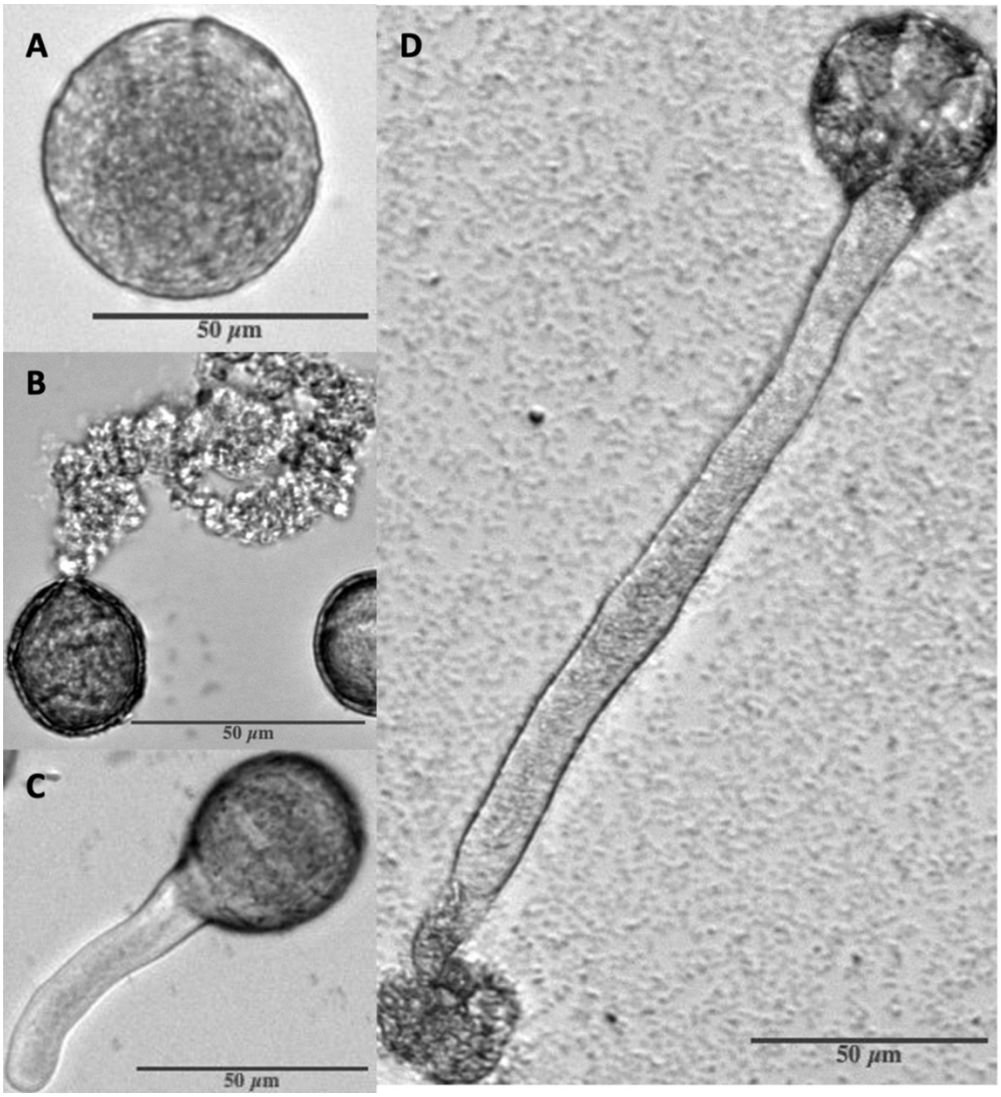

Figure 1.1- Observed states of *Eschscholzia californica* (California poppy) pollen grains. (A) Whole, ungerminated pollen grain. (B) Burst pollen grain releasing protoplasm without signs of pollen tube. (C) Germinated pollen grain. (D) Pollen grain which has germinated and subsequently the tip of the pollen tube burst, releasing protoplasm.

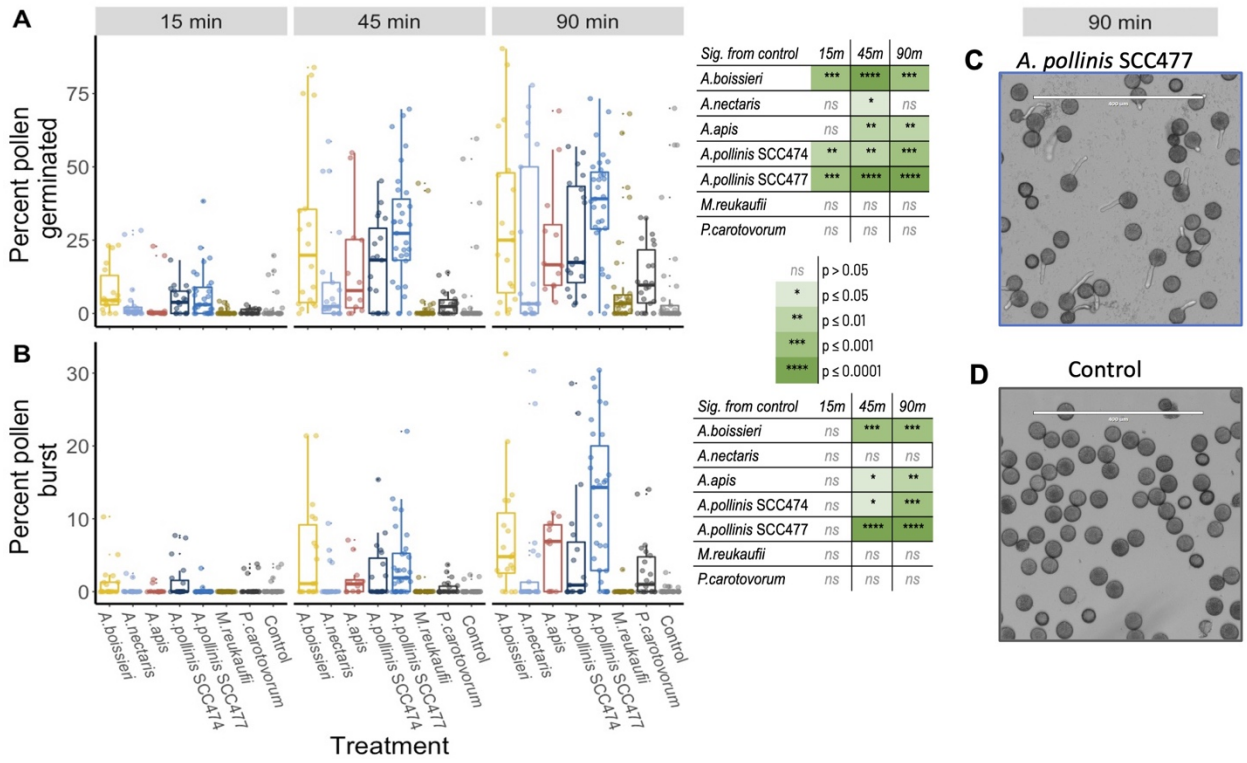

Figure 1.2- Nectar *Acinetobacter* increase pollen germination and bursting. A) Grains that germinated with each microbe treatment. B) Grains that burst with each microbe treatment. For A and B, significance from control used Kruskal Wallis test followed by Dunn's multiple comparisons; 'ns' indicates no significant difference, N=27-36, and a total 41,079 pollen grains. Note difference in scale of y-axes. Center lines correspond to the median, boxes define interquartile range (IQR) and whiskers extend +1.5 IQR. Note difference in scale on y axes. C and D) Cropped images of pollen at 90-minute timepoint when inoculated with *A. pollinis* SCC477 (C), or control with no microbe inoculation (D). See also Appendix I, Figures S1, S2, and S4.

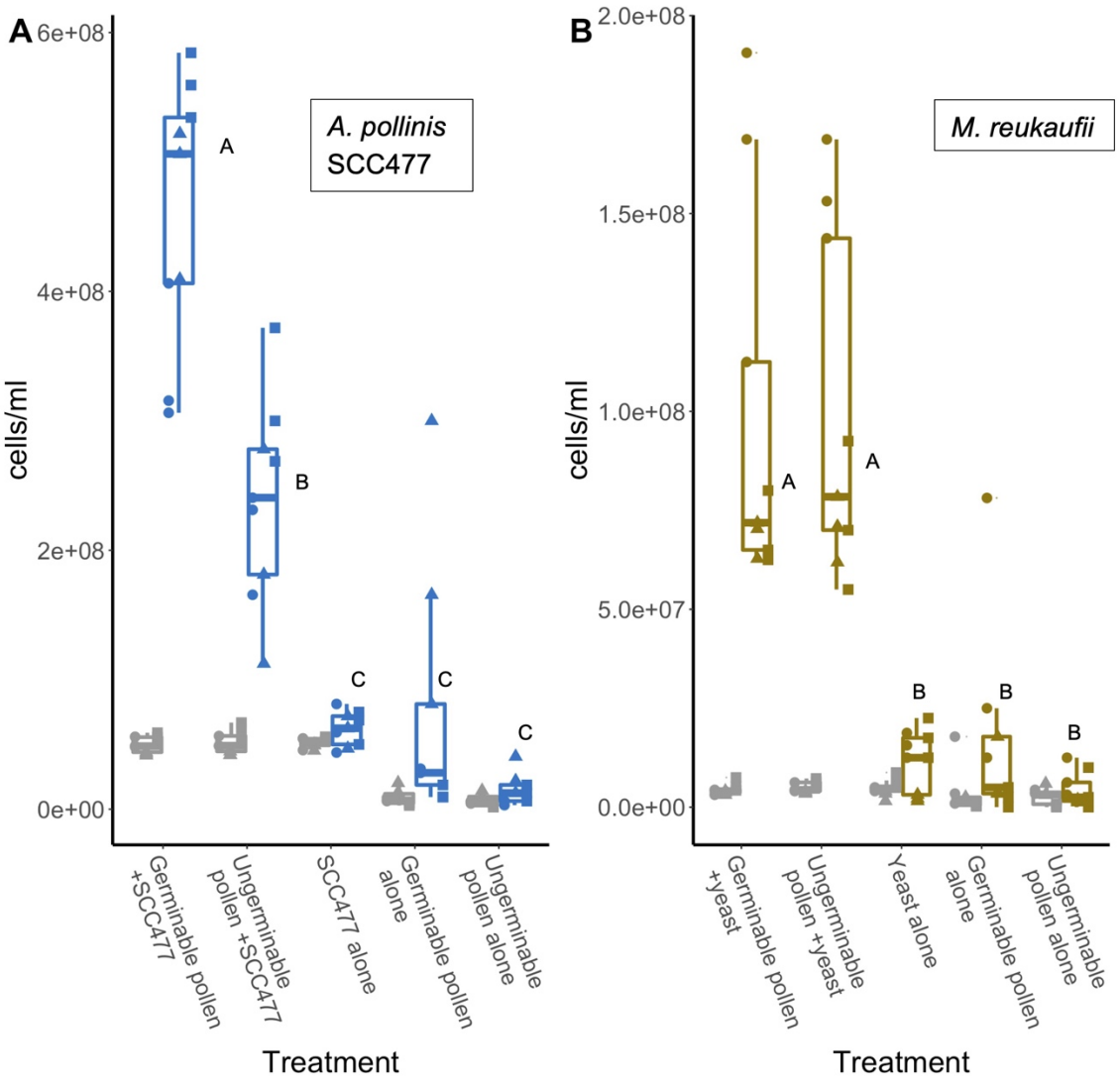

Figure 1.3- *Acinetobacter* growth is enhanced by germinable pollen addition. Standard error bars are shown, significance between treatments marked by lettering based on ANOVA followed by Tukey multiple comparisons. Note difference in scale of y-axes. Data point shape indicates assay replicate. Center lines correspond to the median, boxes define interquartile range (IQR) and whiskers extend +1.5 IQR. Uninoculated pollen had low levels of microbial growth. A) *A. pollinis* SCC477 data represents three assays, 3 biological replicates of each treatment per assay, N=9. B) *M. reukaufii* data represents three assays, 3 biological replicates of each treatment per assay, N=9. See also Appendix I, Figure S4.

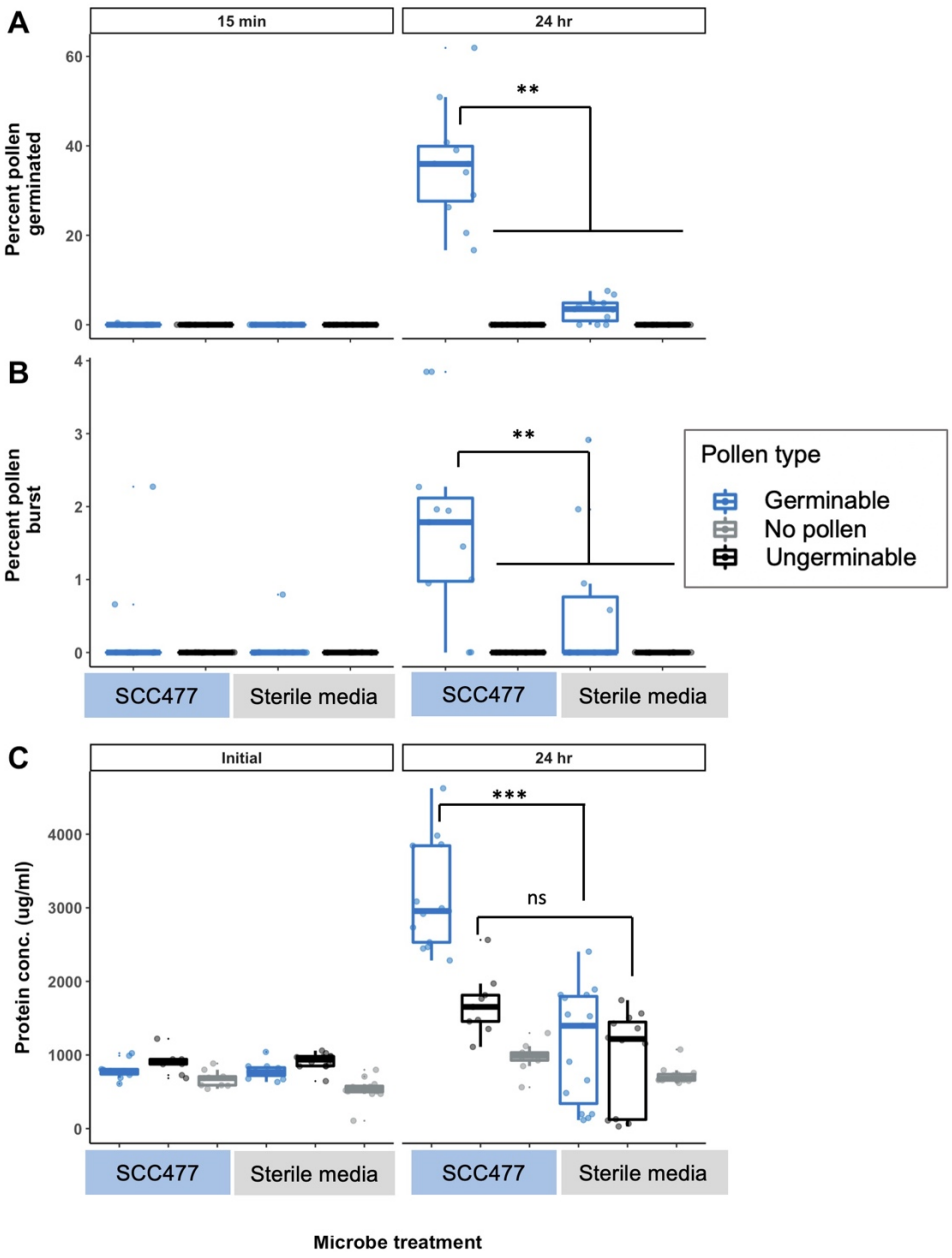

Figure 1.4- Pollen germination and bursting due to *A. pollinis* SCC477 exposure results in increased release of protein from germinable pollen. Standard error bars are shown, significance between treatments based on Kruskal-Wallis followed by Dunn's multiple comparisons and marked by brackets; 'ns' indicates no significant difference (p=0.09). Center lines correspond to the median, boxes define interquartile range (IQR) and whiskers extend +1.5 IQR. Data represents three assays, 3-8 biological replicates of each treatment per assay, N=9-15 and a total 14,544 pollen grains. Assays done in artificial nectar with 30% (w/v) sucrose. Note difference in scale of y-axes. A) Pollen germination at 15 minutes and 24 hours in response to SCC477. B) Pollen bursting at 15 minutes and 24 hours C) Protein concentrations among pollen types with exposure to SCC477. See also Appendix I, Figures S3, S4.

References

1. Leach, M.E., and Drummond, F. (2018). A review of native wild bee nutritional health. Int. J. Ecol. 2018, 1–10.
2. McKinstry, M., Prado-Irwin, S.R., Adames, T.R., and Snow, J.W. (2020). Retained metabolic activity in honey bee collected pollen has implications for pollen digestion and effects on honey bee health. Apidologie 51, 212–225.
3. Roulston, T.H., and Cane, J.H. (2000). Pollen nutritional content and digestibility for animals. Plant Syst. Evol 222, 187–209.
4. Southworth, D. (1973). Cytochemical reactivity of pollen walls. J. Histochem. Cytochem. 21, 73–80.
5. Shi, D.Q., and Yang, W.C. (2010). Pollen germination and tube growth. In Plant Developmental Biology (Springer Berlin Heidelberg), pp. 245–282.
6. Wang, R., and Dobritsa, A.A. (2018). Exine and aperture patterns on the pollen surface: their formation and roles in plant reproduction. In Annual Plant Reviews online, pp. 589–628.
7. Li, F.S., Phyo, P., Jacobowitz, J., Hong, M., and Weng, J.K. (2019). The molecular structure of plant sporopollenin. Nat. Plants 5, 41–46.
8. Wu, W., Wang, K., Qiao, J., Dong, J., Li, Z., and Zhang, H. (2019). Improving nutrient release of wall-disrupted bee pollen with a combination of ultrasonication and high shear technique. J. Sci. Food Agric. 99, 564–575.
9. Herrera, C.M. (2017). Scavengers that fit beneath a microscope lens. Ecology 98, 2725–2726.
10. Pozo, M.I., Lievens, B., and Jacquemyn, H. (2015). Impact of microorganisms on nectar chemistry, pollinator attraction and plant fitness. Nectar Prod. Chem. Compos. Benefits to Anim. Plants, 1–40.
11. Álvarez-Pérez, S., and Herrera, C.M. (2013). Composition, richness and nonrandom assembly of culturable bacterial-microfungal communities in floral nectar of Mediterranean plants. FEMS Microbiol. Ecol. 83, 685–699.
12. Fridman, S., Izhaki, I., Gerchman, Y., and Halpern, M. (2012). Bacterial communities in floral nectar. Environ. Microbiol. Rep. 4, 97–104.
13. Sharaby, Y., Rodríguez-Martínez, S., Lalzar, M., Halpern, M., and Izhaki, I. (2020). Geographic partitioning or environmental selection: What governs the global distribution of bacterial communities inhabiting floral nectar? Sci. Total Environ. 749, 142305.
14. Tsuji, K., and Fukami, T. (2018). Community-wide consequences of sexual dimorphism: evidence from nectar microbes in dioecious plants. Ecology 99, 2476–2484.
15. Heil, M. (2011). Nectar: Generation, regulation and ecological functions. Trends Plant Sci. 16, 191–200.
16. Vannette, R.L., and Fukami, T. (2018). Contrasting effects of yeasts and bacteria on floral nectar traits. Ann. Bot. 121, 1343–1349.
17. Dhami, M.K., Hartwig, T., and Fukami, T. (2016). Genetic basis of priority effects: Insights from nectar yeast. Proc. R. Soc. B Biol. Sci. 283.
18. Álvarez-Pérez, S., Lievens, B., Jacquemyn, H., and Herrera, C.M. (2013). Acinetobacter nectaris sp. nov. and Acinetobacter boissieri sp. nov., isolated from floral nectar of wild Mediterranean insect-pollinated plants. Int. J. Syst. Evol. Microbiol. 63, 1532–1539.
19. Alvarez-Perez, S., Baker, L.J., Morris, M.M., Tsuji, K., Sanchez, V.A., Fukami, T., Vannette, R.L., Lievens, B., and Hendry, T.A. (2021). Acinetobacter pollinis sp. nov., Acinetobacter baretiae sp. nov. and Acinetobacter rathckeae sp. nov., isolated from floral nectar and honey bees. Int. J. Syst. Evol. Microbiol. 71.
20. Kim, P.S., Shin, N.R., Kim, J.Y., Yun, J.H., Hyun, D.W., and Bae, J.W. (2014). Acinetobacter apis sp. nov., isolated from the intestinal tract of a honey bee, Apis mellifera. J. Microbiol. 52, 639–645.
21. Nepi, M., Cresti, L., Maccagnani, B., Ladurner, E., and Pacini, E. (2005). From the anther to the proctodeum: Pear (Pyrus communis) pollen digestion in Osmia cornuta larvae. J. Insect Physiol. 51, 749–757.
22. Grant, B.R. (1996). Pollen digestion by Darwin's finches and its importance for early breeding. Ecology 77, 489–499.
23. Turner, V. (1984). Banksia pollen as a source of protein in the diet of two Australian marsupials Cercartetus nanus and Tarsipes rostratus. Oikos 43, 53–61.
24. Marr, D.L. (1998). The effect of Microbotryum violaceum spores on pollen germination in Silene acaulis. Int. J. Plant Sci. 159, 221–227.
25. Rowe, D.E., and Stortz-Lintz, D.L. (1993). Responses of alfalfa pollen and callus to filtrates from two isolates of Fusarium oxysporum. Sex. Plant Reprod. 6, 11–15.

26. Kimura, Y., Yoshinari, T., Shimada, A., and Hamasaki, T. (1995). Isofunicone, a pollen growth inhibitor produced by the fungus, Penicillium sp. Phytochemistry 40, 629–631.
27. Orenstein, J., Nachmias, A., Colon, L.T., and Hoogendorn, J. (1994). The effect of a Verticillium dahliae phytotoxin on germination of potato pollen. Isr. J. Plant Sci. 42, 29–36.
28. Qin, Y., Wysocki, R.J., Somogyi, A., Feinstein, Y., Franco, J.Y., Tsukamoto, T., Dunatunga, D., Levy, C., Smith, S., Simpson, R., et al. (2011). Sulfinylated azadecalins act as functional mimics of a pollen germination stimulant in Arabidopsis pistils. Plant J. 68, 800–815.
29. Tsukamoto, Y., and Matsubara, S. (1968). Studies on germination of chrysanthemum pollen II: Occurrence of a germination promoting substance. Plant Cell Physiol. 9, 237–245.
30. Zhang, D., Wengier, D., Shuai, B., Gui, C.P., Muschietti, J., McCormick, S., and Tang, W.H. (2008). The pollen receptor kinase LePRK2 mediates growth-promoting signals and positively regulates pollen germination and tube growth. Plant Physiol. 148, 1368–1379.
31. Mo, Y., Nagel, C., and Taylor, L.P. (1992). Biochemical complementation of chalcone synthase mutants defines a role for flavonols in functional pollen. Proc. Natl. Acad. Sci. U. S. A. 89, 7213–7217.
32. Wengier, D.L., Mazzella, M.A., Salem, T.M., McCormick, S., and Muschietti, J.P. (2010). STIL, a peculiar molecule from styles, specifically dephosphorylates the pollen receptor kinase LePRK2 and stimulates pollen tube growth in vitro. BMC Plant Biol. 10, 33.
33. Herrera, C.M., De Vega, C., Canto, A., and Pozo, M.I. (2009). Yeasts in floral nectar: A quantitative survey. Ann. Bot. 103, 1415–1423.
34. Vannette, R.L. (2020). The floral microbiome: Plant, pollinator, and microbial perspectives. Annu. Rev. Ecol. Evol. Syst. 51, 363–386.
35. Pozo, M.I., and Jacquemyn, H. (2019). Addition of pollen increases growth of nectar-living yeasts. FEMS Microbiol. Lett. 366.
36. Haslett, J.R. (1983). A photographic account of pollen digestion by adult hoverflies. Physiol. Entomol. 8, 167–171.
37. Tang, W., Kelley, D., Ezcurra, I., Cotter, R., and McCormick, S. (2004). LeSTIG1, an extracellular binding partner for the pollen receptor kinases LePRK1 and LePRK2, promotes pollen tube growth in vitro. Plant J. 39, 343–353.
38. Higashiyama, T. (2010). Peptide signaling in pollen pistil interactions. Plant Cell Physiol. 51, 177–189.
39. Williams, J.H., and Reese, J.B. (2019). Evolution of development of pollen performance. Curr. Top. Dev. Biol. 131, 299–336.
40. Linskens, H.F., and Schrauwen, J. (1969). The release of free amino acids from germinating pollen. Acta Bot. Neerl. 18, 605–614.
41. Stanley, R.G., and Linskens, H.F. (1965). Protein diffusion from germinating pollen. Physiol. Plant. 18, 47–48.
42. Eisikowitch, D., Lachance, M.A., Kevan, P.G., Willis, S., and Collins-Thompson, D.L. (1990). The effect of the natural assemblage of microorganisms and selected strains of the yeast Metschnikowia reukaufii in controlling the germination of pollen of the common milkweed Asclepias syriaca. Can. J. Bot. 68, 1163–1165.
43. Charkowski, A.O. (2018). The changing face of bacterial soft-rot diseases. Annu. Rev. Phytopathol. 56, 269–288.
44. Heslop-Harrison, J. (1979). Aspects of the structure, cytochemistry and germination of the pollen of rye. Ann. Bot. 44, 2–47.
45. Engel, P., Martinson, V.G., and Moran, N.A. (2012). Functional diversity within the simple gut microbiota of the honey bee. Proc. Natl. Acad. Sci. 109, 11002–11007.
46. Vuong, H.Q., McFrederick, Q.S., and Angert, E. (2019). Comparative genomics of wild bee and flower isolated Lactobacillus reveals potential adaptation to the bee host. Genome Biol. Evol. 11, 2151–2161.
47. Kwong, W.K., Engel, P., Koch, H., and Moran, N.A. (2014). Genomics and host specialization of honey bee and bumble bee gut symbionts. Proc. Natl. Acad. Sci. U. S. A. 111, 11509–11514.
48. Nicolson, S.W., and Thornburg, R.W. (2007). Nectar chemistry. In Nectaries and Nectar (Springer Netherlands), pp. 215–264.
49. Brewbaker, J.L., and Kwack, B.H. (1963). The essential role of calcium ion in pollen germination and pollen tube growth. Am. J. Bot. 50, 859.
50. Álvarez-Pérez, S., Tsuji, K., Donald, M., Van Assche, A., Vannette, R.L., Herrera, C.M., Jacquemyn, H., Fukami, T., and Lievens, B. (2021). Nitrogen assimilation varies among clades of nectar- and insect-associated Acinetobacters. Microb. Ecol.

51. Herrera, C.M., Canto, A., Pozo, M.I., and Bazaga, P. (2010). Inhospitable sweetness: nectar filtering of pollinator-borne inocula leads to impoverished, phylogenetically clustered yeast communities. Proc. R. Soc. B Biol. Sci. 277, 747–754.
52. Stevenson, P.C., Nicolson, S.W., and Wright, G.A. (2017). Plant secondary metabolites in nectar: impacts on pollinators and ecological functions. Funct. Ecol. 31, 65–75.
53. Hausmann, S.L., Tietjen, B., and Rillig, M.C. (2017). Solving the puzzle of yeast survival in ephemeral nectar systems: exponential growth is not enough. FEMS Microbiol. Ecol. 93, 150.
54. Pozo, M.I., Lachance, M.-A., and Herrera, C.M. (2012). Nectar yeasts of two southern Spanish plants: the roles of immigration and physiological traits in community assembly. FEMS Microbiol. Ecol. 80, 281–293.
55. Prado, A., Marolleau, B., Vaissière, B.E., Barret, M., and Torres-Cortes, G. (2020). Insect pollination: an ecological process involved in the assembly of the seed microbiota. Sci. Rep. 10, 1–11.
56. Voulgari-Kokota, A., McFrederick, Q.S., Steffan-Dewenter, I., and Keller, A. (2019). Drivers, diversity, and functions of the solitary-bee microbiota. Trends Microbiol., 1–10.
57. Voulgari-Kokota, A., Grimmer, G., Steffan-Dewenter, I., and Keller, A. (2019). Bacterial community structure and succession in nests of two megachilid bee genera. FEMS Microbiol. Ecol. 95.
58. McFrederick, Q.S., and Rehan, S.M. (2016). Characterization of pollen and bacterial community composition in brood provisions of a small carpenter bee. Mol. Ecol. 25, 2302–2311.
59. Vannette, R.L., and Fukami, T. (2014). Historical contingency in species interactions: Towards niche-based predictions. Ecol. Lett. 17, 115–124.
60. Barendse, G.W.M., Pereira, A.S.R., Berkers, P.A., Driessen, F.M., Van Eyden-Emons, A., and Linskens, H.F. (1970). Growth hormones in pollen, styles and ovaries of Petunia hybrida and of Lillium species. Acta Bot. Neerl. 19, 175–186.
61. Lin, H.R., Shu, H.Y., and Lin, G.H. (2018). Biological roles of indole-3-acetic acid in Acinetobacter baumannii. Microbiol. Res. 216, 30–39.
62. Zheng, Y.Y., Lin, X.J., Liang, H.M., Wang, F.F., and Chen, L.Y. (2018). The long journey of pollen tube in the pistil. Int. J. Mol. Sci. 19.
63. Leroux, C., Bouton, S., Kiefer-Meyer, M.-C., Fabrice, N., Mareck, A., Guénin, S., Fournet, F., Ringli, C., Pelloux, J., Driouich, A., et al. (2015). PECTIN METHYLESTERASE48 Is Involved in Arabidopsis Pollen Grain Germination. Plant Physiol.
64. Dresselhaus, T., and Franklin-Tong, N. (2013). Male-female crosstalk during pollen germination, tube growth and guidance, and double fertilization. Mol. Plant 6, 1018–1036.
65. Muhlemann, J.K., Younts, T.L.B., and Muday, G.K. (2018). Flavonols control pollen tube growth and integrity by regulating ROS homeostasis during high-temperature stress. Proc. Natl. Acad. Sci. 115, E11188–E11197.
66. Williams, J.H. (2012). The evolution of pollen germination timing in flowering plants: Austrobaileya scandens. AoB Plants 12, 1–12.
67. Moutinho, A., Hussey, P.J., Trewavas, A.J., and Malhó, R. (2001). cAMP acts as a second messenger in pollen tube growth and reorientation. Proc. Natl. Acad. Sci. U. S. A. 98, 10481–10486.
68. Sousa, E., Kost, B., and Malho, R. (2008). Arabidopsis phosphatidylinositol-4-monophosphate 5-kinase 4 regulates pollen tube growth and polarity by modulating membrane recycling. Plant Cell 20, 3050–3064.
69. Gebert, M., Dresselhaus, T., and Sprunck, S. (2008). F-actin organization and pollen tube tip growth in Arabidopsis are dependent on the gametophyte-specific armadillo repeat protein ARO1. Plant Cell 20, 2798–2814.
70. Hwang, J.U., and Yang, Z. (2006). Small GTPases and spatiotemporal regulation of pollen tube growth. Plant Cell Monogr. 3, 95–116.
71. Duan, Q., Kita, D., Johnson, E.A., Aggarwal, M., Gates, L., Wu, H.M., and Cheung, A.Y. (2014). Reactive oxygen species mediate pollen tube rupture to release sperm for fertilization in Arabidopsis. Nat. Commun. 5, 3129.
72. Obermeyer, G., and Feijó, J. (2017). Pollen tip growth: From biophysical aspects to systems biology (Springer).
73. Parre, E., and Geitmann, A. (2005). Pectin and the role of the physical properties of the cell wall in pollen tube growth of Solanum chacoense. Planta 220, 582–592.
74. McFrederick, Q.S., Thomas, J.M., Neff, J.L., Vuong, H.Q., Russell, K.A., Hale, A.R., and Mueller, U.G. (2017). Flowers and wild megachilid bees share microbes. Microb. Ecol. 73, 188–200.
75. Rering, C.C., Beck, J.J., Hall, G.W., McCartney, M.M., and Vannette, R.L. (2018). Nectar-inhabiting microorganisms influence nectar volatile composition and attractiveness to a generalist pollinator. New Phytol. 220, 750–759.

76. Rebolleda Gómez, M., and Ashman, T.L. (2019). Floral organs act as environmental filters and interact with pollinators to structure the yellow monkeyflower (Mimulus guttatus) floral microbiome. Mol. Ecol. 28, 5155–5171.
77. Dharampal, P.S., Carlson, C., Currie, C.R., and Steffan, S.A. (2019). Pollen-borne microbes shape bee fitness. Proc. R. Soc. B Biol. Sci. 286.
78. Pérez-Gutiérrez, M.A., Suárez-Santiago, V.N., Fernández, M.C., Salinas Bonillo, M.J., and Romero-García, A.T. (2015). Pollen morphology and post-tetrad wall development in the subfamily Fumarioideae (Papaveraceae). Rev. Palaeobot. Palynol. 222, 33–47.
79. Pérez-Gutiérrez, M.A., Fernández, M.C., Salinas-Bonillo, M.J., Suárez-Santiago, V.N., Ben-Menni Schuler, S., and Romero-García, A.T. (2016). Comparative exine development from the post-tetrad stage in the early-divergent lineages of Ranunculales: the genera Euptelea and Pteridophyllum. J. Plant Res. 129, 1085–1096.
80. Punt, W., Hoen, P.P., Blackmore, S., Nilsson, S., and Le Thomas, A. (2007). Glossary of pollen and spore terminology. Rev. Palaeobot. Palynol. 143, 1–81.
81. Schindelin, J., Arganda-Carreras, I., Frise, E., Kaynig, V., Longair, M., Pietzsch, T., Preibisch, S., Rueden, C., Saalfeld, S., Schmid, B., et al. (2012). Fiji: An open-source platform for biological-image analysis. Nat. Methods 9, 676–682.
82. De Vos, K. (2017). Cell counter.
83. Dynamic Ventures Inc. (2021). CountThings.
84. Sogawa, K., Watanabe, M., Sato, K., Segawa, S., Ishii, C., Miyabe, A., Murata, S., Saito, T., and Nomura, F. (2011). Use of the MALDI BioTyper system with MALDI–TOF mass spectrometry for rapid identification of microorganisms. Anal. Bioanal. Chem. 400.
85. Seuylemezian, A., Aronson, H.S., Tan, J., Lin, M., Schubert, W., and Vaishampayan, P. (2018). Development of a custom MALDI-TOF MS database for species-level identification of bacterial isolates collected from spacecraft and associated surfaces. Front. Microbiol. 9, 780.
86. RStudio Team (2020). RStudio: Integrated Development for R. Rstudio PBC.
87. R Core Team (2020). R: a language and environment for statistical computing.
88. Ogle, D., Wheeler, P., and Dinno, A. (2020). FSA: Fisheries Stock Analysis.
89. Lenth, R. (2020). emmeans: Estimated Marginal Means, aka Least-Squares Means.

Chapter II:

Symbiotic bacteria and fungi proliferate in diapause and may enhance overwintering survival in a solitary bee[2]

[2] Chapter II was published in *The ISME Journal*, Volume 18, Issue 1, January 2024, wrae089, https://doi.org/10.1093/ismejo/wrae089

Authors: Shawn M. Christensen[1]; Sriram N. Srinivas[1]; Quinn S. McFrederick[2]; Bryan N. Danforth[3]; Stephen L. Buchmann[4]; Rachel L. Vannette[1]

Affiliations: 1- University of California Davis, Department of Entomology and Nematology; 2- University of California Riverside, Department of Entomology; 3- Cornell University, Department of Entomology; 4- The University of Arizona, Department of Ecology and Evolutionary Biology

Contributions: SMC, QSM, BND, SLB, and RLV contributed to selection of this bee and floral study system and sampling design, SMC performed lab work with contributions by SNS, SMC performed fieldwork with contributions from QSM, BND, SLB, and RLV, SMC performed bioinformatic and statistical analyses, SMC and RLV wrote the paper, and all authors contributed to revisions.

Abstract

Host-microbe interactions underlie the development and fitness of many macroorganisms, including bees. Whereas many social bees benefit from vertically transmitted gut bacteria, current data suggests that solitary bees, which comprise the vast majority of species diversity within bees, lack a highly specialized gut microbiome. Here we examine the composition and abundance of bacteria and fungi throughout the complete life cycle of the ground-nesting solitary bee *Anthophora bomboides standfordiana*. In contrast to expectations, immature bee stages maintain a distinct core microbiome consisting of Actinobacterial genera (*Streptomyces*, *Nocardiodes*) and the fungus *Moniliella spathulata*. Dormant (diapausing) larval bees hosted the most abundant and distinctive bacteria and fungi, attaining 33 and 52 times their initial copy number, respectively. We tested two adaptive hypotheses regarding microbial functions for diapausing bees. First, using isolated bacteria and fungi, we found that *Streptomyces* from brood cells inhibited the growth of multiple pathogenic filamentous fungi, suggesting a role in pathogen protection during overwintering, when bees face high pathogen pressure. Second, sugar alcohol composition changed in tandem with major changes in fungal abundance, suggesting links with bee cold tolerance or overwintering biology. We find that *Anthophora bomboides* hosts a conserved core microbiome that may provide key fitness advantages through larval development and diapause, which raises the question of how this microbiome is maintained and faithfully transmitted between generations. Our results suggest that focus on microbiomes of mature or active insect developmental stages may overlook stage-specific symbionts and microbial fitness contributions during host dormancy.

Introduction

The ecological and evolutionary success of a wide range of insect species has hinged on partnerships with microbes [1,2]. Bacterial and fungal metabolism can facilitate novel resource use for insect hosts use via synthesis of limiting nutrients [3], evasion or detoxification of diet defenses [4], digestion of recalcitrant substrates [5], or serve as food themselves [6]. Bacteria and fungi may also provide insect hosts

defense from predation [7,8], pathogens [9,10], or food spoilage [11] yet the insect host breadth and life cycle dynamics of such interactions remain poorly understood.

Most specialized bee-microbe interactions are described in adult corbiculate social bees [12–14]. Their microbiomes function in digestion of pollen, regulation of immunity, and suppression of pathogen growth [15–17]. The vast majority of bee species, however, are solitary; lacking cooperative brood care, foraging, and feeding [18]. Unlike social bees, solitary bee species studied to date generally have less specific and less consistent microbiomes [19,20].

A solitary bee spends up to 80% of its life developing inside a sealed brood cell [18]; during this time, the developing bee undergoes significant changes in metabolism and morphology- most profoundly during diapause and metamorphosis, respectively [21–24]. Brood cells are created and provisioned with pollen and nectar by the adult female: in some cases provisions can be dominated by lactobacilli, however these bacteria do not persist through development [25–27]. Annual life cycles, solitary nesting, complete metamorphosis, and lack of direct brood care are hypothesized to impede the development of a specialized core microbiome in solitary bees [13,23]- instead, they are thought to acquire and filter microbes from the environment anew each generation, excepting occasional endosymbiotic bacteria [28], resulting in variable microbial communities among individuals and populations.

Here, we characterize the composition, abundance, and potential functions of the bacterial and fungal microbiome of the solitary bee *Anthophora bomboides stanfordiana* Kirby, 1837 (Hymenoptera: Apidae) over 8 developmental stages, from two geographic sites, over two years using amplicon sequencing, qPCR, microbial isolations, and *in vitro* trials and assays. We describe a uniquely consistent core microbiome throughout brood development of this solitary bee species and test adaptive hypotheses regarding microbial effects on bee ecology and metabolism.

Study system

Anthophora bomboides stanfordiana (from here: *A. bomboides)* is a gregariously nesting solitary bee, inhabiting bluffs along the western coast of North America. *Anthophora bomboides* is a generalist

forager (polylectic), but at our sites, prefers nectar from radish (*Raphanus sativus*) and pollen from lupine (*Lupinus arboreus*) (Figure 2.1, other forage noted in Supplemental Methods). Adult nest in densely populated sites (nests within centimeters, not connected) containing tens to over a hundred thousand bees [29]. Nests are dug using fresh water from a nearby seep or creek to soften the hard dirt (Figure 2.1A) [30]. Once a brood cell is excavated, the inside is lined with a thick waxy secretion. This lining has a cheesy aroma and has been studied in closely related *Anthophora abrupta;* it is produced in the female's hypertrophied Dufour's gland and consists mostly of triglycerides which are converted to solid diglycerides during cell construction [31]. The lining is eaten by the larva as food just after the pollen provision is consumed, just before diapause as a prepupa (Fig 1A) and is thought to be highly specialized for consumption [31,32].

The brood provision is initially very liquid, containing ~630 µl of nectar (Figure 2.1) [30]. After hatching from the egg, larvae (1st-2nd instars) consume the nectar, then pollen (3rd-4th instars), and finally the cell lining; the white larva becomes yellow prepupa, defecates, and diapauses from fall through early spring (Figure 2.1). In early spring the prepupae exit diapause and pupate; adults emerge in late spring (Figure 2.1) [30]. Two nest sites on the California coast were sampled in this study: McClure's Beach (Point Reyes National Seashore, Marin County, CA, USA) and Bodega Head (Bodega Bay Marine Lab, Sonoma County, CA, USA). The sites are 9.8 miles apart and separated by a 5 mile open stretch of ocean. Both nesting sites have been active for at least four decades [30]. Because of the largely Mediterranean climate along the coast, the nesting period is warm and quite dry, but winters are wet and cool.

Methods

Sample collection and processing

Sites:

McClure's Beach (Point Reyes National Seashore, CA, USA) is the larger nesting site, with roughly 2000-3000 nests estimated in early June of 2021 which would indicate around 1000-1500 or more active females given females are likely to have started a second nest by that time [30]. It is located in a

WSW facing eroded bluff made of hard granitic sedimentary substrate (70% sand, 12.2% silt, 14.5% clay) and is ~150' from the ocean. The Bodega Head nesting aggregation (Bodega Head Reserve, CA, USA) is smaller, estimated 250-500 nests; 100-250 active females (June 2021) and located on gently sloping sides and tops of eroded ditches. The substrate is finer and darker (76.5% sand, 9% silt, 14.1% clay). The site is also on the Pacific Ocean, though higher than McClure's, ~50' above sea level. The two sites are 9.8 miles apart, as the crow flies, separated by a 5-mile stretch of open water (Bodega Bay). Soil makeup determined by Cornell Soil Health Lab.

Weather and Climate:

Because of the largely Mediterranean climate, the nesting period is warm and quite dry (10.2/ 22.2°C average low/high; ~1.5" rain total from May-Sept), but winter is wetter and cooler (5.0/15.7°C average low/high; ~18.7" rain total from Nov-Feb) and there are on average 7.3 days where it drops to or below freezing (Nov-Feb). Data from Bear Valley Visitor's center on Point Reyes via PRISM, averages for 2006-2015.

Collection:

Samples were collected from 2021-2023 at Point Reyes National Seashore (permit #: PORE-2020-SCI-0022) and Bodega Head (SCSP permit issued 2/24/2020). Adults were collected in June with a net while foraging or as they emerged from their nests in the early morning. To collect brood cell samples, small chunks of the cliff in the nesting area were separated using a soil knife and rock pick. These were then carefully dissected to separate brood cells, which are distinct and can be entirely removed from the surrounding soil matrix. Brood cells were then carefully opened from the top with sterilized tweezers or scoopulas (70% ethanol). Tweezers and/or scoopula were re-sterilized before being used to remove brood cell contents into sterile tubes and between brood cell samples. Egg-2nd instar stage brood cells have a high proportion of nectar in provisions; in some cases, a pipette was used to transfer these provisions. Upon collection, samples were rated for how 'clean' the extraction of provision was (eg. some had more dirt fall in, or a larva was punctured by the tweezers and soil then stuck to it, etc). The developmental stage, location, and date of collection were also recorded. Developmental stages are

described in Table 2.1. Tubes with collected samples were placed immediately into a cooler for transport back to the lab. Some were vortexed in a buffer (Phosphate Buffered Saline, PBS) and plated for bacterial and fungal isolation (Tryptic Soy Agar, TSA and Yeast Media, YM) or plated directly. The samples that were used for DNA extraction were moved directly from the cooler into a -80C freezer until sample processing.

Table 2.1

Stage	Approximate Phenology	Description, classification criteria	Samples (collected, bacteria, fungi **)	Image
Egg-2nd instar	Apr- Jul	Provision consists of majority nectar and is therefore very liquid. Egg or very small larvae may or may not have been found in the provision, and was not specifically separated or included. Egg through 2nd instar larvae.	N=13, 13, 8	
3rd-4th instar	May- Jul	Provision: nectar has been mostly consumed, leaving pollen of play-dough consistency.	N=11, 11, 11	
		Larvae: cream- colored and not yet full size, active and consuming provision. Larvae separated from provision for analysis. 3rd to 4th instar larvae.	N=10, 6, 7	
Summer Prepupae*	Jun-Aug	Prepupae: Have finished provision and consumed the cell lining. Color shifts to anywhere from pale yellow to bright orange at this stage. Defecation occurs, and prepupa enters diapause.	N=11, 8, 11	
October prepupae	Oct	Prepupae: In diapause, less turgid than late summer but otherwise appearance unchanged.	N=10, 6, 10	
December prepupae	Dec	Prepupae: In diapause, similar in size and appearance to prior two stages.	N=12, 12, 12	
Pupa	Mar- May	After diapause is broken, pupation occurs. No cocoon is spun. Collected pupae ranged in melanization from entirely pale yellow to near entirely melanized, extent was noted.	N=7, 6, 5	

Unemerged adult	Apr- May	Adults collected as they chewed out of their brood cells, or became active upon breaking open of brood cell. Hairs present, wings fully formed.	N=7, 7, 7	
Adult	Apr- Jul	Free-flying adult females collected while foraging or when leaving their nest after they were seen entering said nest. Adults were dissected, crops and guts were isolated for analysis	Guts: N=10, 1, 9 Crops: N=10, 1, 1	
* Bees remain prepupae from the time they consume the lining/defecate through diapause, thus the use of "Summer" to describe this initial prepupal stage. **First number corresponds to total samples collected and submitted for sequencing, second corresponds to number of samples which passed filtering after 16S rRNA gene sequence analysis (bacteria), and third corresponds to number of samples which passed filtering in ITS region sequence analysis (fungi).				

Flowers, water, and soil were also collected from each location to better understand the environmental microbes that the bees encounter (Table 2.2). *Anthophora bomboides* females use fresh water to soften the dirt that they nest in, and often do so in aggregate at a specific location on the spring's edge. This water was collected into sterile collection tubes from each site at the section that was actively in use by the aggregation at the time of collection. Flowers of each species were collected in June, when adults are foraging, and bulked upon collection into sterile tubes. Nesting substrate, here called "soil", was collected from within the aggregate nesting area at each site, from within 2" of the cliff surface, several inches from any nests, but within the nesting area. It was collected by chiseling away the exposed surface and then scraping underlying material into a collection tube with a sterile soil knife.

Table 2.2				
Type	Species	Description	Samples (collected, bacteria, fungi **)	
Flowers	Lupinus arboreus Sims	Yellow bush lupine: preferred pollen source One from each site, each sample containing 5-7 bulked flowers	N=2	N= 12, 11, 11
	Raphanus sativus L.	Wild radish: preferred nectar source Two from McClure's, one from Bodega site, each sample containing ~10-15 flowers	N=3	
	Eschscholzia californica Cham.	California poppy: pollen source McClure's, 2 bulked flowers	N=1	
	Carpobrotus edulis L.	Ice plant: nectar source Bodega, 1 flower	N=1	
	Cacklile maritima Scop.	Sea rocket: nectar source McClure's, 10 bulked flowers	N=1	
	Grindelia stricta DC.	Gum plant: nectar and/or pollen source McClure's, 3 bulked flowers	N=2	
	Erigeron glaucus Ker Gawl.	Seaside daisy: nectar and/or pollen source McClure's, 3 bulked flowers	N=2	
Soil	NA	Nesting material from the surrounding nest site, but not touching any nest, ~2" into nesting surface. (one per site*)	N=2, 0, 0	
Water	NA	Water from the site where adult females collect water for nest construction. Two from each site	N=4, 4, 4	
Blanks	NA	No sample added, to ensure sterility of extraction kit. Blanks were spaced out across rounds of extractions and used in DECONTAM.	N=4, 0, 0	

* Soil samples were collected from both sites, both failed to pass through the initial DADA2 pipeline due to very low reads, which was confirmed with qPCR (Figure 2.4), so a second, more relaxed DADA2 pipeline was run for the soil samples to determine general composition, see Figure S1.
**First number corresponds to total samples collected and submitted for sequencing, second corresponds to number of samples which passed filtering after 16S rRNA gene sequence analysis (bacteria), and third corresponds to number of samples which passed filtering in ITS region sequence analysis (fungi).

Sample pre-processing

For collected brood cell samples that had a visible larva and remaining pollen provision (3rd-4th instar), the larvae were separated from the provision and proceeded as two separate samples. Larvae and prepupae were all rinsed gently by pipetting in and removing sterile PBS (2x) before DNA extraction to

remove dirt that was introduced in the opening of the brood cells or clinging provision material. For all bee samples, the cleanest samples of each stage, as rated upon collection, were used. Free-flying adult females were dissected, separating the crop and gut as two separate samples per bee. Water samples were centrifuged at 13k for 3 minutes to concentrate the sample for DNA extraction. Top water was removed, and the remaining 100ul was used to resuspend the pelleted solids for extraction. Flower samples were immersed in PBS and vortexed at max speed for 60 seconds to dislodge microbes into the PBS, then whole flower material was removed, and the tubes were centrifuged at 13k for 3 minutes. Top PBS was removed, and the remaining 100ul was used to resuspend the pelleted solids.

Microbe isolation and identification

Brood cells, flowers, and water samples that were not used for DNA extraction were plated to isolate bacteria and fungi. These were plated either directly or after suspension in PBS onto both TSA +cycloheximide and YM+ chloramphenicol plates. Once colonies grew (1-5 days), representative colonies (based on morphology) were picked onto separate isolation plates of the same type and allowed to grow. Strains were then named based on isolation site (BH= Bodega Head, PR = Point Reyes (McClures); and saved as glycerol stocks in the -80. A subset of these were then identified via colony PCR (27F/1492R for bacteria, ITS1F/2 or NLR1/4 for fungi) followed by Sanger sequencing at the UC Davis DNA sequencing core, and NCBI BLAST.

DNA Extraction

All samples were added whole to DNA extraction, following preprocessing. Extraction for all samples was done per manufacturer's instructions with the DNeasy PowerSoil Pro kit. Four blanks were included in DNA extractions (Table 2.1). Extracted DNA was stored in the included extraction buffer at -80ºC for amplicon sequencing and qPCR.

Amplicon sequencing

Amplicon sequencing of extracted DNA was done to assess bacterial and fungal community composition using the 16S rRNA (V5/6) gene and ITS region at the Integrated Microbiome Resource

(IMR) at Dalhousie University in Halifax, Nova Scotia. Phusion Plus high-fidelity polymerase was used with fusion primers, which include the sequences below with Illumina adaptors + indices for multiplexing; sequencing was then performed on Illumina MiSeq [33,35]. Samples were de-multiplexed at IMR. For bacteria, primers 799F/1115R amplifying V5/V6 region of the 16S gene were used to limit mitochondria and chloroplast amplification (799F= 5'-AACMGGATTAGATACCCKG-3'/ 1115R= 5'-AGGGTTGCGCTCGTTG-3')[37]. These primers amplify a ~300bp length target sequence. For fungi, primers ITS1F/ITS2 were used (ITS1F= 5'-CTTGGTCATTTAGAGGAAGTAA-3'/ ITS2=5'-GCTGCGTTCTTCATCGATGC-3'). These primers amplify the variable length ITS1/2 region. Sequences were analyzed in R (4.1.1)[34] with primarily the DADA2 package (1.22.0) [36], phyloseq (1.38.0) [38], vegan (2.6.4)[39], microbiome (1.23.1)[40] and ggplot2 (3.4.2)[41]. See code for further details.

Bacteria:

Reads were filtered and trimmed with the following parameters (others were default): maximum expected error was set to 2 for forward reads and 5 for reverse reads (to account for lower quality of reverse reads), reads were truncated at 280 and 220, respectively, to discard bases with quality scores <~30). Primers were removed by trimming the respective primer length. Error rates, dereplication, denoising, merging, and chimera removal were done with default parameters; see supplemental code (Bacteria, code1) and data ('16S_track_reads'). ASVs were inferred via DADA2 (1.22.0) and then taxonomy was assigned using the Silva 138.1 N99 database for bacteria [42]. Mitochondria and chloroplast assigned reads were removed. Decontam package (1.14.0)[43] was used to identify and remove potential contaminants by comparing blanks to samples; 5 were found and removed at the threshold parameter of 0.5. Samples with less than 300 reads were then removed from further analysis, leaving N=86 samples; see supplemental code (Bacteria, code2). Samples lost (37) were: 4/4 blanks, 9/10 adult crop, 9/10 adult gut, 2/2 dirt (analyzed independently), 1/1 ice plant flower, 4/10 3rd-4th instar larvae, 3/11 Summer prepupae, 4/10 Oct. prepupae, 1/7 pupae.

Fungi:

Primers were removed using Cutadapt [47]. Reads were filtered and trimmed using default parameters, aside from the length minimum, which was set to 70 to remove extremely short reads. Error rates, dereplication, denoising, merging, and chimera removal were done with default parameters; see supplemental code (Fungi, code1) and data ('ITS_track_reads'). ASVs were inferred via DADA2 (1.22.0). We assigned fungal reads with the UNITE 9.0 general release dynamic database (29.11.2022)[49]. Non-fungal assigned reads were then removed, and Decontam package (1.14.0)[43] was used to remove potential contaminants by comparing blanks to samples; two were found and removed at threshold=0.5. Samples with fewer than 300 reads were then removed from further analysis, leaving N=93 samples. Samples lost (26) were: 4/4 blanks, 5/13 1st-2nd instar, 3/10 3rd-4th instar larvae, 1/1 dirt sample (analyzed independently, Figure S1), 9/10 adult crops, 1/10 adult guts, 1/1 gum flower, 2/7 pupae.

Community differences:

To evaluate the compositional differences in microbial communities based on occurrence inside or outside of the brood cell, as well as for stage specific community separation, amplicon sequence data was used to create separate Bray-Curtis (BC) dissimilarity matrices for both bacteria and fungi. These were ordinated with NMDS (Figure 2C,D). PERMANOVA was run based on BC distances to determine differences in community composition by sample type (in brood cell, out of brood cell, water, flowers) for both bacteria and fungi.

Relative abundance of Actinobacteria and *Moniliella* inside vs outside of brood cell:

Data was subset to ASVs assigned to the Actinobacterial class (or *Moniliella spathulata* species). Samples were grouped based on whether they occur inside or outside of the brood cell (egg through unemerged adult: in brood cell; adult, flower and water samples: outside of brood cell). The total relative abundance of Actinobacteria (or *Moniliella spathulata*) assigned ASVs were compared between the groups with the Base R 'stats' package (4.1.1) [34] 'kruskal.test' function.

Defining the core microbiome:

Detection of a core microbiome occurs using prevalence and abundance (detection) thresholds, and these can vary widely by study system, environment, and goals of the analysis [51,53]. Therefore, we used the 'microbiome' package "plot_core" function to visualize a wide range of prevalence (0 to 100%) and abundance (0.01% to 20%) thresholds for both bacteria and fungi in the style of a heatmap (Figure 2.3) for clarity, and to allow for nuance in interpretation of what may be considered core taxa.

Abundance of *Streptomyces* by stage:

Data was subset to ASVs assigned to the genus *Streptomyces*, and samples were grouped based on season, with egg- summer prepupa as 'summer', October and December prepupa as 'overwintering', and pupa- unemerged adults as 'spring'. Differences in relative abundance of *Streptomyces* of these groups was evaluated with the Base R 'stats' package (4.1.1) [34] 'kruskal.test' function followed by the 'FSA' package (0.9.4)[44] 'dunnTest' function with Bonferroni p-value correction [45]. To determine 'actual' abundance, we combined the qPCR data with the amplicon data by multiplying the total bacterial copy number by the proportion assigned to *Streptomyces* in each sample.

qPCR- Microbial copy number

Bacteria:

Bacterial copy number was quantified with standard DNA intercalating dye (SYBR) based qPCR. The same extracted samples that were sent for amplicon sequencing were run through this procedure. Identical primers (799F= 5'-AACMGGATTAGATACCCKG-3' /1115R= 5'-AGGGTTGCGCTCGTTG-3') were used so that compositional and quantification could be directly compared and merged. A 1:10 dilution of extracted DNA was determined after dilution testing was done with a representative subset of samples; 1:10 dilution gave in-range Cq values. Master mix, per reaction, was composed of 5ul SSO Advanced Universal SYBR Supermix (Catalog# 1725271), 0.3ul of each primer (10uM), 3.4ul Molecular grade water, and 1ul of extracted DNA (diluted 1:10 in Molecular grade water). Reactions were performed in triplicate for each sample, and arranged semi-randomly across plates to avoid possible

correlations of plate and developmental stage. Blanks and standards were included in each plate, and a Cq cutoff for blanks was established at 31.

To translate Cq values to copy number, we purchased a plasmid containing the relevant sequence from *Nocardiodes luteus (*ASV_5) from Eurofins at a known concentration. This was diluted in 10-fold steps; the dilution steps of 1.17E+6 through 0.117 molecules/ul, plus a blank, were used to create a standard curve, which had an R^2= 0.983. The equation of this line (see code) was used to convert Cq values to log (copy number) and edited to account for dilution.

Using amplicon data, we also adjusted the final qPCR copy number to remove the proportion of reads in each sample that had been assigned to mitochondria (no chloroplast reads were assigned). Flower and water samples had to be concentrated to ensure sufficient DNA for sequencing during pre-processing and thus bacteria in these samples could not be reliably quantified with qPCR.

Fungi:

Fungal copy number was quantified with probe-based (Taq-Man®) qPCR using a previously established system, FungiQuant [46]. Because the ITS region is highly variable in length, we did not use the same approach as above, as SYBR will intercalate throughout the length of an amplicon, potentially resulting in higher fluorescence readings for samples with a greater proportion of longer ITS amplicons. For these reasons, the fungal quantification was done with FungiQuant, using the 18S rRNA gene primers FungiQuant-F= 5′-GGRAAACTCACCAGGTCCAG-3′ and FungiQuant-R = 5′-GSWCTATCCCCAKCACGA-3′, along with the fluorescent probe FungiQuant-Prb = (6FAM) 5′-TGGTGCATGGCCGTT-3′ (MGBNFQ). As with bacteria, dilution testing of samples was done to bring Cq values into the optimal range, and a 1:20 dilution was picked. Master mix, per reaction, was composed of 5ul PCR Biosystems qPCRBIO Probe Mix (No-ROX) (Catalog# 17-512B), 0.3ul of each primer (10uM), 0.3ul fluorescent probe (10uM), 3.1ul molecular grade water, and 1ul of extracted DNA (diluted 1:20 in molecular grade water). Reactions were performed in triplicate for each sample and arranged

semi-randomly across plates to avoid possible correlations of plate and developmental stage. Blanks and standards were included in each plate.

To translate Cq values to copy number, we purchased a plasmid containing the relevant sequence from *Moniliella oedocephalis* on NCBI (#NG_062174) from Eurofins at a known concentration. This was diluted in 10-fold steps and the dilutions steps of 1.28E+6 through 0.128 molecules/ul, plus a blank, were used to create a standard curve, which had an R^2= 0.983. The equation of this line (see code) was used to convert Cq values to log(copy number), and edited to account for dilution. To evaluate differences in copy number between stages for both bacteria and fungi, we used the Base R 'stats' package (4.1.1) [34] 'kruskal.test' function followed by the 'FSA' package (0.9.4)[44] 'dunnTest' function with BH p-value correction [48].

Inhibition

Strains of *Streptomyces* were isolated by plating brood cell contents on Tryptic Soy Agar (TSA) with added cycloheximide. Colonies were picked by hand and replated on TSA until isolated, then glycerol stocks were created. *Streptomyces* isolates were identified to closest taxa based on Sanger sequencing of the 16S rRNA gene (primers 27F/1492R) using NCBI BLAST (Table 3) [50]. To ensure that the isolates were representative of the diversity of *Streptomyces* in the brood cells (Figure S7A), we aligned the 16S rRNA gene sequences from the isolates with the 300bp amplified region from our community ASV sequencing data using MUSCLE and found that the isolates likely represent two of the three most abundant *Streptomyces* ASVs (Figure S7B, C) [60]. Additionally, the 16S rRNA gene sequences were aligned with those of known *Streptomyces* from NCBI using MAFFT with default parameters (method= L-INS-i) and a phylogenetic tree was constructed using conserved sites (1386 sites, method= neighbor-joining, model= Jukes-Cantor, bootstrap resampling = 1000) (Figure S8) [62].

Thelonectria was isolated in much the same way, but from an infected *A. bomboides* pupa that had developed external filamentous fungal growth. *Moniliella spathulata* was isolated from a 1st instar *A. bomboides* provision (though it also occurred in nearly every plated brood cell sample, and all identified

to same BLAST ID). *Ascosphaera apis* and *Aspergillus flavus* were isolated from infected *Bombus impatiens* larvae previously in the Vannette lab. All fungal isolation occurred with Yeast Media Agar with added chloramphenicol. Identification was based on Sanger sequencing of the ITS or 18S rRNA D1/D2 region (primers ITS1F/ITS2 for *Thelonectria;* NL1/NL4 for *Ascosphaera apis*; ITS86F/ITS4 *Aspergillus flavus,* NL1/NL4 and ITS1/ITS4 for *Moniliella spathulata*) followed by NCBI BLAST [50] (Table 2.3).

Table 2.3

Strain	*BLAST ID*	*Isolation source*	*Accession numbers*
BH34	*Streptomyces endophyticus strain YIM65594*	1st instar *A. bomboides* provision	27F/1492R (PP576370)
BH55	*Streptomyces endophyticus strain YIM65594*	Egg stage *A. bomboides* provision	27F/1492R (PP576373)
BH97	*Streptomyces endophyticus strain YIM65594*	October *A. bomboides* prepupa	27F/1492R (PP576371)
BH104	*Streptomyces endophyticus strain YIM65594*	October *A. bomboides* prepupa	27F/1492R (PP576372)
FFP4	*Thelonectria sp.* strain OTU1563	*A. bomboides* pupa, infected	ITS1F/ITS2 (PP554508)
AA1	*Ascosphaera apis*	*Bombus impatiens* larva	NL1/NL4 (PP564911)
BAIF1	*Aspergillus flavus*	*Bombus impatiens* larva	ITS86F/ITS4 (PP554507)
BH004	*Moniliella spathulata*	1st instar *A. bomboides* provision	ITS1F/ITS2 (PP554509)
			NL1/NL4 (PP564910)

In order to ensure that both the bacteria and fungi could grow on the same media, for all inhibition trials we used TSA without any antimicrobials. For consistency, we used a template to mark the underside of all of the plates, it included in the very center a cross "+" then two parallel lines, 30mm long and each 20mm from the center point. These served as guides for inoculations. *Streptomyces* strains were inoculated with 1ul hoops from stock plates of the TSA without antifungals onto the 30mm parallel lines. Five replicate plates were made for each comparison (25 per trial, including 5 control plates). These were allowed to grow for 10 days, then, from stock plates of each fungus (also TSA, no antimicrobials), plugs

were inserted into the center "+" of each plate. Care was taken to ensure that plugs were all taken from just inside the leading edge of the fungal hyphae on the stock plates. These were allowed to grow for seven days. Measurements were taken on the backs of the plate and measured the distance from the leading edge of the growing fungi to the center "+", directly perpendicular to the parallel lines, on both sides. A tabletop light pad was used for imaging to qualitatively assess the density of the fungal hyphae, ensuring even back-lighting for the plates.

Radius measurements (two per plate, each side of the '+') were averaged for each replicate plate. Kruskal-Wallis was run with the Base R 'stats' (4.1.1) package 'kruskal.wallis' function as radius by inhibition treatment. This was followed with multiple comparisons with the 'FSA' package (0.9.4)[44] 'dunnTest' function, but as we were only interested in comparisons to the negative control, we then subset to those four comparisons. P value correction done with 'stats' package 'p.adjust' function using a Bonferroni correction [45].

Sugar and Sugar Alcohols

Samples of whole larvae, prepupae and pupae, as well as one pollen provision from a 4th instar larva were extracted for sugar and sugar alcohol analysis. Whole samples were placed in tubes with metal beads and 1mL of 100% ethanol and run on a bead beater for 8 minutes at full speed with 20s breaks every minute. These were then centrifuged for 30 seconds at 10k rcf. For each sample, the top 700ul of ethanol was moved to a new tube, 700ul 100% hexane was added, and then vortexed for 30 seconds. To this, 100ul MilliQ water was added, and vortexed for another 30 seconds. Once hexane had separated from the aqueous phase, it was removed (800ul). The remaining 1mL of aqueous phase was centrifuged for 2 minutes at 16k rcf, and the bottom 500ul was filtered through a 0.2 micron syringe filter and placed in a new tube in a lyophilizer for 6 hours, without heat. The dried samples were kept in a -20C freezer until analysis, at which time they were re-suspended in 300ul 1:1 water: acetonitrile. Standards of erythritol, sorbitol, fructose, glucose, sucrose, xylose and maltose were made at 0.5 mg/mL, standards of glycerol and trehalose were made at 5mg/mL and 1mg/mL respectively, all in 1:1 water: acetonitrile.

Separation of sugars was performed on Thermo UltiMate 3000 HPLC system according to the Waters Application Note: WA60110, except for the following: column was Phenomenex Luna Omega 3um SUGAR (50x2.1mm, Part#: 00B-4775-AN), and flow rate was 0.2mL/min; detection was by CAD (Corona Veo; Dionex). Each sample was run twice, standards were run 2-5 times. Analysis of peaks was performed with Thermo Fisher Chromeleon software. Peak identities were assigned based on retention times of standards, and unassigned peaks were then named by their retention times. Peak area was calculated by the software and this data was exported for analysis.

Analysis:

To identify differences in sample groups based on SSA profiles we used Principal Components Analysis (PCA) 'stats' package, Base R [34]. Data was first normalized by Hellinger transformation. The 'factoextra' package was used to plot PCA and biplot of components. After calculation of Bray-Curtis distance matrix, PERMANOVA ('vegan' package; [39] and pairwise PERMANOVA (package 'RVAideMemoire' 0.9.83) were used to determine differences in composition of SSA by sample group, p-value correction by FDR [48].

Results

Anthophora bomboides *brood cell microbial communities are distinct from the environment and dominated by Actinobacteria and* Moniliella spathulata *yeast*

For both bacteria and fungi, brood cell microbial composition was distinct from environmental sources and from adult gut samples (Figure 2C,D; S2, SI Methods Table 1). Actinobacteria were predominant during all stages of brood cell development in significantly higher relative abundance compared to samples from outside of the brood cell (K-W χ^2 = 37.6, df = 1, *P* value = 8.7e-10; Figure 2A). All sample groups contained Actinobacteria, but brood cell samples had 84.9% (n = 69, sd = 17.9) relative abundance, adult bee samples had 29.9% relative abundance (n = 2, sd = 12.7), and environmental samples had 18.8% relative abundance (n = 15, sd = 20.4).

To determine if Actinobacteria are specifically affiliated with *A. bomboides* we compared relative abundance of the Actinobacteria assigned ASVs (489 total) in brood cell and environmental samples (Figure S3). With a 0.1% detection threshold, 60% were found exclusively in the brood cell samples (294 ASVs), 17% were found in both brood cell and environmental samples (64 ASVs), and 25% were only detected in environmental samples (123 ASVs). Of the 64 ASVs shared between brood and environmental samples, 54% were found in only one environmental sample, mostly flower samples likely visited by foraging *A. bomboides* (*Raphanus sativus, Erigeron glaucus*). These 64 shared ASVs make up on average 9% of the reads in environmental samples (sd = 13.56). Six Actinobacteria ASVs are shared between the adult bee gut samples and the brood cells, comprising an average of only 1.6% of the reads within the brood cell samples (sd = 1.85).

Fungal communities within brood cells were dominated by *Moniliella spathulata* across all stages except the pupal stage (Figure 2B). *Moniliella spathulata* was detected in every brood cell where it comprised on average 72.3% of sequences (n = 71, sd = 29.6), significantly greater than in adult bees or environmental sources (Fig 2B, K-W χ^2 = 43.9, df = 1, *P* value = 3.3e-11). *M. spathulata* was detected in all but one adult GI tract sample, where its average relative abundance was only 10.9% (n = 10, sd = 16.1). Three environmental samples (*Raphanus sativus* bulked 15flowers, *Carpobrotus edulis* flower, water sample) contained *M. spathulata;* the mean relative abundance in all environmental samples was 0.7% (n = 12, sd = 1.57).

Anthophora bomboides *brood cells host a core microbiome composed of select Actinomycete genera and* Moniliella spathulata *yeast*

We next evaluated the presence and composition of a core microbiome in *A. bomboides* brood cells. Bacterial core was defined at the genus level for samples inside the brood cell, because the genera seemed to remain quite consistent despite diversity at the ASV level. At a prevalence of 65% and detection threshold of 0.1%, six genera (*Streptomyces, Arthrobacter, Nocardioides, Mycobacterium, Pseudarthrobacter,* and *Rhodococcus*) comprise a bacterial core. At the stricter prevalence cutoff of 90%, *Streptomyces* and *Nocardioides* remain core genera (Figure 2.3A). Regardless of the specific numerical

cutoff, the top eight genera that could constitute the core are all Actinobacteria (marked with * on Figure 2.3A).

The fungal core microbiome was defined at the ASV level for samples inside the brood cell. Two ASVs in particular, ASV_1 and ASV_2, both assigned to *Moniliella spathulata,* are present in 97% of samples at a detection threshold of 0.5% and in 88% of samples at a detection threshold of 5% (Figure 2.3B). ASV_6, also belonging to *Moniliellaceae*, could be considered core at lower thresholds, but no other ASVs approach inclusion in the fungal core within the brood cell (Figure 2.3B).

Microbial abundance peaks in during bee diapause

To quantify abundance of bacteria and fungi throughout the bee life cycle, we conducted qPCR using the same bee samples as above. Bacterial copy number increased through bee development (Figure 4; K-W χ^2= 66.7, df = 10, *P* value = 1.9e-10). Specifically, bacterial copy number increases through larval development, peaking during December, mid-diapause, and decreasing after pupation; bacterial copy number in December prepupae is 33 times higher than in egg-2nd instar (1.3e6, 3.7e4).

Fungal qPCR was conducted using FungiQuant [46]. Fungal copy number also changed through development (Figure 4, K-W χ^2 = 67.0, df = 10, *P* value = 1.6e-10) increasing by a factor of 52 between egg-2nd instar stage and summer prepupae (2.8e5, 1.5e7), coinciding with consumption of the brood cell lining and defecation. Fungal copy number remained high through December before dropping by a factor of 83 between December prepupal stage and pupal stage (4.3e6, 5.2e4). Soil samples from each site were included, both showed very low density of fungi and bacteria.

Stages within the brood cell have shifting bacterial and fungal communities, Streptomyces *dominates in overwintering stages*

We compared bacterial and fungal communities at different stages inside the brood cell to determine whether these communities shift at finer taxonomic scales and found that the community changed in consistent patterns through brood cell development (Figure 2.5, Appendix II- Figure S4). Microbial communities within the brood cell consistently contain a high proportion of Actinobacteria and

Moniliella spathulata, but the relative composition changed between stages after the summer prepupa stage (*P* value < 0.05, Figure 2.5A). Fungal community composition was overall consistent between stages, but was distinct in summer prepupae and pupae (Appendix II, Figure S5).

We further examined how the relative abundances of the top six bacterial core genera change with developmental stage. The most abundant genus, *Streptomyces*, peaks in abundance in overwintering prepupae, with average relative abundance of 48.5% (sd = 35.2, during October and December). *Streptomyces* relative abundance in the overwintering stages is significantly greater than summer (egg through summer prepupae, avg. 13.7% sd = 13.8, *P* value = 6e-4) and spring (pupae and unemerged adults, avg. 13%, sd = 16.1, *P* value= 0.003) stages by Dunn's test (Figure 2.5C).

Streptomyces *isolated from brood cells inhibits growth of filamentous fungi*

Fungal pathogens can thrive in the wet conditions of the overwintering period, which also coincided with peak abundance of *Streptomyces.* To test the hypothesis that brood-isolated *Streptomyces* inhibits growth of filamentous fungi, we used a plate-based co-inoculation assay. Representative *Streptomyces* isolates from *A. bomboides* brood cells (BH34, BH55, BH97, BH104; Figure S6, S7) were tested against *Ascosphaera apis*, a devastating pathogen of bee brood, as well as *Thelonectria*, which we isolated from an infected pupa of *A. bomboides. Streptomyces* isolates from the brood cells were able to inhibit both pathogens. Although *Streptomyces* strains varied in their fungal growth suppression, *A. apis* was significantly inhibited by both BH34 (*P* value < 0.05) and BH97 (*P* value < 0.05) and *Thelonectria* was significantly inhibited by BH34 (*P* value < 0.01) and BH55 (*P* value< 0.05) on day 7 of co-inoculation (Figure 6 A,B,E). As BH34 was able to inhibit both pathogenic fungi, we then tested whether it would also inhibit *Aspergillus flavus*- another generalist bee pathogen, or *Moniliella spathulata*- the core fungal taxa, using the same methods. We found that BH34 was also able to significantly inhibit the growth of both *Aspergillus flavus* (*P* value < 0.01, day 4) and brood cell isolated *Moniliella spathulata (P* value < 0.01, day 7; Figure 6C, D).

Sugar alcohol profiles distinguish developmental stages and coincide with changes in fungal abundance

The genus *Moniliella* is known for its industrial production of sugar alcohols and energy storing carbohydrates such as erythritol, glycerol, and trehalose [52,54]. In insects, trehalose is protective against environmental stress, such as temperature extremes, dehydration, oxidation, and starvation [55,56]. To determine if *A. bomboides* stages exhibit changes in sugar and sugar alcohol composition in development that may coincide with proliferation of fungi, of which the vast majority are *Moniliella*, we analyzed 4th instar larvae (before fungal proliferation), prepupae (highest fungal abundance), and pupae (when fungal abundance drops, and *Moniliella* is no longer dominant; see Figs. 2, 4) to determine their composition of sugar and sugar alcohols (SSA) via HPLC-CAD. We found that the stages with high fungal abundance (prepupal, diapausing stages) have distinct SSA composition as compared to 4th instar and pupal stages (*P* value < 0.01 by pairwise PERMANOVA; *P* values FDR corrected, Figure 7A). Specifically, glucose/sorbitol and fructose decline in relative abundance as bees develop from late-stage larvae to prepupae, while the disaccharide trehalose increases to high relative abundance in summer prepupae, coinciding with peak fungal abundance (*Moniliella*, Figure 2.4). Trehalose remains the SSA with the highest relative abundance throughout diapause (Figure 7B).

Discussion

Our study provides a detailed characterization and demonstration of the potential for complex interplay of insect development with microbiome composition and abundance. In contrast to previously studied solitary bee species, we identified a complex core microbiome in the brood cells of the solitary bee *Anthophora bomboides* which increases in abundance during diapause and persists through development; these findings are unique in several ways.

Stage specific vulnerabilities

We find that *A. bomboides* hosts a distinct core microbiome of Actinobacteria and *M. spathulata* which increases in abundance and shifts in composition during diapause. Diapause is a programmed metabolic depression that allows an organism to wait out seasonal environmental conditions, it occurs in

many organisms and is often a required stage before maturation [22]. Despite its importance for surviving these otherwise unsuitable conditions, insects are vulnerable to predation, freezing, drying out, and pathogen infection during diapause [7,57–59,61]. Although the microbiome is known to mitigate environmental stressor impacts on hosts [7,14,63,64], the roles of microbial symbionts during diapause are poorly studied [65,66]. Several studies show decreased microbial abundance and activity during diapause [67,68], but other studies suggest its importance. In dormancy, the bacterial communities of animals change in composition and abundance [69–71], can impact host gene expression [72], lipid accumulation, and survival [73], as well as provide pathogen suppression [9], and are hypothesized to contribute to nutrient recycling systems while host systems are suppressed [74,75].

The most common cause of brood mortality in *A. bomboides,* and solitary bees in general, is fungal infection during overwintering [59,76]. Though diapausing insects retain innate immunity [77], it may be reduced or altered during this time [78,79]. We found that bacteria in general, and *Streptomyces* specifically, attain the highest abundances during the winter months of diapause, with *Streptomyces* absolute abundance increasing by 46-fold between early provisions and December prepupae. This, combined with the demonstrated ability of brood-isolated *Streptomyces* to inhibit fungal pathogens of bees, suggests a defensive mutualism. *Streptomyces* are commonly found in soil, and many species and strains can produce antibiotics or antifungals, however, recent work has shown that insect-associated *Streptomyces* are more likely to inhibit pathogens than those found in soil, implying symbiont selection [80,81]. This is also supported by the many examples of other insect-*Streptomyces* defensive mutualisms [82–85]. Alternatively, lowered bee immune defenses may allow *Streptomyces* to proliferate, or *Streptomyces* may be responding to season independently of the host, thus further experiments are required to demonstrate the hypothesized mutualism. However, other bee species tend to exhibit low or undetectable microbial populations following defecation and in diapause, suggesting distinct biology in *A. bomboides* that supports symbiont growth.

Overwintering can lead to more subtle effects on survival via indirect chill injuries, which lead to a gradual failure to maintain homeostasis [22] and increased oxidative stress [86]. Many insects use antifreeze compounds, such as trehalose and glycerol, to reduce ice crystal formation and stabilize proteins [22]. *Moniliella,* the ubiquitous yeast found with developing *A. bomboides*, are best known for their prolific production of sugar alcohols and trehalose [87]. By comparing pre-, during, and post- diapausing stages, we found that shifts in sugar alcohol composition corresponded to shifts in fungal abundance, with high levels of trehalose co-occurring with peak fungal abundance during diapause. Although insects are also capable of producing sugar alcohols and trehalose [88], and xerophilic yeasts may produce sugar alcohols to enhance their own survival in habitats with low water activity [89], other insect studies have shown microbiome correlation with [63], and direct contribution to, cold tolerance [72]. The temporal linkage of *M. spathulata* abundance and trehalose production suggests that symbionts could be involved in the production of compounds suporting host cold tolerance. As *Moniliella spathulata* is also known to be oleaginous and able to accumulate lipids up to > 60% of its dry weight, a role in lipid metabolism is also possible [90,91]. Energy (lipid) storage for diapause can be reliant on microbial presence; recent work in mosquitos showed that depleting microbial communities in pre-diapausing females prevents lipid accumulation, which rapidly and significantly lowers survival during diapause [73]. Broadly, it is possible that the developing bees are outsourcing some aspects of metabolism to their associated microbes while their own metabolism is suppressed during diapause [22]. These, as well as additional adaptive and nonadaptive hypotheses will require further investigation.

Transmission and acquisition

Previous work on solitary bee microbiomes indicates that shared flowers are the major mode of microbiome acquisition, resulting in variable microbial communities within species and between individuals with some exceptions of extreme filtering of environmental microbes resulting in dominance of lactic acid bacteria [20,26,27,92–94]. In *A. bomboides,* however, brood microbiomes are distinct from the environmental samples, and patterns resemble vertical transmission, but this is not confirmed. Minimal

bacterial ASV sharing between brood cells and flowers supports a distinct acquisition mode from that of other solitary bees (Figure S3). Vertical transmission is especially likely for the fungal symbiont, *Moniliella spathulata*, as nearly every brood cell from both sampled sites, even at the earliest stage (Figure 2.2) contained the same two ASVs, indicating tight and effective control of transmission.

Though not generally found in flowers, Actinobacteria commonly inhabit soil environments. Our soil samples, however, were removed from the main sequencing dataset due to very low read count (but see Figure S1), which was confirmed with qPCR (Figure 2.4). We suspect that the low microbial densities may be due to high salt content (ocean spray) [95] and substrate composition, which is more akin to decomposing granite (~ 73% sand), without visible roots or other organic material (see Supplemental Methods for composition). It is possible that with more extensive substrate sampling a link between soil and brood cell compositions could be found.

The core brood cell microbial composition was not consistent with adult GI tracts; ten guts and ten crops were sequenced- only one of each had enough bacterial reads to pass filtering, and low bacterial density was confirmed by qPCR (Figure 2.4). Fungal communities in the crop also had low density, whereas gut fungi were more abundant and more closely resembled environmental communities, not brood cells (Figure 2.2). This suggests a non-GI method of transmission; for example, in another solitary hymenopteran, the beewolf (*Philanthus*), transfers its core brood associate (*Streptomyces*) to newly provisioned cells using specialized glands in the antennae [9]. Our results suggest a vertical mode of microbiome transmission in *A. bomboides,* but this hypothesis, along with the methods by which they maintain or select for this unique microbial composition, will require further study.

Comparison to other insect microbiomes

The bacterial taxa that associate with *Anthophora bomboides* have not been previously described as core associates of bees (Anthophila) (but see [96,97]). The actinomycete genera *Streptomyces* and *Nocardioides* were present in over 90% of samples and *Moniliella spathulata* was found in nearly every cell as the dominant fungus. Other solitary species with specific bacterial associates commonly host

environmentally acquired lactobacilli, or other floral and environmental microbes [20,26,92–94], whereas the social bee gut microbiome consists of a distinct set of genera not overlapping with the *A. bomboides* core [12,13,98]. A different *Moniliella* species (*M. megachilensis*) and *Streptomyces* have been isolated from brood of solitary *Megachile* bees [96,99], which, like *A. bomboides,* are known to have hypertrophied triglyceride-producing Dufour's glands [100,101]. Though these taxa are rare in bees, they are in some ways comparable to the widely studied microbial associates of fungus farming ants. Ant workers host actinomycetes (*Pseudonocardia, Streptomyces*) to protect the monoculture of cultivated fungus [102–104]. However, the data presented here show that although *Streptomyces* isolated from *A. bomboides* brood cells suppresses the growth of pathogenic fungi, they also suppress the growth of *Moniliella spathulata*, the core fungal taxa (Figure 6D). This observation suggests that microbial communities may exhibit temporal or small-scale physical niche partitioning between *Streptomyces* and *M. spathulata* that allows both to persist, or that conditions used in the plate assay result in different dynamics compared to the brood cell; this remains to be tested.

Why Anthophora?

To date, *A. bomboides* is the only solitary bee which is now documented to associate with a complex and consistent core microbiome in the brood cell. What traits may support this specialized association? We hypothesize that the brood cell lining from the hypertrophied adult Dufour's gland may be involved in maintaining this association. Some species within the genus *Anthophora* are unique in that their Dufour's gland secretion has evolved from a thin waterproof cell lining to a thick, energy dense food source for developing brood [32]. This triglyceride rich lining has been noted as being highly specialized, similar to royal jelly in honey bees or milk in mammals [31]. Adult females produce copious amounts of this secretion, using it to both line the cell and mix into the provision itself [31]. *M. spathulata* is lipophilic and can degrade a wide range of over 150 hydrocarbons, perhaps the larvae's consumption of the lipid lining just prior to diapause facilitates yeast proliferation in this stage [91]. Some Dufour's secretions also

have antibiotic properties, which, if present here, may also exhibit selective pressure in shaping the microbiome [105].

Conclusions

We provide direct evidence of a consistent and abundant microbial community in developing *Anthophora bomboides* solitary bees and antifungal activity of the abundant *Streptomyces,* which suggests a defensive symbiosis. Solitary bees are vulnerable to multiple sources of mortality during development, especially during overwintering. Increasing microbial titer during diapause, consistent composition across brood cells, and microbial phenotypes with clear links to bee life history suggest, but do not yet demonstrate, a mutualistic symbiosis. Specifically, two ASVs of the yeast *Moniliella spathulata* were consistently found at both sampled sites and all developmental stages, with dramatic changes in density corresponding to significant shifts in sugar alcohol composition during overwintering, pointing to a role in cold-tolerance. *Streptomyces* was found to be a potential defensive symbiont, inhibiting a variety of brood-pathogenic fungi, and dominating specifically the overwintering stages. These results highlight a few underappreciated aspects of insect-microbe symbiosis: 1) a complex and consistent microbiome can be maintained in the absence of sociality, 2) bacteria and fungi may affect bee biology during diapause, and 3) the mycobiome may be important and likely deserves additional study. Although much work remains to examine the ecology of this bee-microbiome symbiosis, our study reframes the conditions thought to maintain symbiosis and highlights novel research areas in exploring unique roles of the microbiome during host dormancy.

Data Availability:

All data and code is publicly available through Dryad Data repository at: [doi.org/10.5061/dryad.gtht76ht1]. Sanger sequences of isolates are available on GenBank, details in SI Methods Table 3, accession numbers (PP576370-PP576373; PP554507-PP554509; PP564910-PP564911).

Acknowledgments:

We would like to thank Point Reyes National Seashore, UC Berkeley Point Reyes Field Station, Bodega Head State Marine Reserve, UC Davis Bodega Head Field Station and associated staff for facilitating this research. We thank the Bohart Museum of Entomology, especially Lynn Kimsey, for assistance with bee identification. We appreciate the work of the Dalhousie Integrated Microbiome Resource, especially André Comeau. We also thank Abigail Ray, Danielle Rutkowski, Alexia Martin, Dino Sbardellati, Leta Landucci, Jacob Francis, Jacob Cecala, Amber Crowly-Gall, and Michael Orr for their ideas and assistance.

Figures

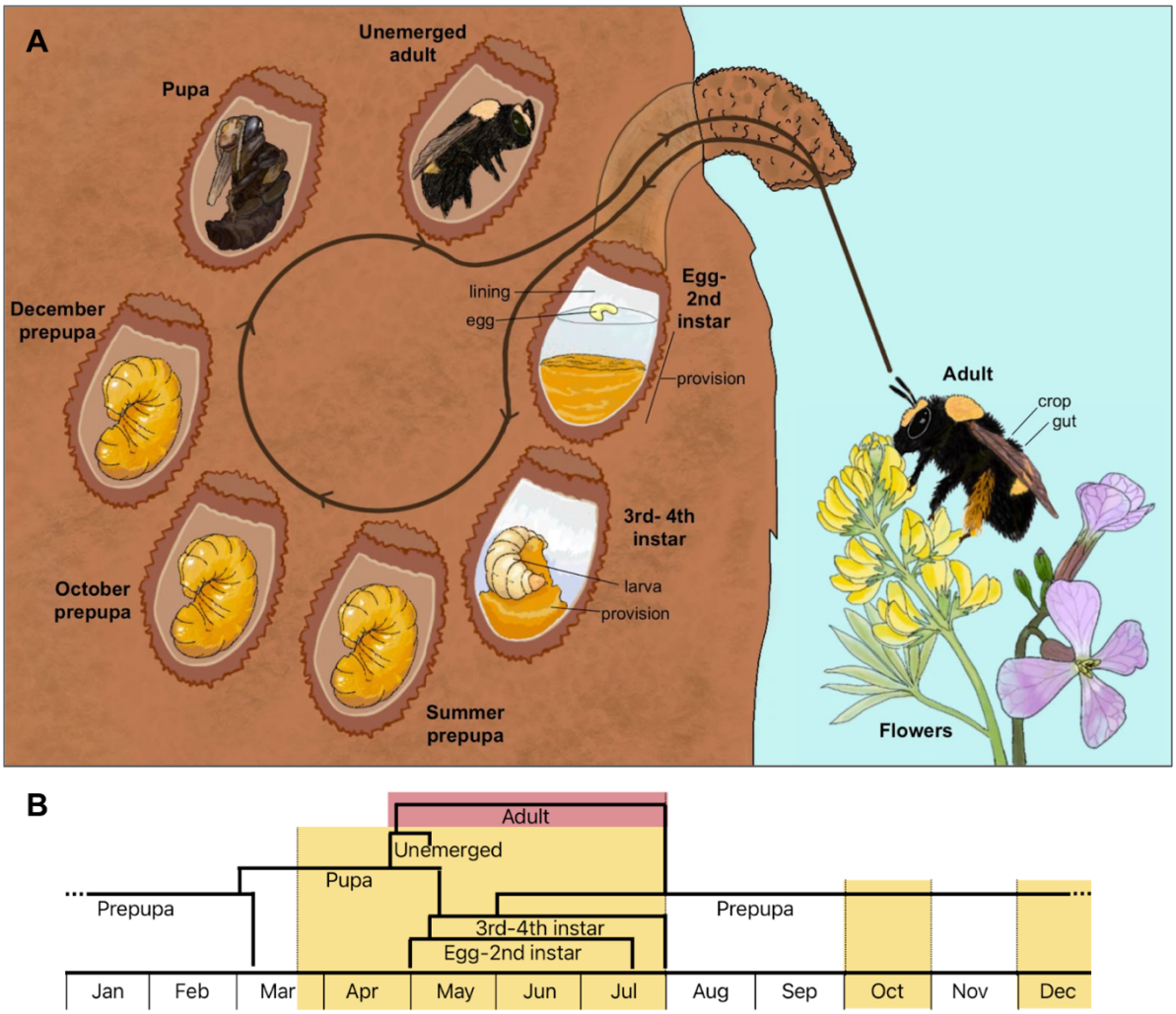

Figure 2.1 - Life cycle of *Anthophora bomboides* indicating sampled stages. (A) Full circle represents one year, with labeled brood cells illustrating stages that were sampled. The egg-2nd instar stage includes pollen provisions that contained liquid nectar, only provision was sampled. The 3rd-4th instar stage contained pollen but no nectar and was separated into larva and provision samples, summer prepupae (collected pre-August) had recently eaten the cell lining, defecated, and turned yellow-orange. Overwintering prepupae collected in October and December are categorized as such. Pupal and unemerged adult stages were collected in spring; the latter were distinguished by complete development of hairs. Active foraging adults were collected and dissected for crop and gut samples. Stages are listed stepwise as they occur for one bee. Black text and lines indicate which parts of the stage were used for further analysis, excepting "lining" and "egg" which are labeled for illustrative purposes. Absence of lines indicate that the whole bee was used as the sample for that stage. **(B)** At the population level, some stages overlap in time. Highlighted sections indicate months when sampling occurred. Yellow indicated that sampled stages occur within the brood cell, red indicates that sampled stage occurs outside of the brood cell. Illustration by S. Christensen.

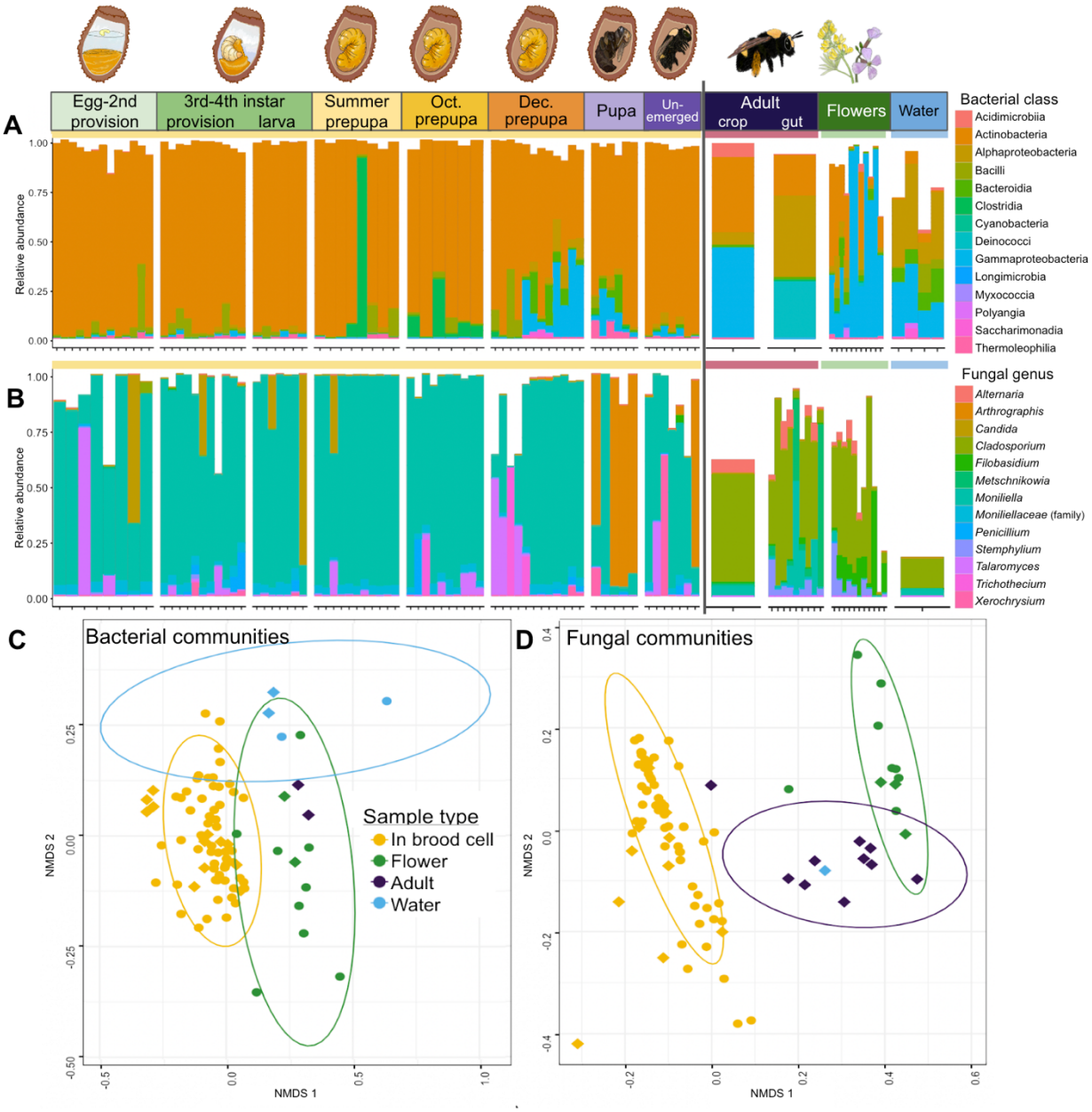

Figure 2.2 - *Anthophora bomboides* brood cell samples are dominated by Actinobacteria and *Moniliella*, differing significantly from adults and environment.

(A-B) Stages arranged in order of development, followed by environmental samples (flowers and water). Dirt samples yielded no sequences after QC and filtering, see Figure S1. Yellow horizontal bar indicates stages/samples which occur within the brood cell, red indicates adults collected outside of the brood cell, green indicates flower samples, and blue indicates water samples where adult bees collect water for nest construction. Each vertical column represents one sample, fill corresponds to proportion of sample reads belonging to each taxa (colors in key). Black vertical line separates inside (left) versus outside (right) of the brood cell. The same samples were sequenced for both bacteria and fungi, but discrepancies occur when a sample was filtered out due to low read count in one sequencing run but not the other, such as the adult gut sequencing well for fungi and poorly for bacteria. **(A)** Top

500 bacterial ASVs, colored by class, via sequencing of V5/V6 region of 16S rRNA gene. Actinobacteria (orange) dominate within the brood cell. Kruskal-Wallis χ^2= 37.6, df = 1, *P* value = 8.7e-10 comparing relative abundance of Actinobacteria from inside brood cell samples (mean 84.9%; yellow horizontal bar; left of vertical black line) to outside brood cell samples (mean 20.1%; red, green, blue bars; right of line). n = 86 samples. **(B)** Top 15 fungal ASVs, via sequenicing of ITS region, colored by genus. *Moniliella* (light blue) dominate within the brood cell. Kruskal-Wallis χ^2 = 43.9, df = 1, *P* value = 3.3e-11 comparing relative abundance of *Moniliella spathulata* from inside brood cell samples (mean 72.3%; yellow bar; left of line) to outside brood cell samples (mean 5.4%; red, green, blue bars; right of line). n = 93 samples. **(C-D)** For both plots, color indicates sample type, shape indicates sample site. Yellow corresponds to samples from inside the brood cell, green corresponds to flower samples, purple to adults that were free-flying outside of the brood cell, and blue to water samples. Circles were sampled from McClure's Beach site, diamonds from Bodega Head site. **(C)** NMDS of weighted Bray-Curtis (BC) distance for bacterial communities (stress = 0.19). PERMANOVA with sample type as a predictor R^2 = 0.07, *F* = 2.2, *P* value < 0.001. **(D)** NMDS of weighted Bray-Curtis distance for fungal communities (stress = 0.1). PERMANOVA with sample type as a predictor R^2 = 0.25, *F* = 10.12, *P* value < 0.001.

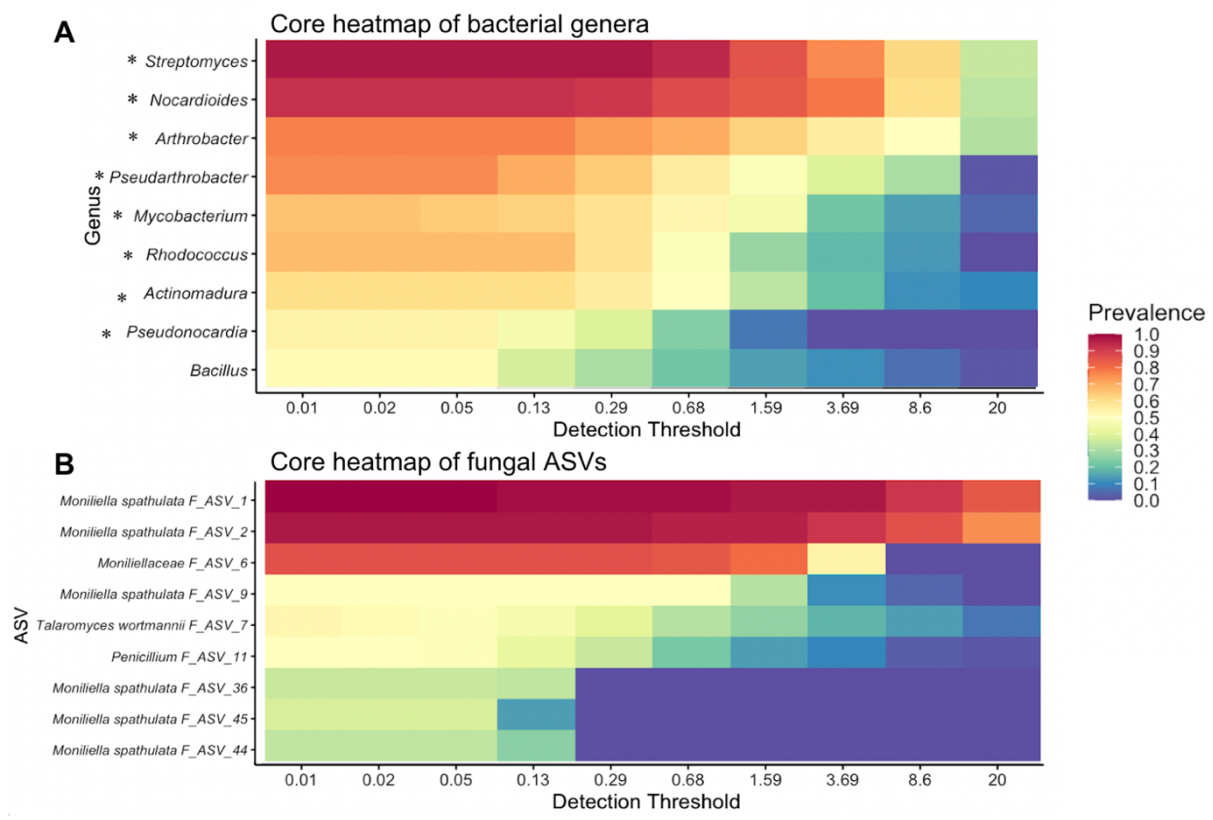

Figure 2.3 - *Anthophora bomboides* brood cells host a core microbiome composed of Actinomycetes and *Moniliella*. Core microbiome heat maps for bacterial genera (A) and fungal ASVs (B), indicating prevalence at increasing detection thresholds. Prevalence is the proportion of samples containing the indicated taxa, detection threshold is the minimum relative abundance that needs to be present in a sample for it to be counted. Together, these separate core taxa (high prevalence and abundance) from other taxa. Top taxa arranged in decreasing order down the y axis, prevalence for each taxa is indicated by color, with 1 (dark red) meaning that the taxa is present in all samples, and 0 (dark blue) indicating it is present in none of the samples at each detection threshold (x axis, % of reads). **(A)** All bacterial genera with an asterisk (*) belong to Actinobacterial class. **(B)** Fungal ASVs labeled at the most specific assigned taxonomic level, see Appendix II, Figure S5 for relative abundance of fungal ASVs 1&2.

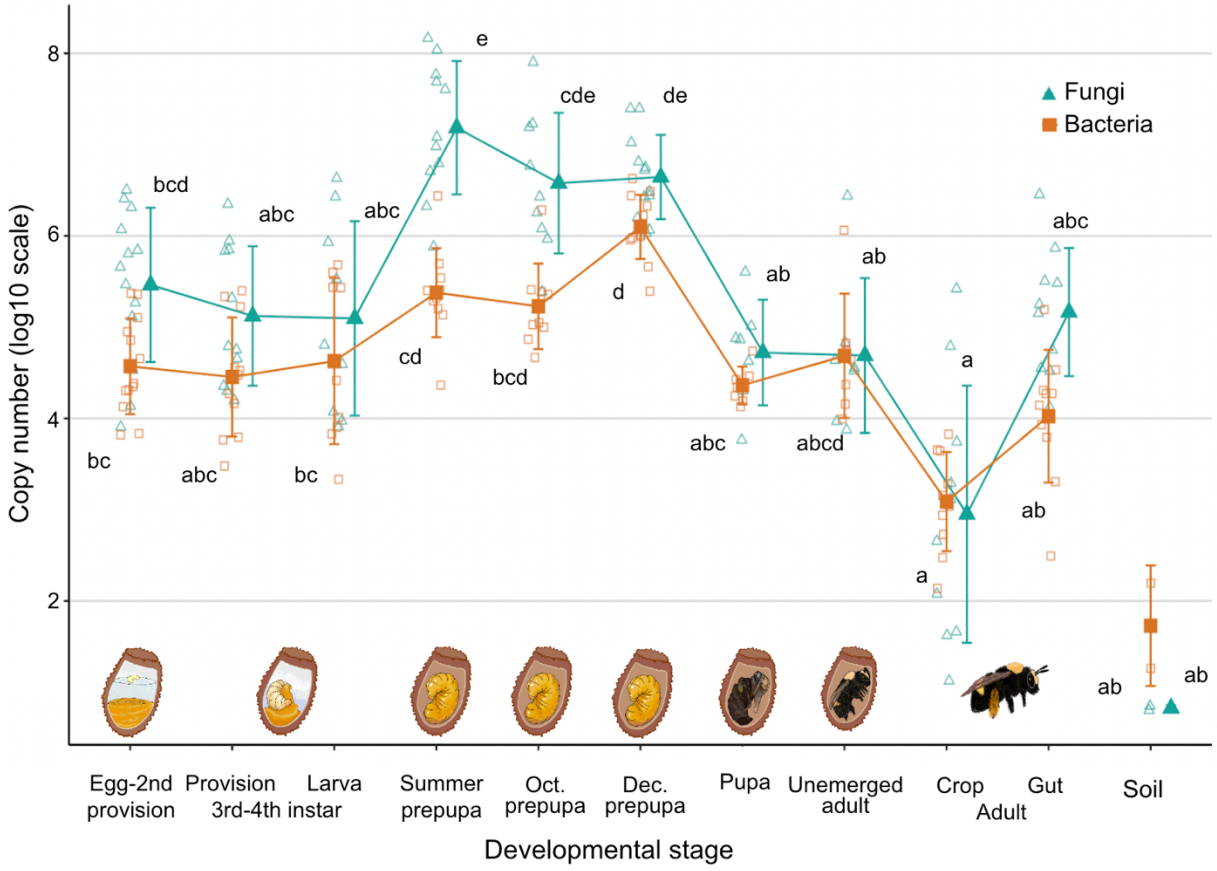

Figure 2.4 - *Anthophora bomboides* microbial copy number is highest in diapausing prepupae. Filled points represent the mean of the log10(copy number) by developmental stage, error bars +/-1 SD log(copy number) of each developmental stage for both bacteria (orange squares) and fungi (teal triangles). Smaller open points represent individual samples. Bacterial copy number has been adjusted to remove non-bacterial reads, as determined by amplicon sequencing with identical primers. Kruskal-Wallis test indicates significant differences in bacterial and fungal copy number based on bee developmental stage, (Bacteria- K-W χ^2= 66.7, df = 10, *P* value = 1.9e-10; Fungi- K-W χ^2 = 67.0, df = 10, *P* value = 1.6e-10). Lettering indicates differences via Dunn's multiple comparisons; above for fungi and below for bacteria (*P value* < 0.01).

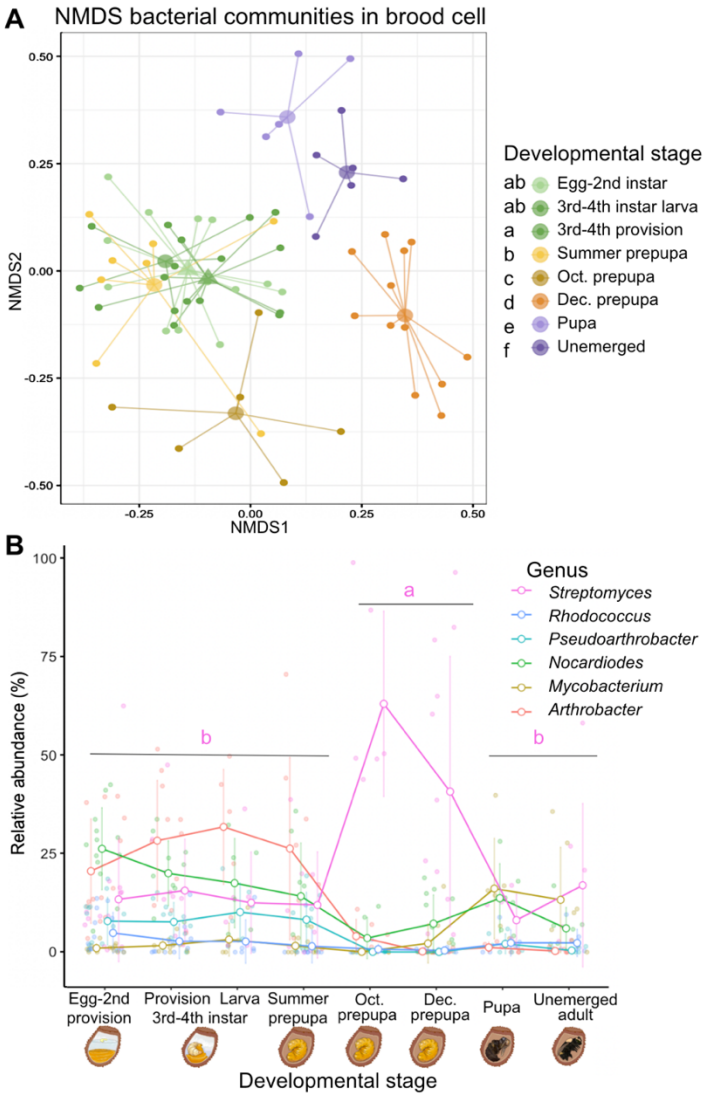

Figure 2.5 - Bacterial communities shift with bee development, with increased *Streptomyces* abundance in overwintering stages. (A) NMDS of bacterial community Bray-Curtis distance with color indicating stage of brood cell development. Larger semi-transparent dots indicate centroids, with lines from centroid to each point in the group. Triangular centroids indicate provision samples. Global PERMANOVA shows significant difference between stages ($R^2 = 0.25$, $F = 2.87$, P value < 0.001). Pairwise PERMANOVA of stages (FDR < 0.05) indicated with lettering on left side of figure key. **(B)** Relative abundance (% of total) of top six bacterial genera across bee developmental stages. Larger open circles represent mean relative abundance of the genus at the indicated developmental stage and are connected by lines. Error bars are (+/- 1 SD). Each smaller shaded point represents the relative abundance of the corresponding genus in one sample. *Streptomyces* relative abundance varies through development (Kruskal-Wallis $\chi^2 = 15.9$, df = 2, P value = 0.0003) and is highest during overwintering (Oct.-Dec.) as compared to summer (egg-summer prepupa; Dunn's test adj. P value < 0.001), or spring stages (pupa-unemerged adult; Dunn's test adj. P value < 0.01).

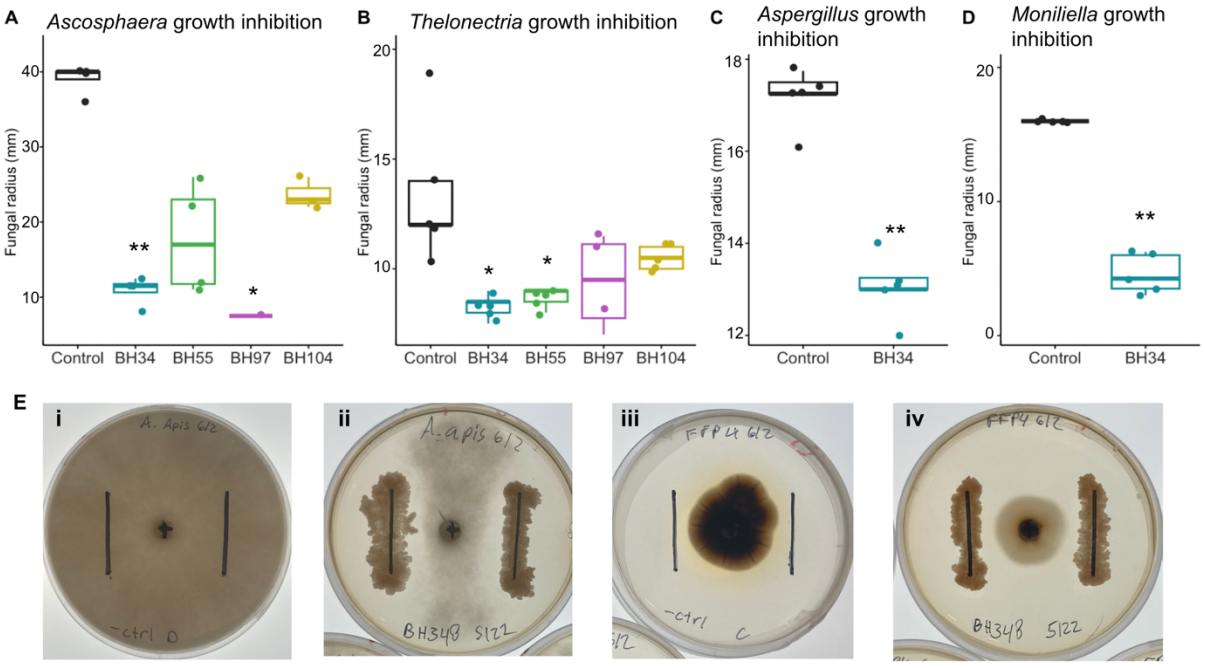

Figure 2.6 - *Streptomyces* isolated from *A. bomboides* brood cells inhibit growth of filamentous fungi. Inhibition is shown by decrease in radius of fungi (mm, y axis) on plates when co-inoculated with isolates of *Streptomyces* (BH104, BH34, BH55, BH97) (x axis, colors) from brood cells as compared to negative control (black). *Streptomyces* isolates plated 10 days prior to inoculation with 6mm diameter fungal plug. Comparisons to control by Dunn test, *P* values adjusted with Bonferroni (*P* value < 0.05 = *, *P* value < 0.01= **). (**A-D**) Center lines correspond to the median, boxes define interquartile range (IQR), and whiskers extend + 1.5 IQR. Note difference in scale of y axes. **(A)** Inhibition of *Ascosphaera apis,* a common pathogen of bee brood, on day 7 of co-inoculation. Data represents 16 plates. BH34 and BH97 significantly reduced the radius of *A. apis.* Note 40 mm radius was the edge of the plate. Kruskal-Wallis $\chi^2 = 12.3$, df = 4, *P* value = 0.014. **(B)** Inhibition of *Thelonectria,* a potential pathogen isolated from an infected pupal cell, on day 7 of co-inoculation. Data represents 24 plates. BH34 and BH55 significantly reduced the radius of *Thelonectria*. Kruskal-Wallis $\chi^2 = 14.5$, df = 4, *P* value = 0.005. **(C)** Inhibition of *Aspergillus flavus*, generalist bee pathogen, by BH34 on day 4 of co-inoculation. Data represents 10 plates. Kruskal-Wallis $\chi^2 = 6.9$, df = 1, *P* value = 0.009. **(D)** Inhibition of *Moniliella spathulata*, ubiquitous brood cell yeast, by BH34 on day 7 of co-inoculation. Data represents 10 plates. BH34 significantly reduced the radius of *Moniliella spathulata.* Kruskal-Wallis $\chi^2 = 7.3$, df = 1, *P* value = 0.007. **I** Plate images of fungi on day 7 of growth, when grown alone and with *Streptomyces* isolate BH034 showing decreased radius and qualitatively reduced hyphal density. i) *A. apis* negative control, ii) *A. apis* with *Streptomyces* isolate BH034, iii) *Thelonectria* negative control, iv) *Thelonectria* with *Streptomyces* isolate BH034. Images were taken on backlit LED screen to ensure identical lighting.

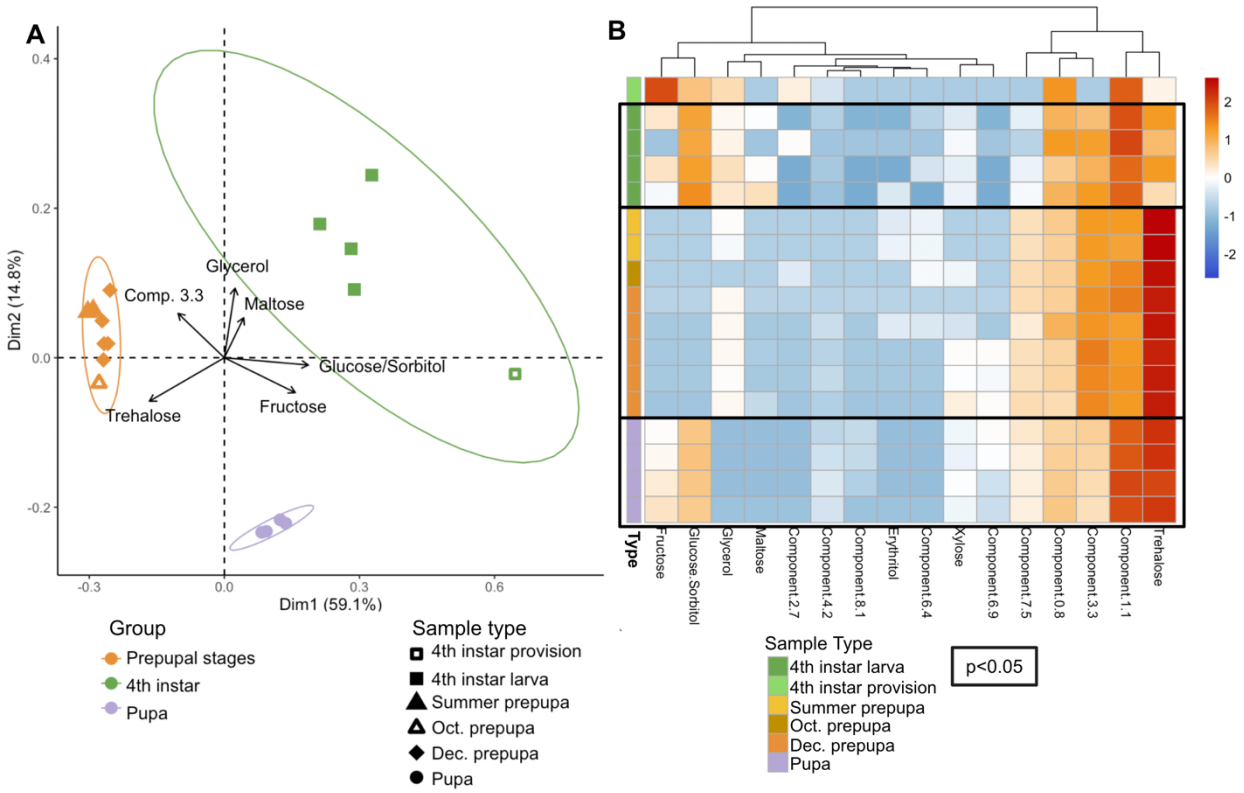

Figure–2.7 - Sugar and sugar alcohol composition differentiates bee developmental stages. (A) Sugar and sugar alcohol (SSA) composition of late larvae through pupal stages mapped by PCA, colored by stage. Ellipses indicate 95% confidence for sample groups. Axes labeled with % variance explained. Biplot of the 6 most influential SSA components; longer arrows indicate greater influence on sample separation, direction indicates the alignment with the mapped PCs. Glucose and sorbitol had overlapping and thus indistinguishable peaks. **(B)** Composition of individual SSAs (columns) of each sample (rows). Samples grouped and colored by stage in the first column. SSA data was Hellinger transformed and scaled to sample (relative abundances) with red indicating high relative abundance of that component (column) for that sample (row) and blue indicating low relative abundance within the sample. Black boxes indicate significant clustering of sample compositions *(P* value < 0.05) via hierarchical clustering (multiscale bootstrap resampling).

References

1. Moran, N.A. (2007). Symbiosis as an adaptive process and source of phenotypic complexity. Proc. Natl. Acad. Sci. 104, 8627–8633. https://doi.org/10.1073/pnas.0611659104.
2. Cornwallis, C.K., van 't Padje, A., Ellers, J., Klein, M., Jackson, R., Kiers, E.T., West, S.A., and Henry, L.M. (2023). Symbioses shape feeding niches and diversification across insects. Nat. Ecol. Evol. 7, 1022–1044. https://doi.org/10.1038/s41559-023-02058-0.
3. Reis, F., Kirsch, R., Pauchet, Y., Bauer, E., Bilz, L.C., Fukumori, K., Fukatsu, T., Kölsch, G., and Kaltenpoth, M. (2020). Bacterial symbionts support larval sap feeding and adult folivory in (semi-)aquatic reed beetles. Nat. Commun. 11, 2964. https://doi.org/10.1038/s41467-020-16687-7.
4. Chung, S.H., Rosa, C., Scully, E.D., Peiffer, M., Tooker, J.F., Hoover, K., Luthe, D.S., and Felton, G.W. (2013). Herbivore exploits orally secreted bacteria to suppress plant defenses. Proc. Natl. Acad. Sci. 110, 15728–15733. https://doi.org/10.1073/pnas.1308867110.
5. Arora, J., Kinjo, Y., Šobotník, J., Buček, A., Clitheroe, C., Stiblik, P., Roisin, Y., Žifčáková, L., Park, Y.C., Kim, K.Y., et al. (2022). The functional evolution of termite gut microbiota. Microbiome 10, 78. https://doi.org/10.1186/s40168-022-01258-3.
6. Chapela, I., Rehner, S., Schultz, T., and Mueller, U. (1995). Evolutionary history of the symbiosis between fungus-growing ants and their fungi. Science 266, 1691–1694. https://doi.org/10.1126/science.266.5191.1691.
7. Berasategui, A., Breitenbach, N., García-Lozano, M., Pons, I., Sailer, B., Lanz, C., Rodríguez, V., Hipp, K., Ziemert, N., Windsor, D., et al. (2022). The leaf beetle Chelymorpha alternans propagates a plant pathogen in exchange for pupal protection. Curr. Biol. 32, 4114-4127.e6. https://doi.org/10.1016/j.cub.2022.07.065.
8. Oliver, K.M., Smith, A.H., and Russell, J.A. (2014). Defensive symbiosis in the real world – advancing ecological studies of heritable, protective bacteria in aphids and beyond. Funct. Ecol. 28, 341–355. https://doi.org/10.1111/1365-2435.12133.
9. Kaltenpoth, M., Göttler, W., Herzner, G., and Strohm, E. (2005). Symbiotic bacteria protect wasp larvae from fungal infestation. Curr. Biol. 15, 475–479. https://doi.org/10.1016/j.cub.2004.12.084.
10. Van Arnam, E.B., Currie, S.R., and Clardy, J. (2018). Defense contracts: molecular protection in insect-microbe symbioses. Chem. Soc. Rev. 47, 1638–1651. https://doi.org/10.1039/C7CS00340D.
11. Shukla, S.P., Plata, C., Reichelt, M., Steiger, S., Heckel, D.G., Kaltenpoth, M., Vilcinskas, A., and Vogel, H. (2018). Microbiome-assisted carrion preservation aids larval development in a burying beetle. Proc. Natl. Acad. Sci. 115, 11274–11279. https://doi.org/10.1073/pnas.1812808115.
12. Kwong, W.K., Medina, L.A., Koch, H., Sing, K.-W., Soh, E.J.Y., Ascher, J.S., Jaffé, R., and Moran, N.A. (2017). Dynamic microbiome evolution in social bees. Sci. Adv. 3, e1600513. https://doi.org/10.1126/sciadv.1600513.
13. Engel, P., Kwong, W.K., Mcfrederick, Q., Anderson, K.E., Barribeau, S.M., Chandler, J.A., Cornman, R.S., Dainat, J., De Miranda, J.R., Doublet, V., et al. (2016). The bee microbiome: Impact on bee health and model for evolution and ecology of host-microbe interactions. mBio 7, e02164-15. https://doi.org/10.1128/mBio.02164-15.
14. Rutkowski, D., Weston, M., and Vannette, R.L. (2023). Bees just wanna have fungi: a review of bee associations with nonpathogenic fungi. FEMS Microbiol. Ecol. 99, fiad077. https://doi.org/10.1093/femsec/fiad077.
15. Engel, P., Martinson, V.G., and Moran, N.A. (2012). Functional diversity within the simple gut microbiota of the honey bee. Proc. Natl. Acad. Sci. 109, 11002–11007. https://doi.org/10.1073/pnas.1202970109.
16. Kwong, W.K., Engel, P., Koch, H., and Moran, N.A. (2014). Genomics and host specialization of honey bee and bumble bee gut symbionts. Proc. Natl. Acad. Sci. U. S. A. 111, 11509–11514. https://doi.org/10.1073/pnas.1405838111.

17. Lee, F.J., Rusch, D.B., Stewart, F.J., Mattila, H.R., and Newton, I.L.G. (2015). Saccharide breakdown and fermentation by the honey bee gut microbiome. Environ. Microbiol. 17, 796–815. https://doi.org/10.1111/1462-2920.12526.
18. Danforth, B.N., Minckley, R.L., and Neff, J.L. (2019). The Solitary Bees: Biology, Evolution, Conservation (Princeton University Press) https://doi.org/10.2307/j.ctvd1c929.18.
19. McFrederick, Q.S., and Rehan, S.M. (2019). Wild bee pollen usage and microbial communities co-vary across landscapes. Microb. Ecol. 77, 513–522. https://doi.org/10.1007/s00248-018-1232-y.
20. Voulgari-Kokota, A., McFrederick, Q.S., Steffan-Dewenter, I., and Keller, A. (2019). Drivers, Diversity, and Functions of the Solitary-Bee Microbiota. Trends Microbiol. 27, 1034–1044. https://doi.org/10.1016/j.tim.2019.07.011.
21. Wasielewski, O., Wojciechowicz, T., Giejdasz, K., and Krishnan, N. (2013). Overwintering strategies in the red mason solitary bee- physiological correlates of midgut metabolic activity and turnover of nutrient reserves in females of Osmia bicornis. Apidologie 44, 642–656. https://doi.org/10.1007/s13592-013-0213-x.
22. Denlinger, D.L. (2022). Insect Diapause (Cambridge University Press) https://doi.org/10.1017/9781108609364.
23. Hammer, T.J., and Moran, N.A. (2019). Links between metamorphosis and symbiosis in holometabolous insects. Philos. Trans. R. Soc. B Biol. Sci. 374, 20190068. https://doi.org/10.1098/rstb.2019.0068.
24. Truman, J.W. (2019). The evolution of insect metamorphosis. Curr. Biol. 29, R1252–R1268. https://doi.org/10.1016/j.cub.2019.10.009.
25. McFrederick, Q.S., Wcislo, W.T., Hout, M.C., and Mueller, U.G. (2014). Host species and developmental stage, but not host social structure, affects bacterial community structure in socially polymorphic bees. FEMS Microbiol. Ecol. 88, 398–406. https://doi.org/10.1111/1574-6941.12302.
26. Hammer, T.J., Kueneman, J., Argueta-Guzmán, M., McFrederick, Q.S., Grant, Lady, Wcislo, W., Buchmann, S., and Danforth, B.N. (2023). Bee breweries: The unusually fermentative, lactobacilli-dominated brood cell microbiomes of cellophane bees. Front. Microbiol. 14, 1114849.
27. Kapheim, K.M., Johnson, M.M., and Jolley, M. (2021). Composition and acquisition of the microbiome in solitary, ground-nesting alkali bees. Sci. Rep. 11, 2993. https://doi.org/10.1038/s41598-021-82573-x.
28. Saeed, A., and White, J.A. (2015). Surveys for maternally-inherited endosymbionts reveal novel and variable infections within solitary bee species. J. Invertebr. Pathol. 132, 111–114. https://doi.org/10.1016/j.jip.2015.09.011.
29. Hanson, T., and Ascher, J.S. (2018). An unusually large nesting aggregation of the digger bee Anthophora bomboides Kirby, 1838 (Hymenoptera: Apidae) in the San Juan Islands, Washington State. Pan-Pac. Entomol. 94, 4–16. https://doi.org/10.3956/2018-94.1.4.
30. Brooks, R. (1983). Biology of Anthophora bomboides standfordiana Cockerell. In Systematics and Bionomics of Anthophora: The Bomboides Group and Species Groups of the New World Entomology. (University of California Publications), pp. 2–25.
31. Norden, B., Batra, S.W.T., Fales, H.M., Hefetz, A., and Shaw, G.J. (1980). Anthophora bees: Unusual glycerides from maternal Dufour's glands serve as larval food and cell lining. Science 207, 1095–1097. https://doi.org/10.1126/science.207.4435.1095.
32. Batra, S., and Norden, B. (1996). Fatty food for their brood: How Anthophora bees make and provision their cells (Hymenoptera: Apoidea). Mem. Entomol. Soc. Wash., 36–44.
33. Comeau, A.M., Douglas, G.M., and Langille, M.G.I. (2017). Microbiome helper: A custom and streamlined workflow for microbiome research. mSystems 2, 10.1128/msystems.00127-16. https://doi.org/10.1128/msystems.00127-16.
34. R Core Team (2020). R: a language and environment for statistical computing. (R Foundation for Statistical Computing).
35. Comeau, A.M., and Kwawukume, A. (2023). Preparing multiplexed 16S/18S/ITS amplicons for the Illumina MiSeq. Protocols.io. https://doi.org/dx.doi.org/10.17504/protocols.io.4r3l277k3g1y/v1.

36. Callahan, B.J., McMurdie, P.J., Rosen, M.J., Han, A.W., Johnson, A.J.A., and Holmes, S.P. (2016). DADA2: High-resolution sample inference from Illumina amplicon data. Nat. Methods 13, 581–583. https://doi.org/10.1038/nmeth.3869.
37. Chelius, M.K., and Triplett, E.W. (2001). The diversity of archaea and bacteria in association with the roots of Zea mays L. Microb. Ecol. 41, 252–263. https://doi.org/10.1007/s002480000087.
38. McMurdie, P.J., and Holmes, S. (2013). Phyloseq: An R package for reproducible interactive analysis and graphics of microbiome census data. PLOS ONE 8, e61217. https://doi.org/10.1371/journal.pone.0061217.
39. Dixon, P. (2003). VEGAN, a package of R functions for community ecology. J. Veg. Sci. 14, 927–930. https://doi.org/10.1111/j.1654-1103.2003.tb02228.x.
40. Lahti, L., and Shetty, S. (2017). Tools for microbiome analysis in R. Version 1.22.0. https://doi.org/10.18129/B9.bioc.microbiome https://doi.org/10.18129/B9.bioc.microbiome.
41. Wickham, H. (2016). ggplot2: Elegant Graphics for Data Analysis (Springer-Verlag New York) https://doi.org/10.1007/978-0-387-98141-3.
42. Quast, C., Pruesse, E., Yilmaz, P., Gerken, J., Schweer, T., Yarza, P., Peplies, J., and Glöckner, F.O. (2013). The SILVA ribosomal RNA gene database project: improved data processing and web-based tools. Nucleic Acids Res. 41, D590–D596. https://doi.org/10.1093/nar/gks1219.
43. Callahan, B., Davis, N.M., and Ernst, F.G.M. (2023). decontam: Identify contaminants in marker-gene and metagenomics sequencing data. Version 1.20.0 (Bioconductor version: Release (3.17)). https://doi.org/10.18129/B9.bioc.decontam https://doi.org/10.18129/B9.bioc.decontam.
44. Ogle, D.H., Doll, J.C., and Wheeler, A.P. (2023). FSA: Simple fisheries stock assessment methods. Version 0.9.5.
45. Bonferroni, C.E. (1936). Teoria statistica delle classi e calcolo delle probabilità (Seeber).
46. Liu, C.M., Kachur, S., Dwan, M.G., Abraham, A.G., Aziz, M., Hsueh, P.-R., Huang, Y.-T., Busch, J.D., Lamit, L.J., Gehring, C.A., et al. (2012). FungiQuant: A broad-coverage fungal quantitative real-time PCR assay. BMC Microbiol. 12, 255. https://doi.org/10.1186/1471-2180-12-255.
47. Martin, M. (2011). Cutadapt removes adapter sequences from high-throughput sequencing reads. EMBnet.journal 17, 10–12. https://doi.org/10.14806/ej.17.1.200.
48. Benjamini, Y., and Hochberg, Y. (1995). Controlling the false discovery rate: A practical and powerful approach to multiple testing. J. R. Stat. Soc. Ser. B Methodol. 57, 289–300. https://doi.org/10.1111/j.2517-6161.1995.tb02031.x.
49. Nilsson, R.H., Larsson, K.-H., Taylor, A.F.S., Bengtsson-Palme, J., Jeppesen, T.S., Schigel, D., Kennedy, P., Picard, K., Glöckner, F.O., Tedersoo, L., et al. (2019). The UNITE database for molecular identification of fungi: handling dark taxa and parallel taxonomic classifications. Nucleic Acids Res. 47, D259–D264. https://doi.org/10.1093/nar/gky1022.
50. Altschul, S.F., Gish, W., Miller, W., Myers, E.W., and Lipman, D.J. (1990). Basic local alignment search tool. J. Mol. Biol. 215, 403–410. https://doi.org/10.1016/S0022-2836(05)80360-2.
51. Shade, A., and Handelsman, J. (2012). Beyond the Venn diagram: the hunt for a core microbiome. Environ. Microbiol. 14, 4–12. https://doi.org/10.1111/j.1462-2920.2011.02585.x.
52. Liang, P., Cao, M., Li, J., Wang, Q., and Dai, Z. (2023). Expanding sugar alcohol industry: Microbial production of sugar alcohols and associated chemocatalytic derivatives. Biotechnol. Adv. 64, 108105. https://doi.org/10.1016/j.biotechadv.2023.108105.
53. Neu, A.T., Allen, E.E., and Roy, K. (2021). Defining and quantifying the core microbiome: Challenges and prospects. Proc. Natl. Acad. Sci. 118, e2104429118. https://doi.org/10.1073/pnas.2104429118.
54. Kobayashi, Y., Yoshida, J., Iwata, H., Koyama, Y., Kato, J., Ogihara, J., and Kasumi, T. (2013). Gene expression and function involved in polyol biosynthesis of Trichosporonoides megachiliensis under hyper-osmotic stress. J. Biosci. Bioeng. 115, 645–650. https://doi.org/10.1016/j.jbiosc.2012.12.004.

55. Crowe, J.H., Crowe, L.M., and Chapman, D. (1984). Preservation of membranes in anhydrobiotic organisms: the role of trehalose. Science 223, 701–703. https://doi.org/10.1126/science.223.4637.701.
56. Elbein, A.D., Pan, Y.T., Pastuszak, I., and Carroll, D. (2003). New insights on trehalose: a multifunctional molecule. Glycobiology 13, 17R-27R. https://doi.org/10.1093/glycob/cwg047.
57. Storey, J.M., and Storey, K.B. (2005). Cold Hardiness and Freeze Tolerance. In Functional Metabolism: Regultion and Adaptation (John Wiley & Sons, Inc.), pp. 473–503. https://doi.org/10.1002/047167558X.ch17.
58. Wang, Q., Xu, X., Zhu, X., Chen, L., Zhou, S., Huang, Z.Y., and Zhou, B. (2016). Low-temperature stress during capped brood stage increases pupal mortality, misorientation and adult mortality in honey bees. PLoS ONE 11, e0154547. https://doi.org/10.1371/journal.pone.0154547.
59. Minckley, R.L., and Danforth, B.N. (2019). Sources and frequency of brood loss in solitary bees. Apidologie 50, 515–525. https://doi.org/10.1007/s13592-019-00663-2.
60. Edgar, R.C. (2004). MUSCLE: multiple sequence alignment with high accuracy and high throughput. Nucleic Acids Res. 32, 1792–1797. https://doi.org/10.1093/nar/gkh340.
61. Torson, A.S., Yocum, G.D., Rinehart, J.P., Kemp, W.P., and Bowsher, J.H. (2015). Transcriptional responses to fluctuating thermal regimes underpinning differences in survival in the solitary bee Megachile rotundata. J. Exp. Biol. 218, 1060–1068. https://doi.org/10.1242/jeb.113829.
62. Katoh, K., Rozewicki, J., and Yamada, K.D. (2019). MAFFT online service: multiple sequence alignment, interactive sequence choice and visualization. Brief. Bioinform. 20, 1160–1166. https://doi.org/10.1093/bib/bbx108.
63. Ferguson, L.V., Dhakal, P., Lebenzon, J.E., Heinrichs, D.E., Bucking, C., and Sinclair, B.J. (2018). Seasonal shifts in the insect gut microbiome are concurrent with changes in cold tolerance and immunity. Funct. Ecol. 32, 2357–2368. https://doi.org/10.1111/1365-2435.13153.
64. Parish, A.J., Rice, D.W., Tanquary, V.M., Tennessen, J.M., and Newton, I.L.G. (2022). Honey bee symbiont buffers larvae against nutritional stress and supplements lysine. ISME J. 16, 2160–2168. https://doi.org/10.1038/s41396-022-01268-x.
65. Denlinger, D.L. (2023). Insect diapause: From a rich history to an exciting future. J. Exp. Biol. 226, jeb245329. https://doi.org/10.1242/jeb.245329.
66. Mushegian, A.A., and Tougeron, K. (2019). Animal-microbe interactions in the context of diapause. Biol. Bull. 237, 180–191. https://doi.org/10.1086/706078.
67. Douglas, A.E. (2000). Reproductive diapause and the bacterial symbiosis in the sycamore aphid Drepanosiphum platanoidis. Ecol. Entomol. 25, 256–261. https://doi.org/10.1046/j.1365-2311.2000.00270.x.
68. Dittmer, J., and Brucker, R.M. (2021). When your host shuts down: larval diapause impacts host-microbiome interactions in Nasonia vitripennis. Microbiome 9, 85. https://doi.org/10.1186/s40168-021-01037-6.
69. Liu, W., Li, Y., Guo, S., Yin, H., Lei, C.-L., and Wang, X.-P. (2016). Association between gut microbiota and diapause preparation in the cabbage beetle: a new perspective for studying insect diapause. Sci. Rep. 6, 38900. https://doi.org/10.1038/srep38900.
70. Didion, E.M., Doyle, M., and Benoit, J.B. (2022). Bacterial communities of lab and field northern house mosquitoes (Diptera: Culicidae) throughout diapause. J. Med. Entomol. 59, 648–658. https://doi.org/10.1093/jme/tjab184.
71. Brown, A.L., Sharp, K., and Apprill, A. (2022). Reshuffling of the coral microbiome during dormancy. Appl. Environ. Microbiol. 88, e01391-22. https://doi.org/10.1128/aem.01391-22.
72. Neelakanta, G., Sultana, H., Fish, D., Anderson, J.F., and Fikrig, E. (2010). Anaplasma phagocytophilum induces Ixodes scapularis ticks to express an antifreeze glycoprotein gene that enhances their survival in the cold. J. Clin. Invest. 120, 3179–3190. https://doi.org/10.1172/JCI42868.
73. Didion, E.M., Sabree, Z.L., Kenyon, L., Nine, G., Hagan, R.W., Osman, S., and Benoit, J.B. (2021). Microbiome reduction prevents lipid accumulation during early diapause in the northern house

mosquito, Culex pipiens pipens. J. Insect Physiol. 134, 104295. https://doi.org/10.1016/j.jinsphys.2021.104295.
74. Wiebler, J.M., Kohl, K.D., Lee, R.E., and Costanzo, J.P. (2018). Urea hydrolysis by gut bacteria in a hibernating frog: evidence for urea-nitrogen recycling in Amphibia. Proc. R. Soc. B Biol. Sci. 285. https://doi.org/10.1098/rspb.2018.0241.
75. Regan, M.D., Chiang, E., Liu, Y., Tonelli, M., Verdoorn, K.M., Gugel, S.R., Suen, G., Carey, H.V., and Assadi-Porter, F.M. (2022). Nitrogen recycling via gut symbionts increases in ground squirrels over the hibernation season. Science 375, 460–463. https://doi.org/10.1126/science.abh2950.
76. Yoder, J.A., Nelson, B.W., Main, L.R., Lorenz, A.L., Jajack, A.J., and Aronstein, K.A. (2017). Water activity of the bee fungal pathogen Ascosphaera apis in relation to colony conditions. Apidologie 48, 159–167. https://doi.org/10.1007/s13592-016-0461-7.
77. Nakamura, A., Miyado, K., Takezawa, Y., Ohnami, N., Sato, M., Ono, C., Harada, Y., Yoshida, K., Kawano, N., Kanai, S., et al. (2011). Innate immune system still works at diapause, a physiological state of dormancy in insects. Biochem. Biophys. Res. Commun. 410, 351–357. https://doi.org/10.1016/j.bbrc.2011.06.015.
78. Crowley, L.D., and Houck, M.A. (2002). The immune response of larvae and pupae of Calliphora vicina (Diptera: Calliphoridae), upon administered insult with Escherichia coli. J. Med. Entomol. 39, 931–934. https://doi.org/10.1603/0022-2585-39.6.931.
79. Ferguson, L.V., and Sinclair, B.J. (2017). Insect immunity varies idiosyncratically during overwintering. J. Exp. Zool. 327, 222–234. https://doi.org/10.1002/jez.2067.
80. Seipke, R.F., Kaltenpoth, M., and Hutchings, M.I. (2012). Streptomyces as symbionts: an emerging and widespread theme? FEMS Microbiol. Rev. 36, 862–876. https://doi.org/10.1111/j.1574-6976.2011.00313.x.
81. Chevrette, M.G., Carlson, C.M., Ortega, H.E., Thomas, C., Ananiev, G.E., Barns, K.J., Book, A.J., Cagnazzo, J., Carlos, C., Flanigan, W., et al. (2019). The antimicrobial potential of Streptomyces from insect microbiomes. Nat. Commun. 10, 516. https://doi.org/10.1038/s41467-019-08438-0.
82. Kaltenpoth, M., Goettler, W., Dale, C., Stubblefield, J.W., Herzner, G., Roeser-Mueller, K., and Strohm, E. (2006). 'Candidatus Streptomyces philanthi', an endosymbiotic streptomycete in the antennae of Philanthus digger wasps. Int. J. Syst. Evol. Microbiol. 56, 1403–1411. https://doi.org/10.1099/ijs.0.64117-0.
83. Flórez, L., Biedermann, P.H., Engl, T., and Kaltenpoth, M. (2015). Defensive symbioses of animals with prokaryotic and eukaryotic microorganisms. Nat. Prod. Rep. 32, 904–936. https://doi.org/10.1039/C5NP00010F.
84. Seipke, R.F., Barke, J., Brearley, C., Hill, L., Yu, D.W., Goss, R.J.M., and Hutchings, M.I. (2011). A single Streptomyces symbiont makes multiple antifungals to support the fungus farming ant Acromyrmex octospinosus. PLOS ONE 6, e22028. https://doi.org/10.1371/journal.pone.0022028.
85. Pessotti, R. de C., Hansen, B.L., Reaso, J.N., Ceja-Navarro, J.A., El-Hifnawi, L., Brodie, E.L., and Traxler, M.F. (2021). Multiple lineages of Streptomyces produce antimicrobials within passalid beetle galleries across eastern North America. eLife 10, e65091. https://doi.org/10.7554/eLife.65091.
86. Lalouette, L., Williams, C.M., Hervant, F., Sinclair, B.J., and Renault, D. (2011). Metabolic rate and oxidative stress in insects exposed to low temperature thermal fluctuations. Comp. Biochem. Physiol. A. Mol. Integr. Physiol. 158, 229–234. https://doi.org/10.1016/j.cbpa.2010.11.007.
87. Kobayashi, Y., Iwata, H., Yoshida, J., Ogihara, J., Kato, J., and Kasumi, T. (2015). Metabolic correlation between polyol and energy-storing carbohydrate under osmotic and oxidative stress condition in Moniliella megachiliensis. J. Biosci. Bioeng. 120, 405–410. https://doi.org/10.1016/j.jbiosc.2015.02.014.
88. Becker, A., Schlöder, P., Steele, J.E., and Wegener, G. (1996). The regulation of trehalose metabolism in insects. Experientia 52, 433–439. https://doi.org/10.1007/BF01919312.
89. Segal-Kischinevzky, C., Romero-Aguilar, L., Alcaraz, L.D., López-Ortiz, G., Martínez-Castillo, B., Torres-Ramírez, N., Sandoval, G., and González, J. (2022). Yeasts inhabiting extreme environments

and their biotechnological applications. Microorganisms 10, 794. https://doi.org/10.3390/microorganisms10040794.
90. Kitcha, S., and Cheirsilp, B. (2011). Screening of oleaginous yeasts and optimization for lipid production using crude glycerol as a carbon source. Energy Procedia 9, 274–282. https://doi.org/10.1016/j.egypro.2011.09.029.
91. Mikolasch, A., Berzhanova, R., Omirbekova, A., Reinhard, A., Zühlke, D., Meister, M., Mukasheva, T., Riedel, K., Urich, T., and Schauer, F. (2021). Moniliella spathulata, an oil-degrading yeast, which promotes growth of barley in oil-polluted soil. Appl. Microbiol. Biotechnol. 105, 401–415. https://doi.org/10.1007/s00253-020-11011-1.
92. McFrederick, Q.S., Cannone, J.J., Gutell, R.R., Kellner, K., Plowes, R.M., and Mueller, U.G. (2013). Specificity between Lactobacilli and Hymenopteran hosts is the exception rather than the rule. Appl. Environ. Microbiol. 79, 1803–1812. https://doi.org/10.1128/AEM.03681-12.
93. McFrederick, Q.S., Thomas, J.M., Neff, J.L., Vuong, H.Q., Russell, K.A., Hale, A.R., and Mueller, U.G. (2017). Flowers and wild megachilid bees share microbes. Microb. Ecol. 73, 188–200. https://doi.org/10.1007/s00248-016-0838-1.
94. Cohen, H., McFrederick, Q.S., and Philpott, S.M. (2020). Environment shapes the microbiome of the blue orchard bee, Osmia lignaria. Microb. Ecol. 80, 897–907. https://doi.org/10.1007/s00248-020-01549-y.
95. Li, X., Wang, A., Wan, W., Luo, X., Zheng, L., He, G., Huang, D., Chen, W., and Huang, Q. High salinity inhibits soil bacterial community mediating nitrogen cycling. Appl. Environ. Microbiol. 87, e01366-21. https://doi.org/10.1128/AEM.01366-21.
96. Inglis, G.D., Sigler, L., and Goette, MarkS. (1993). Aerobic microorganisms associated with alfalfa leafcutter bees (Megachile rotundata). Microb. Ecol. 26, 125–143. https://doi.org/10.1007/BF00177048.
97. Hettiarachchi, A., Cnockaert, M., Joossens, M., Gekière, A., Meeus, I., Vereecken, N.J., Michez, D., Smagghe, G., and Vandamme, P. (2023). The wild solitary bees Andrena vaga, Anthophora plumipes, Colletes cunicularius, and Osmia cornuta microbiota are host specific and dominated by endosymbionts and environmental microorganisms. Microb. Ecol., 1–14. https://doi.org/10.1007/s00248-023-02304-9.
98. Handy, M.Y., Sbardellati, D.L., Yu, M., Saleh, N.W., Ostwald, M.M., and Vannette, R.L. (2023). Incipiently social carpenter bees (Xylocopa) host distinctive gut bacterial communities and display geographical structure as revealed by full-length PacBio 16S rRNA sequencing. Mol. Ecol. 32, 1530–1543. https://doi.org/10.1111/mec.16736.
99. Inglis, G.D., Sigler, L., and Goettel, M.S. (1992). Trichosporonoides megachiliensis, a new hyphomycete associated with alfalfa leafcutter bees, with notes on Trichosporonoides and Moniliella. Mycologia 84, 555–570. https://doi.org/10.2307/3760322.
100. Cane, J.H., and Carlson, R.G. (1984). Dufour's gland triglycerides from Anthophora, Emphoropsis (Anthophoridae) and Megachile (Megachilidae) bees (Hymenoptera: Apoidea). Comp. Biochem. Physiol. 78, 769–772. https://doi.org/10.1016/0305-0491(84)90132-9.
101. Hefetz, A. (1987). The role of Dufour's gland secretions in bees. Physiol. Entomol. 12, 243–253. https://doi.org/10.1111/j.1365-3032.1987.tb00749.x.
102. Currie, C.R., Scott, J.A., Summerbell, R.C., and Malloch, D. (1999). Fungus-growing ants use antibiotic-producing bacteria to control garden parasites. Nature 398, 701–704. https://doi.org/10.1038/19519.
103. Currie, C.R. (2001). A community of ants, fungi, and bacteria: A multilateral approach to studying symbiosis. Annu. Rev. Microbiol. 55, 357–380. https://doi.org/10.1146/annurev.micro.55.1.357.
104. Mueller, U.G., Scott, J.J., Ishak, H.D., Cooper, M., and Rodrigues, A. (2010). Monoculture of leafcutter ant gardens. PLOS ONE 5, e12668. https://doi.org/10.1371/journal.pone.0012668.
105. Perito, B., Cremonini, M., Montecchi, T., and Turillazzi, S. (2018). A preliminary study on the antimicrobial activity of sting secretion and gastral glands of the acrobat ant Crematogaster scutellaris. Bull. Insectology, 97–101.

Chapter III:

Complete genome sequence and description of *Streptomyces solapis* sp. nov. and *Streptomyces nidicoloris* sp. nov., novel Actinobacteria isolated from a solitary bee

Abstract

Streptomyces were previously thought to be mostly soil-associated bacteria, but recent work has shown that they are commonly defensive symbionts of macroscopic organisms due to their prolific and diverse secondary metabolite products. We describe *Streptomyces solapis* sp. nov. and *Streptomyces nidicoloris* sp. nov., novel Actinobacteria isolated from developing brood of solitary bee species *Anthophora bomboides*, and present the complete genome sequences of six strains of these new species in comparison to related *Streptomyces*; five strains belong to *Streptomyces solapis* sp. nov. and one strain represents *Streptomyces nidicoloris* sp. nov. These new species are distinguished from previously described species by unique genetic, morphological, and physiological characteristics. The five genomes representing *S. solapis* sp. nov. comprise 9.6 Mb and encode 8,640 predicted genes on average. The genome representing *S. nidicoloris* sp. nov. comprises 9.4 Mb and encodes 8,426 predicted genes. Phylogenetic analysis based on 5 gene multilocus sequence alignment and whole-genome data positions *S. solapis* sp. nov and *S. nidicoloris* sp. nov. within the genus *Streptomyces* with close relation to *S. endophyticus* and *S. fractus*, which were isolated from plant root and termite gut environments, respectively. We provide differential analysis of secondary metabolic potential of the new strains as compared to these related species. The genomic data and comparative analysis indicate that strains of *S. solapis* sp. nov. have novel biosynthetic gene clusters which are unique to the species, some of which differentiate two subclades within it. The difference in subclades corresponds to the differential antifungal activity of these strains observed in Ch. 2. This chapter provides support for the hypothesis that these bee-associated *Streptomyces* have the potential to contribute to pathogen defense of the brood through production of antifungal compounds. Due to the diversity of these strains and average genome size, we hypothesize that these strains are not obligately associated with the host. Further experimental and chemical analyses are required to determine the *in situ* expression of these gene clusters and the resulting bee host survival benefit of maintaining these symbiotic strains.

Introduction

The genus *Streptomyces* (Actinomycetota) encompasses a diverse, ecologically complex and economically important group of bacteria[1–3]. *Streptomyces* are most well known for their production of natural products, including compounds with antibiotic, antifungal, anticancer, antiparasitic, and immunosuppressive properties[4]. *Streptomyces*-derived antibiotics were among the first to be discovered (e.g. Streptomycin), and many are still widely used to treat variety of infections in people and to protect crops and domesticated animals[3,5].

This plethora of secondary metabolites is due to the genetic and ecological complexity and diversity within the genus *Streptomyces*. Members typically have large genomes, 6-12 Mb as compared to ~5 Mb for the average bacteria[1,6]. These large genomes almost always include biosynthetic gene clusters (BGCs), which are sets of genes that make the enzymatic "machinery" to produce various secondary metabolites[5]. Unlike the primary metabolites, which an organism requires to function, grow, and reproduce, secondary metabolites perform other beneficial functions, such as eliminating competing microbes, scavenging iron, manipulating a host, attracting organisms for spore dispersal, or signaling to other members of the species[7]. The BGCs and the secondary metabolites they produce can vary considerably between species, and for many of these metabolites, roles are yet unknown[1].

Streptomyces typically grow as multicellular vegetative hyphae (filamentous) with highly coordinated metabolism, phenology, and responses to the environment. They are generally nonmotile and produce spores for dispersal to new habitats. While they are highly prevalent and abundant in soil, *Streptomyces* are also symbionts of multicellular eukaryotes, especially plants and invertebrates[8–10].

In Ch. 2, four *Streptomyces* strains were isolated from samples of the solitary bee *Anthophora bomboides* during development in the brood cell[11]. These strains were found to inhibit fungal growth to various degrees, and were abundant in bee brood cell habitats, prompting further investigation to characterize them and sequence their genomes. Two additional *Streptomyces* strains were isolated after the publication of the chapter. Ch. 2 described *Streptomyces* as a core taxa within the developing brood cell of *Anthophora bomboides* and determined that the *Streptomyces* abundance increased dramatically

during the overwintering period, when bee immunity is suppressed and fungal infection is most prevalent. Notably, the bees hosted a diversity of *Streptomyces*, not a single species or strain but rather over 100 unique ASVs. We determined that the diversity of ASVs assigned to Actinobacteria (including *Streptomyces*) was not due to spillover from environmental sources (i.e. flowers, water), as the ASV overlap between brood cell and environmental samples was low; 316 ASVs of Actinobacteria were found in the brood cells, and less than 18% of these (64 ASVs) were also found in the environmental samples. The strains isolated and sequenced in this chapter match to two of the three most common *Streptomyces* ASVs that were found in the brood cell; these matching ASVs are found in 56% of brood cell samples (Ch. 2, Fig. S7). Additionally, the strains sequenced here were isolated from different brood cells, at different developmental stages and seasons, during three different years (Table 3.1), yet five of the six represent strains of the same species. Though it is possible that the bees are acquiring these ASVs from environmental sources that we did not sample, the combination of very consistent *Streptomyces* presence, low overlap of ASVs between brood cells and environment, high prevalence of ASVs matching the sequence of the isolates, and consistent re-isolation of *S. solapis* sp. nov. from the brood cells over time indicates some level of association or possibly specialization of these bacteria with the host (Ch. 2, Fig. S3).

This chapter aims to describe two new species: *Streptomyces solapis* sp. nov. and *Streptomyces nidicoloris* sp. nov. and to provide genomic sequences and analysis that can contribute to our understanding of the genetic underpinnings of host-microbe symbiosis.

Materials and Methods

Isolation and Cultivation

Samples of solitary bee *Anthophora bomboides* were collected from Point Reyes National Seashore and Bodega Head Marine Reserve (permit #: PORE-2020-SCI-0022 and SCSP permit issued 2/24/2020). Six isolates were obtained from various stages of the solitary bee *Anthophora bomboides* life cycle (Table 3.1). These brood cells were collected and then *Streptomyces* were isolated from samples via repeated streak plating on tryptic soy agar (TSA) and underwent preliminary identification via 16S Sanger sequencing as described in Ch. 2. Once single-colony isolates were obtained, these were cryopreserved as glycerol stocks at -70° C.

Table 3.1

Isolate_ID	Proposed species	Source	Collection date	Coverage avg.	GC	Genome size	Contigs	Coding density	Predicted genes	Completeness	Contamination
BH034	*Streptomyces solapis* sp. nov T	Early provision	4 Jun. '21	80	0.710	9621129	3	0.894	8716	99.89	1.29
BH055	*Streptomyces solapis* sp. nov	Egg stage provision	9 Jun. '21	196	0.709	9659588	3	0.892	8797	99.46	1.29
BH097	*Streptomyces solapis* sp. nov	Overwintering oct	25 Oct. '22	29	0.710	9674327	6	0.893	8774	99.46	0.43
BH104	*Streptomyces solapis* sp. nov	Overwintering oct	25 Oct. '22	214	0.709	8757701	6	0.893	8026	99.89	1.29
BH105	*Streptomyces solapis* sp. nov	Pupa	12 May '23	419	0.709	9672763	4	0.894	8891	99.46	1.29
BH106	*Streptomyces nidicoloris* sp. nov T	Pupa	12 May '23	400	0.707	9455321	2	0.895	8426	98.61	0.43

Phenotypic Characterization

Morphology

To determine morphological characteristics, I plated each strain from freezer stock onto multiple media types (TSA, Maltose Yeast Media- MYM, Oatmeal Agar- OA, see Appendix III Table S3) and inoculated into liquid media (Supplemented Grace's Media- SGM, Gibco) then observed every other day for 7 days, noting changes in media color (diffusible pigments), colony shape, color, and finish; these are standard characteristics for bacterial species description. I used a dissection microscope to examine whether the strain produced spores on each media, standard practice for *Streptomyces*. From liquid media, I spotted 10 µl onto a glass slide every other day for 7 days to look for morphological changes in growth, especially fragmentation of the filaments, as this trait was observed to differ between close relatives *S. fractus* and *S. endophyticus*[12,13].

Salt tolerance

Salt tolerance was also observed in related species *S. fractus* and was thus tested for all available strains[12]. To test salt tolerance, SGM was modified with various concentrations of salt (NaCl) at 0%, 5%,10% w/v. Isolates were grown on plates and one colony (1ul loop) was added to 5ml of each media. Growth was determined after 5 days by increased optical density after resuspension via agitation, as compared to the control (media without inoculation).

Temperature range

To test heat resistance, I streaked from SGM cultures of each isolate onto TSA and grew them at 25°C, 28°C, and 37°C for 5 days, checking for growth every other day. Determination of heat tolerance is standard for bacterial species description.

Geosmin production

Geosmin production is a common trait for *Streptomyces* species, and is what gives soil its "earthy" smell[14]. After initial observations that BH106 was less distinctly "earthy" smelling than the other new isolates, geosmin production for each was inferred. The isolates were plated on TSA and allowed to grow for 5 days wrapped in parafilm, then each plate was opened and smelled to infer geosmin production. This was repeated twice.

Genomic Analysis

DNA was extracted from isolated strains using the Qiagen PowerSoil Pro kit, DNA concentration was assessed via NanoDrop. Sanger sequencing of the 16S rRNA gene using universal bacterial primers (27F/1492R) traces confirmed that the strains belong to *Streptomyces* using NCBI BLAST (16S ribosomal RNA sequences database)[15,16]. The genomes were sequenced using Pacific Bioscience (PacBio) long read sequencing, and assembled with Flye (v 2.9.3), the quality and completeness were calculated with CheckM (v1.2.2), which determined completeness of >99% for 5 genomes, and over 98.5% for 1 genome[17,18]. All bee isolate genomes had very low CheckM contamination, max 1.29%. Coverage ranged from 29x (BH97) to 419x (BH105) (mean= 223x, median= 205x). The genome sizes ranged from 8.75Mb

(BH104) to 9.67Mb (BH97), on average the bee isolated strains were 9.47Mb with 70.9% GC (range 70.7-71.0%). For details see Table 3.1.

Similarity to known strains was determined in several ways. The full 16S rRNA gene was extracted from the genomes (as annotated by Prokka) and NCBI BLAST was then used to determine closest potential relatives[15,19]. This determined that *Streptomyces fractus* isolated from the termite gut (*Amitermes hastatus*) was a close relative, but the species did not yet have a genome sequence[12]. We therefore ordered the strain and had it sequenced as well, but used NanoPore technology at the Max Planck Institute for Chemical Ecology provided by our collaborators. The *S. fractus* genome was 99.89% complete, with 1.65% contamination.

Digital DNA-DNA hybridization (dDDH) was used to estimate the genetic relatedness between bacterial genomes based on the digital analysis of genomic sequences. It serves as a digital approximation of the traditional DNA-DNA hybridization (DDH) method, which is used to determine genomic similarity and to classify bacterial species, with d0 < 70% indicating species separation[20]. The DSMZ type strain genome server was used for dDDH with their continuously updated library of known genomes to determine genome overlap/relatedness among the strains and other previously sequenced *Streptomyces*[21,22]. It uses dDDH to compare the genomes for relatedness and generated a whole genome phylogeny using D5 distance formula and "GreedyWithTrimming" distance algorithm, while the 16S phylogeny used the "CharacterCoverage" distance algorithm[21]. Determination of closest type strain genomes was done in two complementary ways. First, all uploaded genomes were compared against all type strain genomes available in the TYGS database via the MASH algorithm, a fast approximation of intergenomic relatedness, and the ten type strains with the smallest MASH distances chosen per user genome[23]. Second, an additional set of ten closely related type strains was determined via the 16S rDNA gene sequences. These were extracted from the user genomes using RNAmmer and each sequence was subsequently BLASTed against the 16S rDNA gene sequence of each of the 21,293 type strains available in the TYGS database on June 10, 2024 [24]. This was used as a proxy to find the best 50 matching type strains (according to the bit score) for each uploaded genome and to subsequently calculate precise

distances using the Genome BLAST Distance Phylogeny approach (GBDP) under the algorithm 'coverage' and distance formula d5. These distances were finally used to determine the 10 closest type strain genomes for each of the uploaded genomes.

Pairwise comparison of genome sequences

For the phylogenomic inference, all pairwise comparisons among the set of genomes were conducted using Genome BLAST Distance Phylogeny (GBDP) and accurate intergenomic distances inferred under the algorithm 'trimming' and distance formula d5 [25]. 100 distance replicates were calculated each. Digital DDH values and confidence intervals were calculated using the recommended settings of the GGDC 4.0.

Phylogenetic inference

The resulting intergenomic distances were used to infer a balanced minimum evolution tree with branch support via FastME 2.1.6.1 including SPR postprocessing[26]. Branch support was inferred from 100 pseudo- bootstrap replicates each. The trees were rooted at the midpoint and visualized with PhyD3 (Figure 3.2)[27]. The type-based species clustering used a 70% dDDH radius around each of the 54 type strains[21]. The resulting groups are shown in Figure 3.2. Subspecies clustering was done using a 79% dDDH threshold.

Average nucleotide identity

Average Nucleotide Identity (ANI) is a widely used metric for estimating the genetic similarity between bacterial genomes. It provides a quantitative measure of the average nucleotide identity shared between the aligned regions of two genomic sequences and is commonly used in microbial taxonomy and genomics to distinguish species[28]. We utilized fastANI (v.1.34) to determine average nucleotide identity among the isolates and with other known genomes, using a cutoff of 95% to determine species level relatedness[28].

Annotation

The genomes of the *Streptomyces* isolates were annotated with Prokka v1.14.6[19]. Prokka was executed on the UC Davis FARM high-performance computing cluster, with default settings, the

kingdom argument was set to “Bacteria” and genus argument set to “Streptomyces”, to optimize processing time. Prokka employs Prodigal for predicting protein-coding sequences, RNAmmer and Aragorn for identifying rRNA and tRNA genes, and HMMER for small non-coding RNA detection[24,29–31]. Functional annotations are through homology searches against UniProt and RefSeq databases[32–34]. Additionally, functional domains are annotated by searching against the Pfam database using HMMER[35]. From Prokka output, Ghost Koala server was used to assign KO numbers to the amino acid sequences, and these were fed to KEGG Mapper to group genes to modules and pathways[36,37]. This annotation was also used for extracting multilocus sequence alignment gene sequences.

The genomes were analyzed for biosynthetic gene clusters (BGCs) using antiSMASH web server (antibiotics & Secondary Metabolite Analysis SHell, v7.0), a specialized software tool designed for the identification and annotation of secondary metabolite biosynthetic gene clusters [38]. The analysis was conducted using the default settings of antiSMASH, which was configured to include all cluster types. AntiSMASH employs a combination of rule-based heuristics and profile hidden Markov models to predict and annotate BGCs, as well as algorithms to identify putative novel gene clusters by comparing them with known clusters in the Minimum Information about a Biosynthetic Gene cluster (MIBiG) repository[39].

The output from antiSMASH included a comprehensive list of predicted BGCs with annotations, including cluster types, core biosynthetic genes, and additional tailoring and transport genes. The results were manually curated and visualized using the antiSMASH interactive HTML output, followed by export and integration with results from related genomes.

Multilocus sequence alignment

A five gene multilocus sequence alignment was performed using genes commonly used for phylogeny in existing *Streptomyces* literature (*atpD, gyrB, recA, rpoB* and *trpB*)[40,41]. The five genes were extracted from the Prokka annotation files of each isolate and reference genome and concatenated. Multiple sequence alignments were performed using MAFFT (Multiple Alignment using Fast Fourier Transform, v 7.0) online server to align the concatenated sequences[42]. The alignment parameters were

configured to include the default settings unless otherwise specified. The "Auto" strategy was initially used to allow MAFFT to select the appropriate algorithm based on sequence length and similarity and picked MAFFT-L-INS-i (most accurate). Following alignment, a phylogenetic tree was constructed using conserved sites (2,278) with the neighbor-joining (NJ) method within MAFFT. MAFFT computed the distance matrix using the Jukes-Cantor (JC69) model and resampling level of 1000 for bootstrap values.

Results

Genome sequencing and analysis showed that the six new bee isolated strains represent two novel *Streptomyces* species. This is based on whole genome comparison methods (dDDH, ANI) as well as multilocus sequence alignment (MLSA) and subsequent phylogenetic analyses, combined with comparative morphology and physiology[43]. Each of these methods complement one another and support the delineation of these two new species.

Genome comparisons

Whole genome comparisons:

Digital DNA-DNA hybridization (dDDH) was used to estimate the genetic relatedness between bacterial genomes, with d0 < 70% indicating species separation[20]. Average Nucleotide Identity (ANI) was also used to distinguish species, with a cutoff of 95% for species separation[44].

Digital DNA-DNA Hybridization showed that the new strains have d0 <70% to any named species with a genome sequence available in the DSMZ database (Table S3, Appendix III)[22]. The closest dDDH matches were *Streptomyces endophyticus* YIM65594 which had a d0 of 67.7% with BH106, and *Streptomyces fractus* MV32 which had a d0 of 55.9% with BH034 (Appendix III, Table S3)[12,13]. Additionally, the average nucleotide identities between these strains and other named species were less than the accepted species boundary of 95% ANI, as the closest named species genome was *S. endophyticus* with an ANI of 93.4% with BH106; and *S. fractus* with an ANI of 92.8%, also with BH106, while all of the other new strains were below 93% ANI with any species with previously sequenced genomes.

When comparing dDDH and ANI among the new strains, we find that two distinct species are present, with BH034, BH055, BH097, BH104 and BH105 clustering together in one clade, while BH106 is a distinctly separate species. This is shown by within-clade ANI values of >96% when comparing the strains within the first clade, whereas BH106 has <93% ANI with all of the other five new strains. dDDH was also supportive of two species, as within- clade d0 >70% (aside from BH104 which had d0 of 69%

with BH034 and BH094), but comparing BH106 to the other new strains showed d0 between 60-66%, well below the species cutoff. At an even finer scale, the first species can be subdivided into two subspecies clades, with BH034 and BH097 being nearly identical (ANI 99.9%, d0 99.8), and BH055, BH104, and BH105 having over 99% ANI and d0 of 80-90.9 with one another.

Phylogeny:

The separation of the new bee isolates into two novel species is supported by the whole genome GBDP tree and the five gene multilocus sequence alignment neighbor joining tree (*atpD, gyrB, recA, rpoB* and *trpB*), which both separate BH34-BH105 into one clade, with BH106, *S. fractus*, and *S. endophyticus* as closest neighbors (Fig. 3.1A-B). The two trees are discordant in specific arrangement of BH106, *S. fractus* and *S. endophyticus*. The genome tree has them together in a clade sister to BH34-BH105, with BH106 more closely related to *S. endophyticus* (Fig. 3.1A), whereas the MLSA separates them, with *S. fractus* being sister to BH34-BH104, *S. endophyticus* branching off before that, and BH106 branching off before both of them (Fig. 3.1B). In both cases, however, the five isolates representing *S. solapis* sp. nov. (BH34-BH105) form a distinct clade, with two subclades (BH34/BH97, and BH55/BH104/BH105).

Biosynthetic gene cluster comparisons:

To detect and identify BGCs in the genomes of these new isolates in comparison to those of close relatives, I used antiSMASH, an online server and database with one of the largest compilations of BGC data[38]. Given an annotated genome (Prokka), antiSMASH searches and annotates BGCs based on known arrangements and gene associations, as well as certain domain traits and comparison to characterized BGCs. This allows for prediction of the type of metabolites the cluster may produce and provides a similarity score for predicted clusters to the closest known cluster. The related *Streptomyces* genomes which were used for reference and comparison were: *S. fractus, S. endophyticus, S. kunmingensis,* and one undescribed *Streptomyces* isolate from compost (NBC003), which was identified as potentially related via 16S SSU BLAST and confirmed via ANI.

Streptomyces solapis sp. nov. strains (BH34 ^{T}, BH55, BH97, BH104, BH105) had between 21 and 24 BGCs in their genomes, while *S. nidicoloris* sp. nov. (BH106) had 16 BGCs. *Streptomyces fractus* also had 16 BGCs (15 of the 16 were the same as in BH106); *S. endophyticus* had 19 BGCs, the compost isolate (NBC003) had 22 BGCs, and *S. kunmingensis* had 40 BCGs (Fig. 3.3, Appendix III- Table S4 and Figure S1). I found that our newly isolated *S. solapis* strains contained 12 unique BGCs not found in their close relatives; no unique BGCs were found in the genome of *S. nidicoloris* sp. nov. (BH106) (Figure 3.3). Of these 12 unique BGCs, 10 have less than 50% similarity to any known cluster, and 8 have less than 25% similarity with any known cluster (Table S4, Appendix III).

The unique BGCs span BGC types: one butyrolactone, one lanthipeptide, three non-ribosomal peptide synthase (NRPS) or NRPS-like, one redox-cofactor, one regioselectivity recognizing element (RRE)-containing, two type 2 polyketide synthase (T2 PKS), one type 3 polyketide synthase (T3 PKS), one terpene, and one thioamitide class. Three of the 12 were found uniformly in all of the *S. solapis* sp. nov. strains, while the others, in most cases, belonged to one of the two subclades specifically. Seven BGCs were unique to clade 2 (BH55/BH104/BH105), but only three of these were found in all three of the strains; the others were uniquely present in only one or two of the three strains in the clade (Table S4, Appendix III).

Two BGCs were unique to *S. solapis* clade 1 (BH34 ^{T}/BH97), which were identical in BGC composition. One of these was a Type II Polyketide Synthase (T2PKS) with low similarity score to known clusters (21%). The alignment of this gene cluster with the most similar known clusters (MIBiG 3.1), as well as analysis of domain matches via HMMER indicates that the cluster contains the main biosynthetic genes for production of polyketides (Table 3.2), but it had low similarity to known T2PKS clusters overall (Figure 3.4).

Table 3.2				
Contig ID (BH034)	**Domain/protein**	**Abbreviation**	**Score**	**E-value**
ctg1_7263	Ketoreductase	**KR**	175.5	3.70E-54
ctg1_7279	Ketoreductase	**KR**	150.4	1.70E-46
ctg1_7280	Methyltransferase	MET	27	5.40E-09
ctg1_7284	Ketosynthase	**KS**	760.5	9.40E-232
ctg1_7285	Chain length factor 7	**CLF** -7	681.7	6.60E-208
ctg1_7286	Acyl carrier protein	**ACP**	99.2	2.40E-31
ctg1_7287	Cyclase	CYC	446.6	8.30E-137
ctg1_7289	Ketoreductase	**KR**	187.1	1.00E-57
ctg1_7291	Cyclase	CYC C7-C12	196.6	1.10E-60
ctg1_7295	Ketoreductase	**KR** C9	432.5	1.20E-132
ctg1_7316	Ketoreductase	**KR**	147	1.90E-45
The core components of T2PKS: **ACP, CLF, KS** Optional/Tailoring Enzymes: CYC*, KR, GT, HAL, MET, OXY [45] *sometimes considered core component				

Phenotypic differences

Morphology:

Streptomyces solapis sp. nov.

On Tryptic Soy Agar (TSA) solid media, colonies are irregular in shape and have lobate edges. The surface ranges between tightly wrinkled at the center and flat with some wrinkles at the edge. Colonies are opaque, and with matte surface and viscoelastic texture, which tends to form a glob when picking colonies. Colonies are light tan and secrete brown or tan diffusible pigments (Table 3.3). Odor is classic of geosmin production: earthy and intense. Sporulation was not observed on TSA when isolates were grown alone but was observed on Oatmeal Agar (OA) and Maltose Yeast Media (MYM).

On MYM solid media, colonies are entire with slightly ciliate edges. Dense colonies grow together to form irregular edges that curl back up and over the colonies, away from the media. Surface is pale tan, somewhat matte, bumpy and complex with peeling back of edges. Within several days to a

week, the surface becomes a matte velvety white with sporulation. Colonies are firm and able to be scraped from the agar surface, with some breakage.

In liquid Supplemented Grace's Media (SGM) *S. solapis* initially grows in classical *Streptomyces* form, forming small fluffy spheres. However, after 2-3 days, the filaments fragment into smaller pieces and fall out of solution into a pellet.

Streptomyces nidicoloris sp. nov.

On Tryptic Soy Agar (TSA) solid media, colonies are irregular in shape and have lobate edges that tend to be raised from the media surface on the edges, creating a 'donut'-like appearance of early colonies, which then grow together. For older colonies or lawns, the surface ranges between tightly wrinkled (center) and flat with raised wrinkled edges. Colonies are opaque, cream to tan in color, and with matte surface and viscous to hard texture, they tend to break apart when picking them. Colonies are light tan and secrete pinkish tan diffusible pigments (Table 3.3). Odor is often absent, but occasionally weakly earthy, suggesting geosmin production.

On MYM solid media, colonies are entire with slightly ciliate edges. Dense colonies grow together to form irregular edges which curl back up and over the colonies. Surface is pale tan, matte, bumpy and complex with peeling back of edges. Spore formation was not observed on any media tested.

In liquid SGM *S. nidicoloris* sp. nov. initially grows in classical *Streptomyces* form, forming small fluffy spheres. However, after 2-3 days, the filaments fragment into smaller pieces and fall out of solution into a pellet.

Physiology:

Noticeable diffusible pigments were only produced by the new isolates, with *S. solapis* producing tan-brown pigmentation and *S. nidicoloris* sp. nov. producing a pinkish-tan pigment on TSA. The reference species did not produce noticeable diffusible pigmentation on TSA. Salt tolerance also differentiated the species, with all *S. solapis* strains being salt tolerant (10%) along with *S. fractus,* whereas *S. endophyticus*, *S. kunmingensis* and *S. variegatus* are not salt tolerant. A similar pattern was observed for fragmentation in liquid media and growth at 37°C, where all of the new isolates as well as *S.*

fractus fragmented after several days in liquid media and grew at 37°C, where the other species did not. Spore formation was observed for all *S. solapis* strains on OA, but was not observed for *S. nidicoloris* sp. nov. or for *S. fractus* on any tested media (Table 3.3).

Table 3.3

Strain or species	Diffusible pigment (TSA)	Growth at		Growth with NaCl		Spore formation			Frag. in liquid	Geosmin production (TSA)
		25°C	37°C	5%	10%	TSA	OA	MA		
BH034 (*S. solapis* sp. nov) [T]	w, tan-brown *	+	+	+	+	-	+	-	+	+
BH055 (*S. solapis* sp. nov)	+, dark brown	+	+	+	+	-	+	+	+	+
BH097 (*S. solapis* sp. nov)	+, light brown	+	+	+	+	-	+	-	+	+
BH104 (*S. solapis* sp. nov)	+, light brown	+	+	+	+	-	+	-	+	+
BH105 (*S. solapis* sp. nov)	+, dark brown	+	+	nd	+	-	+/-	nd	+	+
BH106 (*S. nidicoloris* sp. nov) [T]	+, pinkish tan	+	+	nd	+/-	-	-	-	+	+/-
S. fractus MV32 [T]	-	+	+	+[12]	+[12]	-	-	-	+	+
S. endophyticus YIM65594 [T]	-[13]	+[a]	-[12]	+[12]	+/- [12]	nd	nd	nd	-[12]	nd
S. kunmingensis NBRC 14463 [T]	-	+	+/-	+/- [12]	+/- [12]	-	+	+	-	+
S. variegatus B-16380	- **	+	-	nd	-	-	+	+	-	+

+ positive; +/- weak; - not observed; nd no data
* once made yellow exudate on colony surface in response to fungi
**makes red and green pigments on OA media, but they do not diffuse into the surrounding agar

Description of the New Species

Streptomyces solapis sp. nov. [sohl-AY-pis, referring to the Latin 'sola' for solitary and 'apis' for bee, as the species was isolated from *Anthophora bomboides*, a solitary bee species]. The type strain is BH34 [T] and was isolated from a pollen provision in a brood cell of developing *Anthophora bomboides.* It is a gram-positive, filamentous bacterium. It exhibits fragmenting growth in liquid media and inhibits the

growth of several bee associated filamentous fungi (Fig. 2.6) [11]. It grows optimally 25-37°C on Tryptic Soy Agar or in liquid Supplemented Grace's Media. It produces tan-brown diffusible pigment on solid media, and is halotolerant to at least 10% NaCl. It consistently produces spores on Oatmeal Agar (OA). The genome of *Streptomyces solapis* sp. nov. type strain (BH34^T) is 9.6 Mb with a GC content of 71.0%. The type strain genome contains 8,716 predicted genes, including 22 biosynthetic gene clusters (BGCs) identified by antiSMASH. Phylogenetic analysis of the whole genome places it within the genus *Streptomyces*, related to *Streptomyces endophyticus* and *Streptomyces fractus*.

Streptomyces nidicoloris sp. nov. [nih-dee-koh-LOHR-iss, referring to the Latin "nidus" meaning nest, "colere" meaning "to dwell", and together meaning "of the nest dweller", as it was isolated from the nest of the ground nesting solitary bee *Anthophora bomboides*]. The type strain is BH106 and was isolated from an *A. bomboides* pupa with a brood cell. It is a gram-positive, filamentous bacterium. It exhibits fragmenting growth in liquid media. It grows optimally 25-37°C on Tryptic Soy Agar. It produces pink to tan diffusible pigment on solid TSA media and can weakly grow in 10% NaCl. It did not produce spores on any tested media type. The genome of the *Streptomyces nidicoloris* sp. nov. type strain (BH106) is 9.4 Mb with a GC content of 70.7%. It contains 8,426 predicted genes, including 16 BGCs as predicted by antiSMASH. Phylogenetic analysis places this species as sister to *Streptomyces endophyticus* and related to *Streptomyces fractus.*

Discussion

Streptomyces spp. were previously thought to be mostly free-living soil dwelling bacteria not commonly involved in direct symbiosis with hosts[46]. However, there are also many examples of symbiotic *Streptomyces* associated with plants and animals[8–10,47]. These relationships are often mutualisms, with the host providing a consistent growth environment and transmission of the bacteria between generations, and the *Streptomyces* providing protection from infection through production of secondary metabolites[10,48,49]. In Chapter 2, I found that *Streptomyces* is present throughout the development of the bee (*Anthophora bomboides*), but is especially abundant during overwintering, when

the bee faces heightened pathogen pressure. I isolated four of the six strains described here during my research for Ch. 2, and showed that these *Streptomyces* isolates could inhibit the growth of bee fungal pathogens, leading me to sequence the genomes and explore these strains further.

Genomic analysis showed that the bee isolates described here separate into two species, one being a clade of five closely related isolates, here named *Streptomyces solapis* sp. nov., and the other consisting of one isolate, here named *S. nidicoloris* sp. nov. This finding was supported by whole genome comparison methods (ANI, dDDH), as well as MLSA and whole genome trees, which confirmed the strong support for separation of these isolates from known species and into these two new species. The two species most closely related to the new isolates are *S. endophyticus* and *S. fractus* (Fig. 3.1). Both are associated with a host, with *S. endophyticus* being associated with the roots of *Artemisia annua* and *S. fractus* being associated with the gut of the black mound termite (*Amitermes hastatus*)[12,13]. The genome of *S. endophyticus* YIM65594 had been previously sequenced and was available on NCBI, but it was not available in any free culture collections, thus I used only the genome and literature review for comparisons; the genome of *S. fractus* had not been sequenced, so I ordered the strain (MV32^{T}) and had it sequenced, which allowed me to compare with the bee isolated strains, alongside physiological comparisons. Interestingly, the physiology of the bee isolated strains was most like that of *S. fractus*, which was also isolated from a soil-dwelling insect (black mound termite). The similarities included salt tolerance, fragmentation in liquid media, and growth at 37°C, which may be interesting to explore as potential adaptations to host association in further studies[12].

As *Streptomyces* are known for their production of secondary metabolites, I analyzed the composition of biosynthetic gene clusters in the isolate genomes as compared to the most closely related species and found that *S. solapis* sp. nov. strains have unique biosynthetic gene clusters as compared to close relatives. The BGCs are distinct among the two clades of *S. solapis*, with clade 2 (BH55/BH104/BH105) having the highest number of unique BGCs, though they were not all consistently found in all three strains (Fig. 3.3). Clade 1 (BH34^{T}/BH97) showed higher inhibition of *Ascosphaera* apis, a bee fungal pathogen, than clade 2 (Ch. 2, Fig. 3.3) which indicates that one (or both) biosynthetic

gene clusters that differentiate clade 1 from 2 may encode biosynthetic machinery for an antifungal. I explored one of these unique BGCs which had some similarity to a known Type II Polyketide Synthase (T2PKS) BGC. T2PKS produce aromatic polyketides, which commonly have biological activity and are used as antibacterial (erythromycin, tetracycline), anticancer (anthracycline, doxorubicin), antifungal (amphotericin, griseofulvin), and antiparasitic (avermectin) drugs[45]. This medically important metabolite class is most commonly produced by members of the Actinobacteria (like *Streptomyces*)[45,50]. The major steps in aromatic polyketide production are: 1) load acyl carrier protein (ACP), 2) iterative chain extension by ketosynthase (KS domain) and 3) cyclization and/or aromatization via thioesterase (TE domain). Using antiSMASH domain detection and alignment of the BGC with closest known clusters, I found that the T2PKS BGC of clade 1 (BH34^{T}/BH97) do include the major biosynthetic components and essential domains of a T2PKS, but the putative modifier genes are different from those of known clusters, indicating that the product may be a novel aromatic polyketide[50,51].

It is also interesting to note that these two clades were not separated into different bee developmental stages, but instead co-occurred in multiple developmental timepoints (early stages and overwintering stage) (Table 3.1). This, combined with the consistently observed high diversity of *Streptomyces* ASVs throughout bee development, and differences in antifungal activity of these isolates (Fig. 3.3BC, Ch. 2) suggests that the diversity of strains may be somehow beneficial. In many circumstances, tight host-microbe symbiotic relationships lead to genome erosion and tightening specificity between host and microbe as they co-evolve, with the host selecting for specific strain characteristics, products, or functions, and the microbial population becoming more homogeneous and dependent on the host, losing now-extraneous genes as it is vertically transmitted in a protected, consistent environment[52–56]. However, this is not always the case. Some well-established mutualisms involve mixed strains of the symbiotic bacteria[57,58]. In the *Anthophora bomboides* system, *Streptomyces* strain and thus BGC diversity could allow the bee and its microbial community to better cope with changing pathogen stressors, as different strains may be better suited for defense against different fungi, as would be seen in a "bet hedging" strategy[59–61]. Other scenarios are also possible: 1) the bee lacks tight

control of *Streptomyces* transmission, and instead recruits *Streptomyces* regularly from a yet unsampled area of the environment or 2) the symbiosis is in early stages, meaning the predicted genome erosion and reduction in strain diversity has yet to occur.

The *A. bomboides* brood cell houses a complex microbiome. Besides the aforementioned Actinobacteria (*Streptomyces* and others), it also hosts a highly prevalent and abundant fungal associate, *Moniliella spathulata*. This association, as described in Ch. 2, shows a pattern more like traditional vertically transmitted symbionts, exhibiting low diversity of strains (likely only one) and near perfect transmission (found in all but one examined brood cells)[62,63]. Interestingly, the *Streptomyces solapis* BH34^{T} isolated from the brood cell was shown to also inhibit this ubiquitous fungal brood associate, bringing up the question of how these microbes can reliably co-exist in the brood cell. It is possible that regulation of BGC expression is different within the brood cell, or that the two organisms are spatially separated to preclude interaction and inhibition by the *Streptomyces.* This interaction will require further research.

Significance

Pathogenic fungi continue to threaten human health, as well as the productivity of animals and plants cultivated for agriculture[64]. Infection and mortality from pathogenic fungi is an increasing threat due to emerging fungal species, increasing resistance to existing antifungal compounds, and limited antifungal modes of action available for therapeutic use[65]. Much effort has been dedicated to antifungal natural products discovery from soil-dwelling bacteria, marine organisms and other potential sources of novel chemistries[8,66–68]. However, isolation campaign success has been limited by context-specific metabolite production, compound rediscovery, and off-target toxicity for eukaryotic host animals[69]. To overcome these challenges, host-microbe symbiotic systems have been proposed as platforms for antifungal chemistry discovery, but few systems have been leveraged to date. Insect-microbe systems specifically have been shown to hold exceptional potential for novel, safe, and effective antifungal chemistry[8,10,67].

The data presented here and in concert with Ch. 2 support the use of an ecological comparative approach in insect-microbe systems, as I show that host-isolated strains show specific patterns of antifungal activity that are reflected in variation in BGC content. Such variation can be harnessed to refine potential bioactive targets within complex chemical mixtures. For example, clade 1 had higher activity against *Ascosphaera*, and two novel BGCs not found in the other clade (a type 2 polyketide and a non-ribosomal peptide, Fig. 3.3B-C); these can now be specifically targeted in metabolomic screening and extractions to test for activity. These genomes and analysis will allow further exploration of previously undescribed metabolite diversity and may yield novel antifungal agents that could be leveraged for therapeutic use.

Figures

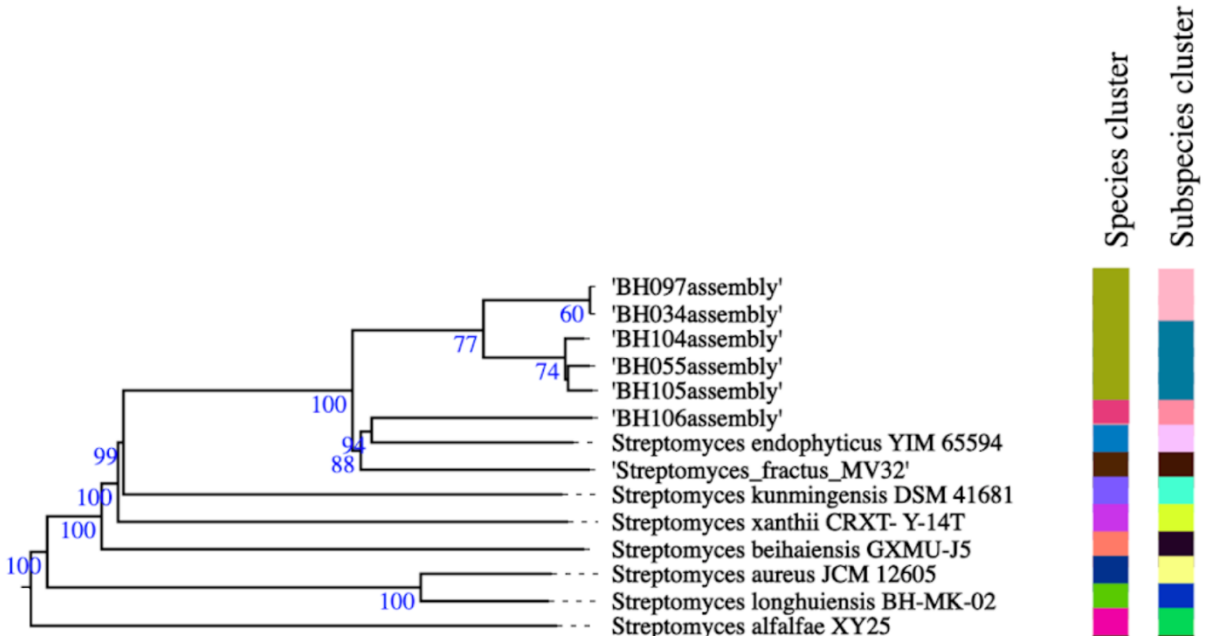

Figure 3.1- A) Subset of genome tree created on DSMZ server, inferred with FastME 2.1.6.1 from GBDP distances calculated from genome sequences. The branch lengths are scaled in terms of GBDP distance formula d5. The numbers at nodes are GBDP pseudo-bootstrap support values > 60 % from 100 replications, with an average branch support of 87.5 %. Species cluster and subspecies cluster are represented by various color blocks and show distinction for the two new proposed species (in green- top, and red- just below), as well as the subspecies clustering within *S. solapis* sp. nov.

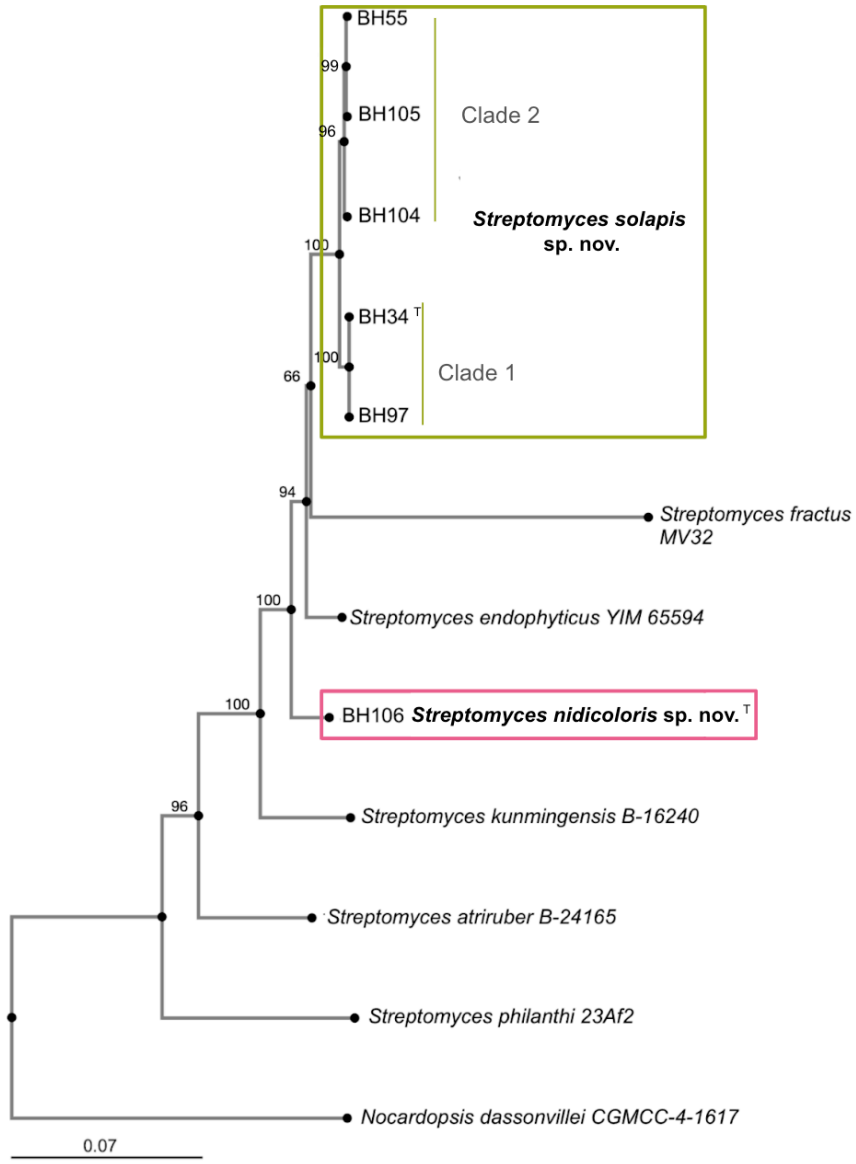

Figure 3.1- B) Five gene multilocus sequence alignment was performed using genes commonly used for phylogeny in existing Streptomyces literature (*atpD, gyrB, recA, rpoB* and *trpB*), alignment performed on MAFFT with MAFFT-L-INS-i. Conserved sites (2,278) were then used to construct a NJ tree using Jukes-Cantor model. The numbers at nodes indicate bootstrap support values >60 % from 1000 replications. Green rectangle (top) outlines the clade of five isolates representing *S. solapis* sp. nov. with the two clusters labeled as Clade 1 and Clade 2. The red rectangle (center) indicates the isolate representing *S. nidicoloris* sp. nov. Branch length indicates base changes per 100 bases, scale bar in bottom left.

	BH034	BH097	BH055	BH104	BH105	BH106	*S. endophyticus*	*S.fractus*
BH034	100.00	99.92	96.60	96.62	96.57	92.69	92.93	92.40
BH097		100.00	96.61	96.62	96.53	92.68	92.97	92.44
BH055			100.00	99.16	99.16	92.52	93.00	92.34
BH104				100.00	99.12	92.60	92.99	92.39
BH105					100.00	92.56	92.99	92.34
BH106						100.00	93.43	92.79
S. endophyticus							100.00	92.05
S.fractus								100.00

Figure 3.2- Whole genome Average Nucleotide Identity (ANI) comparisons between isolated strains and the two most closely related previously described species. ANI was calculated using fastANI (v.1.34). Numbers represent the ANI value of the genome in the row as compared to the column. The color of boxes with ANI values are on a gradient from yellow (lower) to dark green (higher) ANI. The cutoff for species level is 95% ANI.

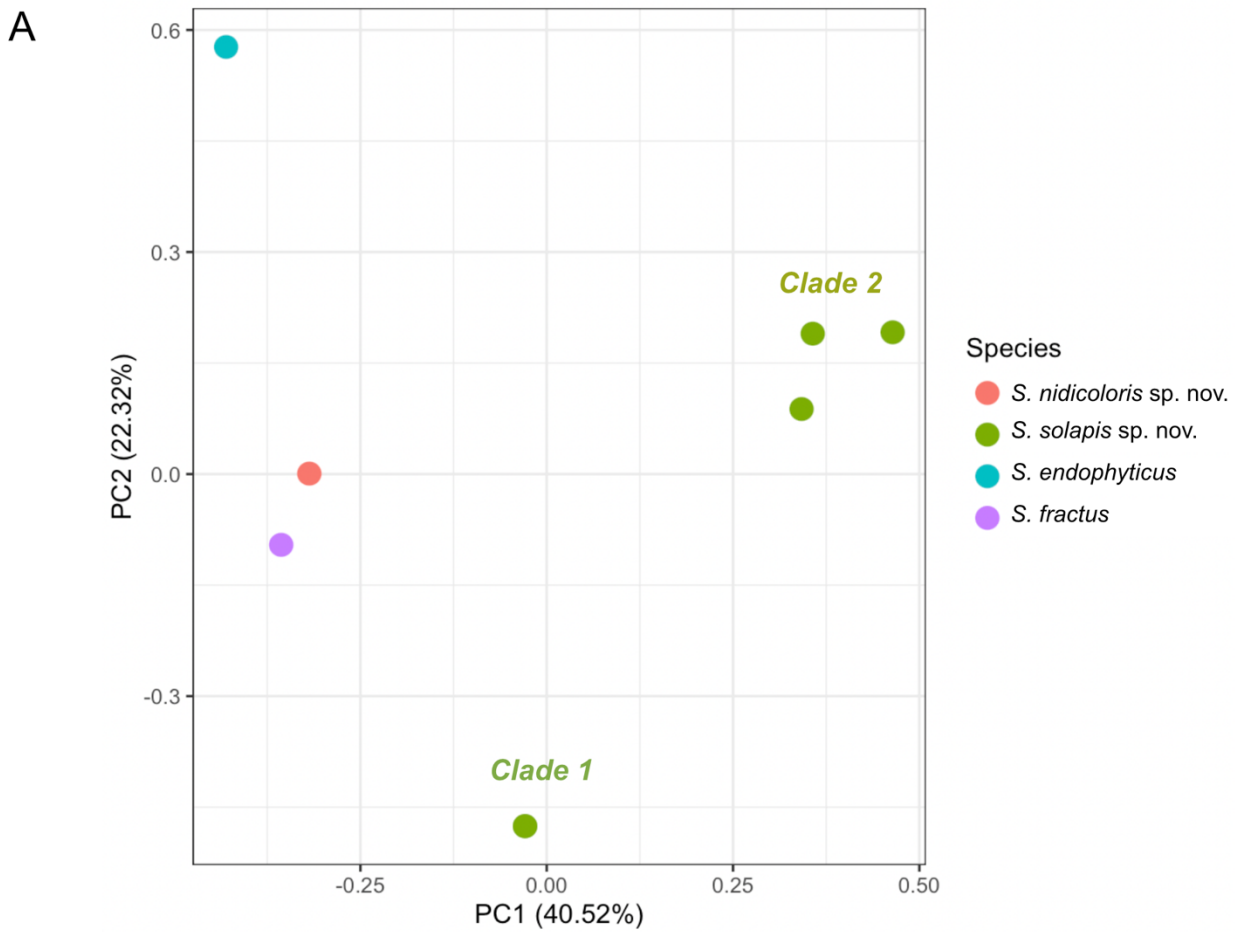

Figure 3.3- A) PCA plot of biosynthetic gene cluster composition, showing distinction of BGC composition based both on species and on subclade. Analysis was limited to differentially present BGCs. Color represents actual or proposed species, labels indicate clade within *S. solapis* sp. nov. BH34^{T} and BH97 are identical in BGC composition and thus the points are directly overlapping. PCA made with prcomp() in R "stats" package (scale= T).

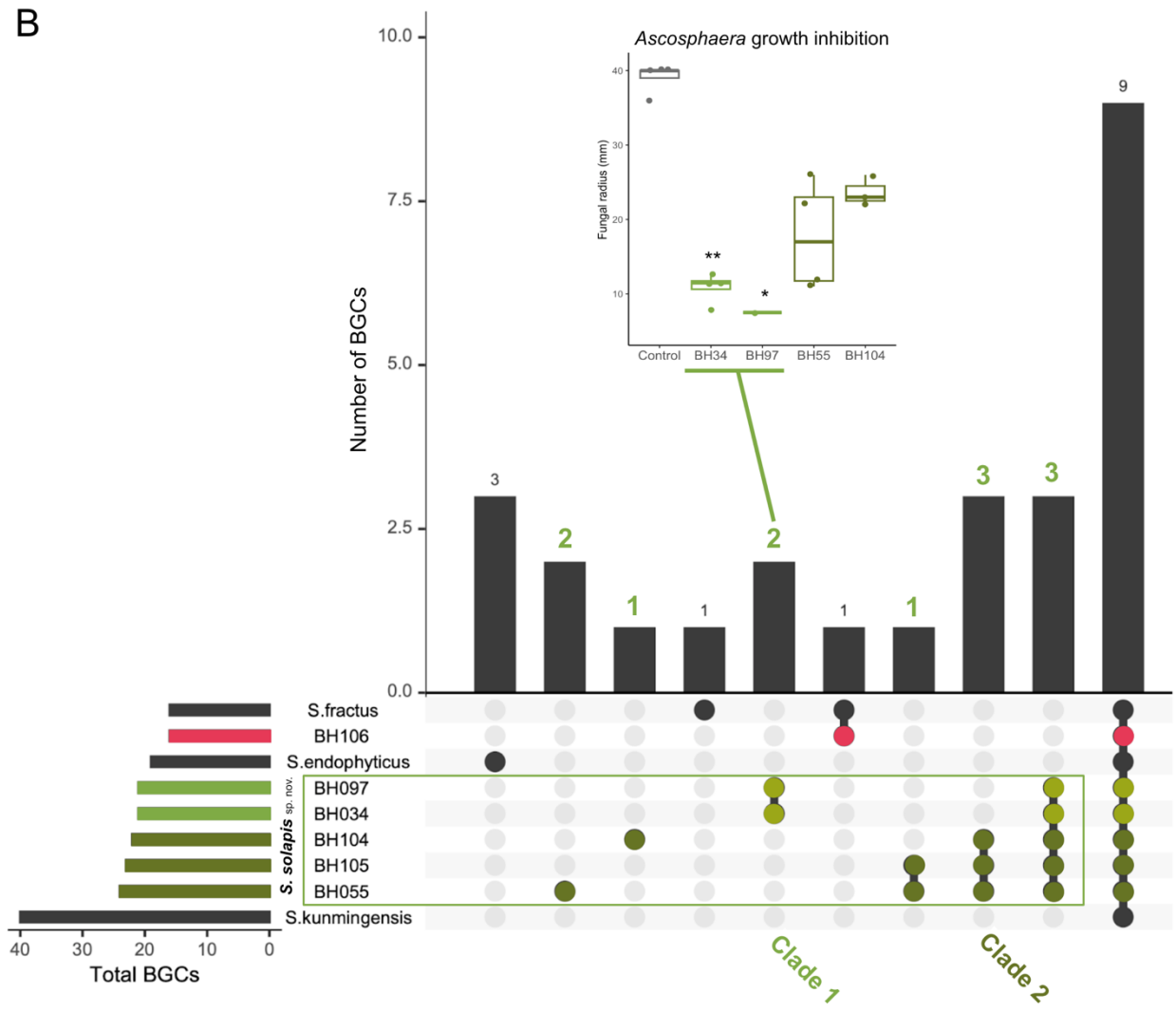

Figure 3.3- B) Upset plot showing biosynthetic gene cluster overlap between bee isolates *(S. solapis* sp. nov., two clades, *S. nidicoloris* sp. nov., *S. endophyticus*, *S. fractus,* and *S. kunmingensis*). Total number of BGCs in each species or group indicated on far left as black horizontal bars. Filled in dots indicate individuals or groups, with the bar directly above the dots indicating the number of unique BGCs in that individual or group. *Streptomyces solapis* sp. nov. as a species has 12 BGCs not found in close relatives (numbers bolded in green), Clade 1 has two biosynthetic gene clusters not found in the other groups. There are no BGCs that specifically distinguish all bee isolates from the other closest species. Made with UpsetR package. Not all comparisons are shown, see Appendix III Figure S1 for all groupings. Inset boxplot: Recolored section of Figure 2.6 showing differential inhibition of fungus *Ascosphaera apis* by four isolates of *S. solapis* sp. nov. BH34^{T} and BH97 are in Clade 1, with higher inhibition than BH55 and BH104, from Clade 2. Green lines connect the isolates belonging to Clade 1, and the bar indicating the two unique BGCs of that clade.

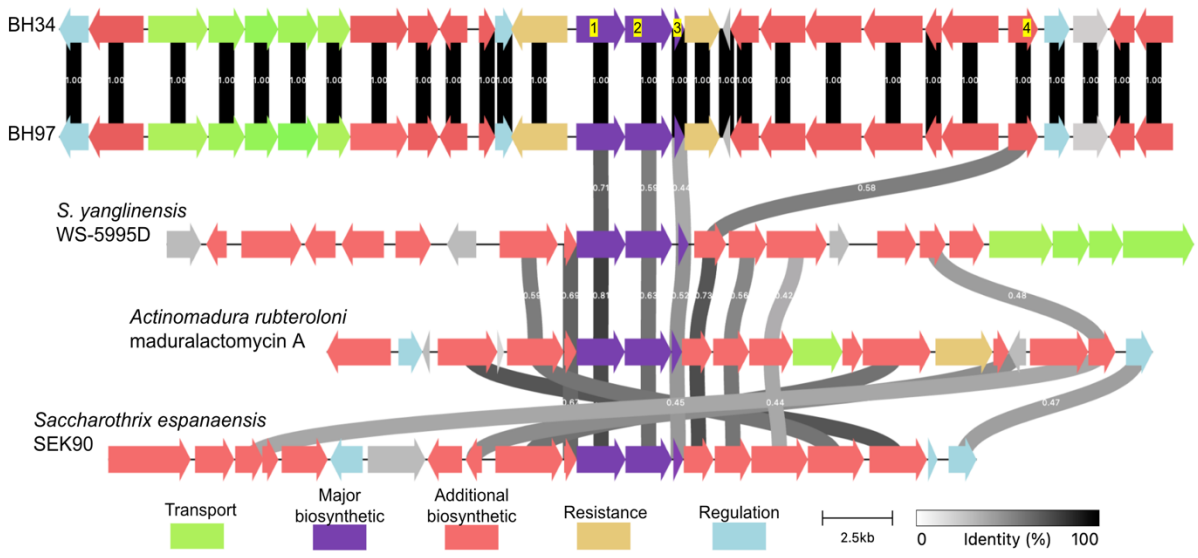

Figure 3.4- Novel Type II Polyketide Synthase (T2PKS) gene cluster in Clade 1 of *S. solapis* sp. nov. Clinker gene cluster alignment showing partial T2PKS BGC region in BH34^T and BH97 as compared to most similar known gene clusters (determined in antiSMASH from MIBiG 3.1 known cluster database). Colored horizontal arrows indicate genes, with different colors representing gene type, as assigned by antiSMASH (green, transport-related; red- tailoring (additional biosynthesis) related; purple, Major biosynthetic genes/ domains for T2PKS; tan, resistance related; light blue, regulatory related; grey indicates unknown or "other" gene group). The alignment is based on sequence homology, and gene blocks with over 40% identity are connected vertically by grey bars, representing synteny between clusters. Highly conserved genes are shown with darker grey/black bars, while less conserved regions have lighter grey bars. The four homologous genes (indicated by yellow numbers 1-4 at top of figure) are homologous to the biosynthetic genes in the known related clusters, whose products constitute the main machinery for polyketide synthesis. The products of genes indicated by 1 and 2 perform the iterative condensation that creates the polyketide backbone. Domain match to T2PKS: 1- E-value: 5.1e-55, Score: 178.9; 2- E-value: 1.7e-25, Score: 81.6. The third gene (indicated by 3 at top of figure) is homologous to the genes encoding an acyl carrier protein (ACP) for carrying intermediates: Domain match to ACP: E-value: 1.8e-15. Score: 48.9. Number 4 indicates the gene homologous to ketoreductase (PKS_KR), a tailoring enzyme, in the related BGCs, Domain match PKS_KR: E-value: 2.9e-12. Score: 38.7. Scores and E-values determined by HMMER in antiSMASH, higher score represents better alignment between the provided sequence and expected sequence pattern for a specific domain, lower E-value indicates confidence that the match did not occur by chance.

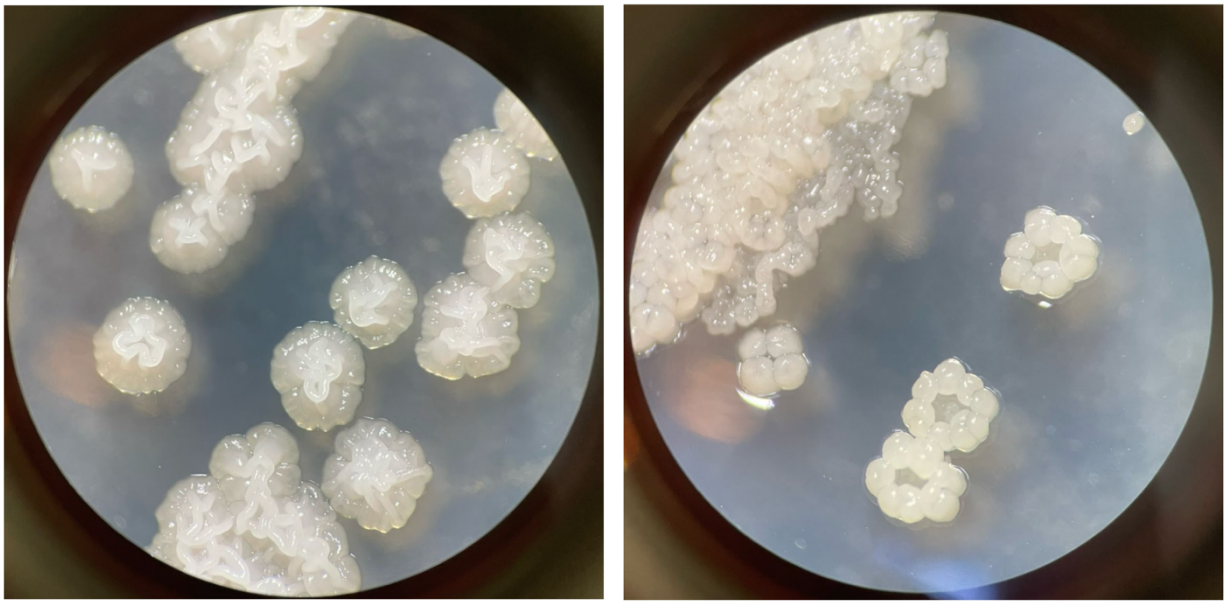

Figure 3.5- Colony appearance of new *Streptomyces* strains. **A)** *Streptomyces solapis* sp. nov. BH105 and **B)** Streptomyces *nidicoloris sp. nov. BH106* on TSA media after 4 days of growth at 28°C. Images taken on dissection microscope with a black background to enhance contrast, at 30x.

References

1. Otani, H., Udwary, D.W., and Mouncey, N.J. (2022). Comparative and pangenomic analysis of the genus Streptomyces. Sci Rep *12*, 18909. https://doi.org/10.1038/s41598-022-21731-1.

2. Chater, K.F. (2006). *Streptomyces* inside-out: a new perspective on the bacteria that provide us with antibiotics. Phil. Trans. R. Soc. B *361*, 761–768. https://doi.org/10.1098/rstb.2005.1758.

3. Procópio, R.E. de L., Silva, I.R. da, Martins, M.K., Azevedo, J.L. de, and Araújo, J.M. de (2012). Antibiotics produced by Streptomyces. Braz J Infect Dis *16*, 466–471. https://doi.org/10.1016/j.bjid.2012.08.014.

4. Alam, K., Mazumder, A., Sikdar, S., Zhao, Y.-M., Hao, J., Song, C., Wang, Y., Sarkar, R., Islam, S., Zhang, Y., et al. (2022). Streptomyces: The biofactory of secondary metabolites. Front. Microbiol. *13*. https://doi.org/10.3389/fmicb.2022.968053.

5. Lee, N., Kim, W., Hwang, S., Lee, Y., Cho, S., Palsson, B., and Cho, B.-K. (2020). Thirty complete Streptomyces genome sequences for mining novel secondary metabolite biosynthetic gene clusters. Sci Data *7*, 55. https://doi.org/10.1038/s41597-020-0395-9.

6. Seshadri, R., Roux, S., Huber, K.J., Wu, D., Yu, S., Udwary, D., Call, L., Nayfach, S., Hahnke, R.L., Pukall, R., et al. (2022). Expanding the genomic encyclopedia of Actinobacteria with 824 isolate reference genomes. Cell Genomics *2*. https://doi.org/10.1016/j.xgen.2022.100213.

7. Deshpande, B.S., Ambedkar, S.S., and Shewale, J.G. (1988). Biologically active secondary metabolites from Streptomyces. Enzyme and Microbial Technology *10*, 455–473. https://doi.org/10.1016/0141-0229(88)90023-3.

8. Chevrette, M.G., Carlson, C.M., Ortega, H.E., Thomas, C., Ananiev, G.E., Barns, K.J., Book, A.J., Cagnazzo, J., Carlos, C., Flanigan, W., et al. (2019). The antimicrobial potential of Streptomyces from insect microbiomes. Nat Commun *10*. https://doi.org/10.1038/s41467-019-08438-0.

9. Matarrita-Carranza, B., Moreira-Soto, R.D., Murillo-Cruz, C., Mora, M., Currie, C.R., and Pinto-Tomas, A.A. (2017). Evidence for Widespread Associations between Neotropical Hymenopteran Insects and Actinobacteria. Front Microbiol *8*, 2016. https://doi.org/10.3389/fmicb.2017.02016.

10. Seipke, R.F., Kaltenpoth, M., and Hutchings, M.I. (2012). Streptomyces as symbionts: an emerging and widespread theme? FEMS Microbiology Reviews *36*, 862–876. https://doi.org/10.1111/j.1574-6976.2011.00313.x.

11. Christensen, S.M., Srinivas, S.N., McFrederick, Q.S., Danforth, B.N., Buchmann, S.L., and Vannette, R.L. (2024). Symbiotic bacteria and fungi proliferate in diapause and may enhance overwintering survival in a solitary bee. The ISME Journal *18*, wrae089. https://doi.org/10.1093/ismejo/wrae089.

12. Rohland, J., and Meyers, P.R. (2015). Streptomyces fractus sp. nov., a novel streptomycete isolated from the gut of a South African termite. Antonie Van Leeuwenhoek *107*, 1127–1134. https://doi.org/10.1007/s10482-015-0404-8.

13. Li, J., Zhao, G.-Z., Zhu, W.-Y., Huang, H.-Y., Xu, L.-H., Zhang, S., and Li, W.-J. (2013). Streptomyces endophyticus sp. nov., an endophytic actinomycete isolated from Artemisia annua L. Int J Syst Evol Microbiol *63*, 224–229. https://doi.org/10.1099/ijs.0.035725-0.

14. Garbeva, P., Avalos, M., Ulanova, D., van Wezel, G.P., and Dickschat, J.S. (2023). Volatile sensation: The chemical ecology of the earthy odorant geosmin. Environmental Microbiology *25*, 1565–1574. https://doi.org/10.1111/1462-2920.16381.

15. Altschul, S.F., Gish, W., Miller, W., Myers, E.W., and Lipman, D.J. (1990). Basic local alignment search tool. J Mol Biol *215*, 403–410. https://doi.org/10.1016/S0022-2836(05)80360-2.

16. Weisburg, W.G., Barns, S.M., Pelletier, D.A., and Lane, D.J. (1991). 16S ribosomal DNA amplification for phylogenetic study. Journal of Bacteriology *173*, 697–703. https://doi.org/10.1128/jb.173.2.697-703.1991.

17. Kolmogorov, M., Yuan, J., Lin, Y., and Pevzner, P.A. (2019). Assembly of long, error-prone reads using repeat graphs. Nat Biotechnol *37*, 540–546. https://doi.org/10.1038/s41587-019-0072-8.

18. Parks, D.H., Imelfort, M., Skennerton, C.T., Hugenholtz, P., and Tyson, G.W. (2015). CheckM: assessing the quality of microbial genomes recovered from isolates, single cells, and metagenomes. Genome Res. *25*, 1043–1055. https://doi.org/10.1101/gr.186072.114.

19. Seemann, T. (2014). Prokka: rapid prokaryotic genome annotation. Bioinformatics *30*, 2068–2069. https://doi.org/10.1093/bioinformatics/btu153.

20. Konstantinidis, K.T., and Tiedje, J.M. (2005). Genomic insights that advance the species definition for prokaryotes. Proceedings of the National Academy of Sciences *102*, 2567–2572. https://doi.org/10.1073/pnas.0409727102.

21. Meier-Kolthoff, J.P., and Göker, M. (2019). TYGS is an automated high-throughput platform for state-of-the-art genome-based taxonomy. Nat Commun *10*, 2182. https://doi.org/10.1038/s41467-019-10210-3.

22. Meier-Kolthoff, J.P., Carbasse, J.S., Peinado-Olarte, R.L., and Göker, M. (2022). TYGS and LPSN: a database tandem for fast and reliable genome-based classification and nomenclature of prokaryotes. Nucleic Acids Research *50*, D801–D807. https://doi.org/10.1093/nar/gkab902.

23. Ondov, B.D., Treangen, T.J., Melsted, P., Mallonee, A.B., Bergman, N.H., Koren, S., and Phillippy, A.M. (2016). Mash: fast genome and metagenome distance estimation using MinHash. Genome Biology *17*, 132. https://doi.org/10.1186/s13059-016-0997-x.

24. Lagesen, K., Hallin, P., Rødland, E.A., Stærfeldt, H.-H., Rognes, T., and Ussery, D.W. (2007). RNAmmer: consistent and rapid annotation of ribosomal RNA genes. Nucleic Acids Res *35*, 3100–3108. https://doi.org/10.1093/nar/gkm160.

25. Auch, A.F., Henz, S.R., Holland, B.R., and Göker, M. (2006). Genome BLAST distance phylogenies inferred from whole plastid and whole mitochondrion genome sequences. BMC Bioinformatics *7*, 350. https://doi.org/10.1186/1471-2105-7-350.

26. Lefort, V., Desper, R., and Gascuel, O. (2015). FastME 2.0: A Comprehensive, Accurate, and Fast Distance-Based Phylogeny Inference Program. Molecular Biology and Evolution *32*, 2798–2800. https://doi.org/10.1093/molbev/msv150.

27. Kreft, Ł., Botzki, A., Coppens, F., Vandepoele, K., and Van Bel, M. (2017). PhyD3: a phylogenetic tree viewer with extended phyloXML support for functional genomics data visualization. Bioinformatics *33*, 2946–2947. https://doi.org/10.1093/bioinformatics/btx324.

28. Ciufo, S., Kannan, S., Sharma, S., Badretdin, A., Clark, K., Turner, S., Brover, S., Schoch, C.L., Kimchi, A., and DiCuccio, M. (2018). Using average nucleotide identity to improve taxonomic assignments in prokaryotic genomes at the NCBI. Int J Syst Evol Microbiol *68*, 2386–2392. https://doi.org/10.1099/ijsem.0.002809.

29. Hyatt, D., Chen, G.-L., LoCascio, P.F., Land, M.L., Larimer, F.W., and Hauser, L.J. (2010). Prodigal: prokaryotic gene recognition and translation initiation site identification. BMC Bioinformatics *11*, 119. https://doi.org/10.1186/1471-2105-11-119.

30. Laslett, D., and Canback, B. (2004). ARAGORN, a program to detect tRNA genes and tmRNA genes in nucleotide sequences. Nucleic Acids Res *32*, 11–16. https://doi.org/10.1093/nar/gkh152.

31. Eddy, S.R. (2011). Accelerated Profile HMM Searches. PLOS Computational Biology *7*, e1002195. https://doi.org/10.1371/journal.pcbi.1002195.

32. The UniProt Consortium (2017). UniProt: the universal protein knowledgebase. Nucleic Acids Research *45*, D158–D169. https://doi.org/10.1093/nar/gkw1099.

33. O'Leary, N.A., Wright, M.W., Brister, J.R., Ciufo, S., Haddad, D., McVeigh, R., Rajput, B., Robbertse, B., Smith-White, B., Ako-Adjei, D., et al. (2016). Reference sequence (RefSeq) database at NCBI: current status, taxonomic expansion, and functional annotation. Nucleic Acids Res *44*, D733-745. https://doi.org/10.1093/nar/gkv1189.

34. Tatusova, T., Ciufo, S., Fedorov, B., O'Neill, K., and Tolstoy, I. (2014). RefSeq microbial genomes database: new representation and annotation strategy. Nucleic Acids Research *42*, D553–D559. https://doi.org/10.1093/nar/gkt1274.

35. Mistry, J., Chuguransky, S., Williams, L., Qureshi, M., Salazar, G.A., Sonnhammer, E.L.L., Tosatto, S.C.E., Paladin, L., Raj, S., Richardson, L.J., et al. (2021). Pfam: The protein families database in 2021. Nucleic Acids Research *49*, D412–D419. https://doi.org/10.1093/nar/gkaa913.

36. Kanehisa, M., Sato, Y., and Morishima, K. (2016). BlastKOALA and GhostKOALA: KEGG Tools for Functional Characterization of Genome and Metagenome Sequences. J Mol Biol *428*, 726–731. https://doi.org/10.1016/j.jmb.2015.11.006.

37. Kanehisa, M., and Sato, Y. (2020). KEGG Mapper for inferring cellular functions from protein sequences. Protein Science *29*, 28–35. https://doi.org/10.1002/pro.3711.

38. Blin, K., Shaw, S., Augustijn, H.E., Reitz, Z.L., Biermann, F., Alanjary, M., Fetter, A., Terlouw, B.R., Metcalf, W.W., Helfrich, E.J.N., et al. (2023). antiSMASH 7.0: new and improved predictions for detection, regulation, chemical structures and visualisation. Nucleic Acids Research *51*, W46–W50. https://doi.org/10.1093/nar/gkad344.

39. Terlouw, B.R., Blin, K., Navarro-Muñoz, J.C., Avalon, N.E., Chevrette, M.G., Egbert, S., Lee, S., Meijer, D., Recchia, M.J.J., Reitz, Z.L., et al. (2023). MIBiG 3.0: a community-driven effort to annotate experimentally validated biosynthetic gene clusters. Nucleic Acids Research *51*, D603–D610. https://doi.org/10.1093/nar/gkac1049.

40. Komaki, H. (2022). Resolution of housekeeping gene sequences used in MLSA for the genus Streptomyces and reclassification of Streptomyces anthocyanicus and Streptomyces tricolor as heterotypic synonyms of Streptomyces violaceoruber. Int J Syst Evol Microbiol *72*. https://doi.org/10.1099/ijsem.0.005370.

41. Labeda, D.P., Dunlap, C.A., Rong, X., Huang, Y., Doroghazi, J.R., Ju, K.-S., and Metcalf, W.W. (2017). Phylogenetic relationships in the family Streptomycetaceae using multi-locus sequence analysis. Antonie Van Leeuwenhoek *110*, 563–583. https://doi.org/10.1007/s10482-016-0824-0.

42. Katoh, K., Rozewicki, J., and Yamada, K.D. (2019). MAFFT online service: multiple sequence alignment, interactive sequence choice and visualization. Briefings in Bioinformatics *20*, 1160–1166. https://doi.org/10.1093/bib/bbx108.

43. Carro, L., Peix, Á., and Velázquez, E. (2021). The Taxonomy of Bacteria in the Genomic Era. In Developmental Biology in Prokaryotes and Lower Eukaryotes, T. G. Villa and T. de Miguel Bouzas, eds. (Springer International Publishing), pp. 289–309. https://doi.org/10.1007/978-3-030-77595-7_12.

44. Goris, J., Konstantinidis, K.T., Klappenbach, J.A., Coenye, T., Vandamme, P., and Tiedje, J.M. (2007). DNA–DNA hybridization values and their relationship to whole-genome sequence similarities. International Journal of Systematic and Evolutionary Microbiology *57*, 81–91. https://doi.org/10.1099/ijs.0.64483-0.

45. Wang, J., Zhang, R., Chen, X., Sun, X., Yan, Y., Shen, X., and Yuan, Q. (2020). Biosynthesis of aromatic polyketides in microorganisms using type II polyketide synthases. Microb Cell Fact *19*, 110. https://doi.org/10.1186/s12934-020-01367-4.

46. Barka, E.A., Vatsa, P., Sanchez, L., Gaveau-Vaillant, N., Jacquard, C., Klenk, H.-P., Clément, C., Ouhdouch, Y., and Van Wezel, G.P. (2016). Taxonomy, Physiology, and Natural Products of Actinobacteria. Microbiol Mol Biol Rev *80*, 1–43. https://doi.org/10.1128/MMBR.00019-15.

47. Nofiani, R., Rudiyansyah, Ardiningsih, P., Rizky, Zahra, S.T.A., Sukito, A., Weisberg, A.J., Chang, J.H., and Mahmud, T. (2023). Genome features and secondary metabolite potential of the marine symbiont Streptomyces sp. RS2. Arch Microbiol *205*, 244. https://doi.org/10.1007/s00203-023-03556-2.

48. Kaltenpoth, M., Schmitt, T., Polidori, C., Koedam, D., and Strohm, E. (2010). Symbiotic streptomycetes in antennal glands of the South American digger wasp genus Trachypus (Hymenoptera, Crabronidae). Physiological Entomology *35*, 196–200. https://doi.org/10.1111/j.1365-3032.2010.00729.x.

49. Ingham, C.S., Engl, T., Matarrita-Carranza, B., Vogler, P., Huettel, B., Wielsch, N., Svatoš, A., and Kaltenpoth, M. (2023). Host hydrocarbons protect symbiont transmission from a radical host defense. Proc Natl Acad Sci U S A *120*, e2302721120. https://doi.org/10.1073/pnas.2302721120.

50. Chen, S., Zhang, C., and Zhang, L. (2022). Investigation of the Molecular Landscape of Bacterial Aromatic Polyketides by Global Analysis of Type II Polyketide Synthases. Angewandte Chemie *134*, e202202286. https://doi.org/10.1002/ange.202202286.

51. Hertweck, C., Luzhetskyy, A., Rebets, Y., and Bechthold, A. (2007). Type II polyketide synthases: gaining a deeper insight into enzymatic teamwork. Nat. Prod. Rep. *24*, 162–190. https://doi.org/10.1039/B507395M.

52. Nechitaylo, T.Y., Sandoval-Calderón, M., Engl, T., Wielsch, N., Dunn, D.M., Goesmann, A., Strohm, E., Svatoš, A., Dale, C., Weiss, R.B., et al. (2021). Incipient genome erosion and metabolic streamlining for antibiotic production in a defensive symbiont. Proceedings of the National Academy of Sciences *118*, e2023047118. https://doi.org/10.1073/pnas.2023047118.

53. Wierz, J.C., Gaube, P., Klebsch, D., Kaltenpoth, M., and Flórez, L.V. (2021). Transmission of Bacterial Symbionts With and Without Genome Erosion Between a Beetle Host and the Plant Environment. Frontiers in Microbiology *12*.

54. Salem, H., Bauer, E., Kirsch, R., Berasategui, A., Cripps, M., Weiss, B., Koga, R., Fukumori, K., Vogel, H., Fukatsu, T., et al. (2017). Drastic Genome Reduction in an Herbivore's Pectinolytic Symbiont. Cell *171*, 1520-1531.e13. https://doi.org/10.1016/J.CELL.2017.10.029.

55. Wilson, A.C.C., and Duncan, R.P. (2015). Signatures of host/symbiont genome coevolution in insect nutritional endosymbioses. Proceedings of the National Academy of Sciences *112*, 10255–10261. https://doi.org/10.1073/pnas.1423305112.

56. Douglas, A.E. (2021). The Symbiotic Habit (Princeton University Press).

57. Nguyen, T.V., Wibberg, D., Vigil-Stenman, T., Berckx, F., Battenberg, K., Demchenko, K.N., Blom, J., Fernandez, M.P., Yamanaka, T., Berry, A.M., et al. (2019). Frankia-Enriched Metagenomes from the Earliest Diverging Symbiotic Frankia Cluster: They Come in Teams. Genome Biology and Evolution *11*, 2273–2291. https://doi.org/10.1093/gbe/evz153.

58. Bongrand, C., and Ruby, E.G. (2019). Achieving a multi-strain symbiosis: strain behavior and infection dynamics. ISME J *13*, 698–706. https://doi.org/10.1038/s41396-018-0305-8.

59. Vorburger, C., and Gouskov, A. (2011). Only helpful when required: a longevity cost of harbouring defensive symbionts. Journal of Evolutionary Biology *24*, 1611–1617. https://doi.org/10.1111/j.1420-9101.2011.02292.x.

60. Fujita, H., Aoki, S., and Kawaguchi, M. (2014). Evolutionary Dynamics of Nitrogen Fixation in the Legume–Rhizobia Symbiosis. PLoS One *9*, e93670. https://doi.org/10.1371/journal.pone.0093670.

61. Heath, K.D., and Stinchcombe, J.R. (2014). Explaining mutualism variation: a new evolutionary paradox? Evolution *68*, 309–317. https://doi.org/10.1111/evo.12292.

62. Su, Q., Wang, Q., Mu, X., Chen, H., Meng, Y., Zhang, X., Zheng, L., Hu, X., Zhai, Y., and Zheng, H. (2021). Strain-level analysis reveals the vertical microbial transmission during the life cycle of bumblebee. Microbiome *9*, 216. https://doi.org/10.1186/s40168-021-01163-1.

63. Paludo, C.R., Menezes, C., Silva-Junior, E.A., Vollet-Neto, A., Andrade-Dominguez, A., Pishchany, G., Khadempour, L., Do Nascimento, F.S., Currie, C.R., Kolter, R., et al. (2018). Stingless bee larvae require fungal steroid to pupate. Scientific Reports. https://doi.org/10.1038/s41598-018-19583-9.

64. Denning, D.W. (2024). Global incidence and mortality of severe fungal disease. The Lancet Infectious Diseases, S1473309923006928. https://doi.org/10.1016/S1473-3099(23)00692-8.

65. Nnadi, N.E., and Carter, D.A. (2021). Climate change and the emergence of fungal pathogens. PLoS Pathog *17*, e1009503. https://doi.org/10.1371/journal.ppat.1009503.

66. Watve, M.G., Tickoo, R., Jog, M.M., and Bhole, B.D. (2001). How many antibiotics are produced by the genus Streptomyces? Arch Microbiol *176*, 386–390. https://doi.org/10.1007/s002030100345.

67. Zhang, Z., Zhou, T., Harunari, E., Oku, N., and Igarashi, Y. (2020). Iseolides A–C, antifungal macrolides from a coral-derived actinomycete of the genus Streptomyces. J Antibiot *73*, 534–541. https://doi.org/10.1038/s41429-020-0304-7.

68. Donald, L., Pipite, A., Subramani, R., Owen, J., Keyzers, R.A., and Taufa, T. (2022). Streptomyces: Still the biggest producer of new natural secondary metabolites, a current perspective. Microbiology Research *13*, 418–465. https://doi.org/10.3390/microbiolres13030031.

69. Roemer, T., and Krysan, D.J. (2014). Antifungal Drug Development: Challenges, Unmet Clinical Needs, and New Approaches. Cold Spring Harb Perspect Med *4*, a019703. https://doi.org/10.1101/cshperspect.a019703.

Discussion

The work presented in this dissertation provides critical insights into the dynamic interactions between microbes, pollen, and bees. By exploring the influence of microbial partners on pollen digestion and microbial contributions to pollinator development and defense, this research advances our understanding of how microbes mediate key processes in pollination biology and pollinator fitness. Each chapter contributes a distinct perspective on these interactions, shedding light on previously understudied mechanisms that govern host-microbe symbioses in pollinators.

Chapter 1 demonstrated that nectar-associated bacteria, specifically *Acinetobacter* species, can induce pollen germination and bursting, allowing these microbes to access nutrient-rich pollen protoplasm[28]. This discovery provides a novel explanation for how some microbes can overcome pollen's protective barriers, through a mechanism that exploits the pollen's mechanism to degrade its own shell, even outside of the plant reproductive processes. The ability of *Acinetobacter* to enhance its fitness by inducing pollen germination reveals a new dimension to the role of microbes in pollination systems[29–32]. These bacteria may play an unrecognized role in facilitating nutrient access not only for themselves but also for the pollinators they interact with, influencing pollinator nutrition. The finding that *Acinetobacter* can specifically induce germination, while other nectar microbes such as *Metschnikowia* do not, suggests potential niche differentiation among floral microbes[33,34]. This phenomenon also raises broader ecological questions regarding potential cooperation of nectar microbes and pollen consumers, which were not addressed here[35,36]. Future research should investigate whether these interactions might influence pollinator health, and the degree to which nectar and bee associated microbes in general utilize this mechanism.

The second chapter of this dissertation shifted focus to the microbial communities associated with the development of a solitary bee, *Anthophora bomboides*. Prior to this work, solitary bee species were thought to pick up microbes anew each year as they interact with the environment, resulting in a

microbiome which resembles a subset of the environmental diversity, and is not generally consistent year to year due to lack of vertical transmission[27,37–40]. This chapter demonstrated that this is not always the case by showing that this solitary bee species can host a consistent, complex microbial community with potential for mutualistic contributions to bee fitness[41]. The core microbiome, dominated by Actinobacteria and *Moniliella spathulata,* was most abundant during diapause, implying that symbiotic microbes play essential roles in enhancing the overwintering survival of these bees, when they are most vulnerable to pathogens and cold stress. Actinobacteria, particularly *Streptomyces* species, were shown to inhibit bee pathogenic fungi, and their presence in bee brood likely confers protection against pathogens. *Moniliella spathulata* abundance was also correlated with increases in metabolites associated with cold tolerance (trehalose) and the genus is known from other studies to produce significant quantities of these metabolites[42–44]. This potential commensalism is supported by the fact that the yeast is highly prevalent and narrowly associated, in that only two ASVs of this fungus comprise the vast majority of bee-associated fungal reads. This result indicates tight and effective control of transmission through generations, a pattern that had not been reported previously in solitary bees[45,46]. These findings are significant, as they highlight the importance of microbial symbionts during development and diapause. Diapause is critical for resilience of insects, especially bee species, as it allows populations to "wait out" adverse seasonal conditions and time their emergence when plants begin flowering[24,47]. The role of microbial symbionts in supporting bees at various stages of development is therefore essential for our understanding and conservation of these critical pollinators, and exploration of microbial communities throughout bee development may lead to new insights into the roles and contributions of bee associated microbes.

Chapter 3 extends the findings from Chapter 2 by characterizing two novel species, *Streptomyces solapis* sp. nov. and *Streptomyces nidicoloris* sp. nov., isolated from the brood cells of *A. bomboides*. *Streptomyces solapis* sp. nov. was found to possess unique biosynthetic gene clusters that distinguish the two clades within the species and correlate with antifungal activity differences. The discovery of these

new species with active antifungal activity from a host-associated environment opens up exciting possibilities for natural product discovery[48]. *Streptomyces* species are renowned for their ability to produce bioactive compounds, including antibiotics and antifungals[49]. As indicated above, the presence of such microbes in bee brood may be part of a symbiotic relationship in which bees actively cultivate beneficial microbes to protect their brood from pathogenic fungi or other environmental threats[50,51]. The identification of these *Streptomyces* strains not only contributes to the growing knowledge of microbial diversity within pollinators but also underscores the potential of symbiotic relationships as reservoirs of novel bioactive compounds[48,52,53].

The findings presented in this dissertation have several broad implications for our understanding of pollination biology, microbial ecology, and host-microbe interactions generally. First, the discovery that nectar bacteria can induce pollen germination fundamentally changes our understanding of pollen digestion. This work suggests that microbes can play an active role in breaking down pollen's protective barriers, enabling themselves and possibly other pollen consumers to access essential nutrients. This has significant implications for both pollinator nutrition and plant reproductive strategies, as it suggests a previously unrecognized link between microbial activity and pollen consumption by pollinators. Second, the identification of a distinct core microbiome in solitary bees, and the potential role of these microbes in enhancing overwintering survival, highlights the importance of microbial symbionts for pollinator health. Given the global decline in pollinator populations, understanding how microbes contribute to pollinator resilience throughout their development could inform conservation strategies aimed at supporting solitary bee species, which are often overlooked compared to social bees. Finally, the characterization of novel *Streptomyces* species with antifungal potential underscores the value of exploring symbiotic relationships in natural ecosystems as sources of new bioactive compounds. These findings have potential future applications in agriculture, where antifungal compounds derived from these microbes could be used to control plant pathogens, and in medicine, where novel antifungal agents are urgently needed.

Future work

While this dissertation has clarified some previously unanswered questions in the fields of microbial symbiosis and pollination ecology, it has also revealed new directions and questions that necessitate further research. Among these, there are several questions whose answers will be important for furthering our understanding of plant physiology, host-microbe mutualisms, and bee biology. First, in relation to microbial impact on pollen germination: Do bees exploit *Acinetobacter*'s ability to extract nutrients from pollen? What metabolite(s), protein(s) or process(es) is/are responsible for the induction of pollen germination by *Acinetobacter*, and can this be applied to study of plant reproduction, bee health, or agriculture? Second, in relation to the developmental microbiome of solitary bees: What is causing the alterations in microbial community through bee development? Does the bee have mechanisms to control the community? How is the community transmitted between generations? Is the microbial community important for host survival through diapause? What is the contribution of microbial symbionts to host diapause survival? Lastly, in relation to *Streptomyces* isolates and genomes: When, and under what conditions, do the *Streptomyces* produce antifungal metabolites, and is this under host control? Do closely related bee species host closely related *Streptomyces*? How widespread is insect developmental symbiosis with *Streptomyces*? By building on this dissertation, future work will be able to uncover the different evolutionary strategies that hosts and symbiotic microbes use and the extent to which they rely on and influence one another.

References – Introduction and Discussion

1. Whitman, W.B., Coleman, D.C., and Wiebe, W.J. (1998). Prokaryotes: The unseen majority. Proceedings of the National Academy of Sciences *95*, 6578–6583. https://doi.org/10.1073/pnas.95.12.6578.

2. Trivedi, P., Leach, J.E., Tringe, S.G., Sa, T., and Singh, B.K. (2020). Plant–microbiome interactions: from community assembly to plant health. Nat Rev Microbiol *18*, 607–621. https://doi.org/10.1038/s41579-020-0412-1.

3. Liu, K., Zhang, Y., Yu, Z., Xu, Q., Zheng, N., Zhao, S., Huang, G., and Wang, J. (2021). Ruminal microbiota–host interaction and its effect on nutrient metabolism. Animal Nutrition *7*, 49–55. https://doi.org/10.1016/j.aninu.2020.12.001.

4. Miller, D.L., Smith, E.A., and Newton, I.L.G. (2021). A bacterial symbiont protects honey bees from fungal disease. mBio *12*, 10.1128/mbio.00503-21. https://doi.org/10.1128/mbio.00503-21.

5. de Paula, G.T., Melo, W.G. da P., Castro, I. de, Menezes, C., Paludo, C.R., Rosa, C.A., and Pupo, M.T. (2023). Further evidences of an emerging stingless bee-yeast symbiosis. Front. Microbiol. *14*. https://doi.org/10.3389/fmicb.2023.1221724.

6. Ogunrinola, G.A., Oyewale, J.O., Oshamika, O.O., and Olasehinde, G.I. (2020). The human microbiome and its impacts on health. International Journal of Microbiology *2020*, 8045646. https://doi.org/10.1155/2020/8045646.

7. Moreau, C.S. (2020). Symbioses among ants and microbes. Current Opinion in Insect Science *39*, 1–5. https://doi.org/10.1016/j.cois.2020.01.002.

8. Hammer, T.J. (2024). Why do hosts malfunction without microbes? Missing benefits versus evolutionary addiction. Trends in Microbiology *32*, 132–141. https://doi.org/10.1016/j.tim.2023.07.012.

9. Kooi, C.J. van der, Vallejo-Marín, M., and Leonhardt, S.D. (2021). Mutualisms and (a)symmetry in plant–pollinator pnteractions. Current Biology *31*, R91–R99. https://doi.org/10.1016/j.cub.2020.11.020.

10. Vannette, R.L. (2020). The floral microbiome: Plant, pollinator, and microbial perspectives. Annual Review of Ecology, Evolution, and Systematics *51*, 363–386. https://doi.org/10.1146/annurev-ecolsys-011720-013401.

11. Martin, V.N., Schaeffer, R.N., and Fukami, T. (2022). Potential effects of nectar microbes on pollinator health. Philosophical Transactions of the Royal Society B: Biological Sciences *377*, 20210155. https://doi.org/10.1098/rstb.2021.0155.

12. LeBuhn, G., and Vargas Luna, J. (2021). Pollinator decline: What do we know about the drivers of solitary bee declines? Current Opinion in Insect Science *46*, 106–111. https://doi.org/10.1016/j.cois.2021.05.004.

13. Katumo, D.M., Liang, H., Ochola, A.C., Lv, M., Wang, Q.-F., and Yang, C.-F. (2022). Pollinator diversity benefits natural and agricultural ecosystems, environmental health, and human welfare. Plant Diversity *44*, 429–435. https://doi.org/10.1016/j.pld.2022.01.005.

14. Khalifa, S.A.M., Elshafiey, E.H., Shetaia, A.A., El-Wahed, A.A.A., Algethami, A.F., Musharraf, S.G., AlAjmi, M.F., Zhao, C., Masry, S.H.D., Abdel-Daim, M.M., et al. (2021). Overview of bee pollination and its economic value for crop production. Insects *12*, 688. https://doi.org/10.3390/insects12080688.

15. Porto, R.G., de Almeida, R.F., Cruz-Neto, O., Tabarelli, M., Viana, B.F., Peres, C.A., and Lopes, A.V. (2020). Pollination ecosystem services: A comprehensive review of economic values, research funding and policy actions. Food Sec. *12*, 1425–1442. https://doi.org/10.1007/s12571-020-01043-w.

16. Danforth, B. (2007). Bees. Current Biology *17*, R156–R161. https://doi.org/10.1016/j.cub.2007.01.025.

17. Roulston, T.H., and Cane, J.H. (2000). Pollen nutritional content and digestibility for animals. Plant Syst. Evol *222*, 187–209. https://doi.org/10.1007/BF00984102.

18. Dobson, H.E.M., and Peng, Y.S. (1997). Digestion of pollen components by larvae of the flower-specialist bee Chelostoma florisomne (Hymenoptera: Megachilidae). Journal of Insect Physiology *43*, 89–100. https://doi.org/10.1016/S0022-1910(96)00024-8.

19. PENG, Y.-S., NASR, M.E., MARSTON, J.M., and FANG, Y. (1985). The digestion of dandelion pollen by adult worker honeybees. Physiological Entomology *10*, 75–82. https://doi.org/10.1111/j.1365-3032.1985.tb00021.x.

20. Brauman, A., Bignell, D.E., and Tayasu, I. (2000). Soil-Feeding Termites: Biology, Microbial Associations and Digestive Mechanisms. In Termites: Evolution, Sociality, Symbioses, Ecology, T. Abe, D. E. Bignell, and M. Higashi, eds. (Springer Netherlands), pp. 233–259. https://doi.org/10.1007/978-94-017-3223-9_11.

21. Lee, F.J., Rusch, D.B., Stewart, F.J., Mattila, H.R., and Newton, I.L.G. (2015). Saccharide breakdown and fermentation by the honey bee gut microbiome. Environmental Microbiology *17*, 796–815. https://doi.org/10.1111/1462-2920.12526.

22. Kwong, W.K., Engel, P., Koch, H., and Moran, N.A. (2014). Genomics and host specialization of honey bee and bumble bee gut symbionts. Proceedings of the National Academy of Sciences of the United States of America *111*, 11509–11514. https://doi.org/10.1073/pnas.1405838111.

23. Engel, P., Kwong, W.K., Mcfrederick, Q., Anderson, K.E., Barribeau, S.M., Chandler, J.A., Cornman, R.S., Dainat, J., De Miranda, J.R., Doublet, V., et al. (2016). The bee microbiome: Impact on bee health and model for evolution and ecology of host-microbe interactions. mBio *7*, e02164-15. https://doi.org/10.1128/mBio.02164-15.

24. Danforth, B.N., Minckley, R.L., and Neff, J.L. (2019). The Solitary Bees: Biology, Evolution, Conservation (Princeton University Press) https://doi.org/10.2307/j.ctvd1c929.18.

25. Danforth, B.N., Minckley, R.L., Neff, J.L., and Fawcett, F. (2019). The Solitary Bee Life Cycle. In The Solitary Bees Biology, Evolution, Conservation. (Princeton University Press), pp. 37–69. https://doi.org/10.2307/j.ctvd1c929.6.

26. Danforth, B.N., Minckley, R.L., Neff, J.L., and Fawcett, F. (2019). The Microcosm of the Brood Cell: A Bestiary of In-Nest Mutualists. In The Solitary Bees Biology, Evolution, Conservation. (Princeton University Press), pp. 224–239. https://doi.org/10.2307/j.ctvd1c929.12.

27. Hammer, T.J., Kueneman, J., Argueta-Guzmán, M., McFrederick, Q.S., Grant, Lady, Wcislo, W., Buchmann, S., and Danforth, B.N. (2023). Bee breweries: The unusually fermentative, lactobacilli-dominated brood cell microbiomes of cellophane bees. Frontiers in Microbiology *14*, 1114849.

28. Christensen, S.M., Munkres, I., and Vannette, R.L. (2021). Nectar bacteria stimulate pollen germination and bursting to enhance microbial fitness. Current Biology *31*, 4373-4380.e6. https://doi.org/10.1016/j.cub.2021.07.016.

29. Steffan, S.A., Dharampal, P.S., Kueneman, J.G., Keller, A., Argueta-Guzmán, M.P., McFrederick, Q.S., Buchmann, S.L., Vannette, R.L., Edlund, A.F., Mezera, C.C., et al. (2023). Microbes, the 'silent third partners' of bee–angiosperm mutualisms. Trends in Ecology & Evolution *0*. https://doi.org/10.1016/j.tree.2023.09.001.

30. Dharampal, P.S., Danforth, B.N., and Steffan, S.A. (2022). Exosymbiotic microbes within fermented pollen provisions are as important for the development of solitary bees as the pollen itself. Ecol Evol *12*, e8788. https://doi.org/10.1002/ece3.8788.

31. Zhou, W., Yan, Y., Mi, J., Zhang, H., Lu, L., Luo, Q., Li, X., Zeng, X., and Cao, Y. (2018). Simulated Digestion and Fermentation in Vitro by Human Gut Microbiota of Polysaccharides from Bee Collected Pollen of Chinese Wolfberry. https://doi.org/10.1021/acs.jafc.7b05546.

32. Calabrese, E.J., and Agathokleous, E. (2021). Pollen biology and hormesis: Pollen germination and pollen tube elongation. Science of the Total Environment *762*, 143072. https://doi.org/10.1016/j.scitotenv.2020.143072.

33. Eisikowitch, D., Lachance, M.A., Kevan, P.G., Willis, S., and Collins-Thompson, D.L. (1990). The effect of the natural assemblage of microorganisms and selected strains of the yeast *Metschnikowia reukaufii* in controlling the germination of pollen of the common milkweed *Asclepias syriaca*. Canadian Journal of Botany *68*, 1163–1165. https://doi.org/10.1139/b90-147.

34. Herrera, C.M. (2017). Scavengers that fit beneath a microscope lens. Ecology *98*, 2725–2726. https://doi.org/10.1002/ecy.1874.

35. Martin, V.N., Schaeffer, R.N., and Fukami, T. (2022). Potential effects of nectar microbes on pollinator health. Philosophical Transactions of the Royal Society B: Biological Sciences *377*, 20210155. https://doi.org/10.1098/rstb.2021.0155.

36. Vannette, R.L., and Fukami, T. (2016). Nectar microbes can reduce secondary metabolites in nectar and alter effects on nectar consumption by pollinators. Ecology *97*, 1410–1419. https://doi.org/10.1890/15-0858.1.

37. Kapheim, K.M., Johnson, M.M., and Jolley, M. (2021). Composition and acquisition of the microbiome in solitary, ground-nesting alkali bees. Scientific Reports *11*, 1–11. https://doi.org/10.1038/s41598-021-82573-x.

38. Lozo, J., Berić, T., Terzić-Vidojević, A., Stanković, S., Fira, D., and Stanisavljević, L. (2015). Microbiota associated with pollen, bee bread, larvae and adults of solitary bee Osmia cornuta (Hymenoptera: Megachilidae). Bulletin of Entomological Research, 470–476. https://doi.org/10.1017/S0007485315000292.

39. Voulgari-Kokota, A., McFrederick, Q.S., Steffan-Dewenter, I., and Keller, A. (2019). Drivers, diversity, and functions of the solitary-bee microbiota. Trends in Microbiology *27*, 1034–1044. https://doi.org/10.1016/j.tim.2019.07.011.

40. McFrederick, Q.S., Wcislo, W.T., Taylor, D.R., Ishak, H.D., Dowd, S.E., and Mueller, U.G. (2012). Environment or kin: whence do bees obtain acidophilic bacteria? Molecular Ecology *21*, 1754–1768. https://doi.org/10.1111/j.1365-294X.2012.05496.x.

41. Christensen, S.M., Srinivas, S.N., McFrederick, Q.S., Danforth, B.N., Buchmann, S.L., and Vannette, R.L. (2024). Symbiotic bacteria and fungi proliferate in diapause and may enhance overwintering survival in a solitary bee. The ISME Journal *18*, wrae089. https://doi.org/10.1093/ismejo/wrae089.

42. Elbein, A.D., Pan, Y.T., Pastuszak, I., and Carroll, D. (2003). New insights on trehalose: a multifunctional molecule. Glycobiology *13*, 17R-27R. https://doi.org/10.1093/glycob/cwg047.

43. Kobayashi, Y., Iwata, H., Yoshida, J., Ogihara, J., Kato, J., and Kasumi, T. (2015). Metabolic correlation between polyol and energy-storing carbohydrate under osmotic and oxidative stress condition in *Moniliella megachiliensis*. J Biosci Bioeng *120*, 405–410. https://doi.org/10.1016/j.jbiosc.2015.02.014.

44. Thoa, V., Khanh, N., Duc Hien, D., Manh, L., and Thanh, V. (2015). Screening of Moniliella yeast with high-level production of erythritol.

45. Bright, M., and Bulgheresi, S. (2010). A complex journey: transmission of microbial symbionts. Nat Rev Microbiol *8*, 218–230. https://doi.org/10.1038/nrmicro2262.

46. Salem, H., Florez, L., Gerardo, N., and Kaltenpoth, M. (2015). An out-of-body experience: the extracellular dimension for the transmission of mutualistic bacteria in insects. Proceedings of the Royal Society B: Biological Sciences. https://doi.org/10.1098/rspb.2014.2957.

47. Denlinger, D.L. (2022). Insect Diapause (Cambridge University Press) https://doi.org/10.1017/9781108609364.

48. Chevrette, M.G., Carlson, C.M., Ortega, H.E., Thomas, C., Ananiev, G.E., Barns, K.J., Book, A.J., Cagnazzo, J., Carlos, C., Flanigan, W., et al. (2019). The antimicrobial potential of Streptomyces from insect microbiomes. Nat Commun *10*. https://doi.org/10.1038/s41467-019-08438-0.

49. Procópio, R.E. de L., Silva, I.R. da, Martins, M.K., Azevedo, J.L. de, and Araújo, J.M. de (2012). Antibiotics produced by Streptomyces. Braz J Infect Dis *16*, 466–471. https://doi.org/10.1016/j.bjid.2012.08.014.

50. Flórez, L., Biedermann, P.H., Engl, T., and Kaltenpoth, M. (2015). Defensive symbioses of animals with prokaryotic and eukaryotic microorganisms. Natural Product Reports *32*, 904–936. https://doi.org/10.1039/C5NP00010F.

51. Oliver, K.M., Smith, A.H., and Russell, J.A. (2014). Defensive symbiosis in the real world – advancing ecological studies of heritable, protective bacteria in aphids and beyond. Functional Ecology *28*, 341–355. https://doi.org/10.1111/1365-2435.12133.

52. Grubbs, K.J., May, D.S., Sardina, J.A., Dermenjian, R.K., Wyche, T.P., Pinto-Tomás, A.A., Clardy, J., and Currie, C.R. (2021). Pollen Streptomyces Produce Antibiotic That Inhibits the Honey Bee

Pathogen Paenibacillus larvae. Frontiers in Microbiology *12*, 115. https://doi.org/10.3389/FMICB.2021.632637/BIBTEX.

53. Kim, D.R., Cho, G., Jeon, C.W., Weller, D.M., Thomashow, L.S., Paulitz, T.C., and Kwak, Y.S. (2019). A mutualistic interaction between Streptomyces bacteria, strawberry plants and pollinating bees. Nature Communications *10*. https://doi.org/10.1038/s41467-019-12785-3.

Appendix I

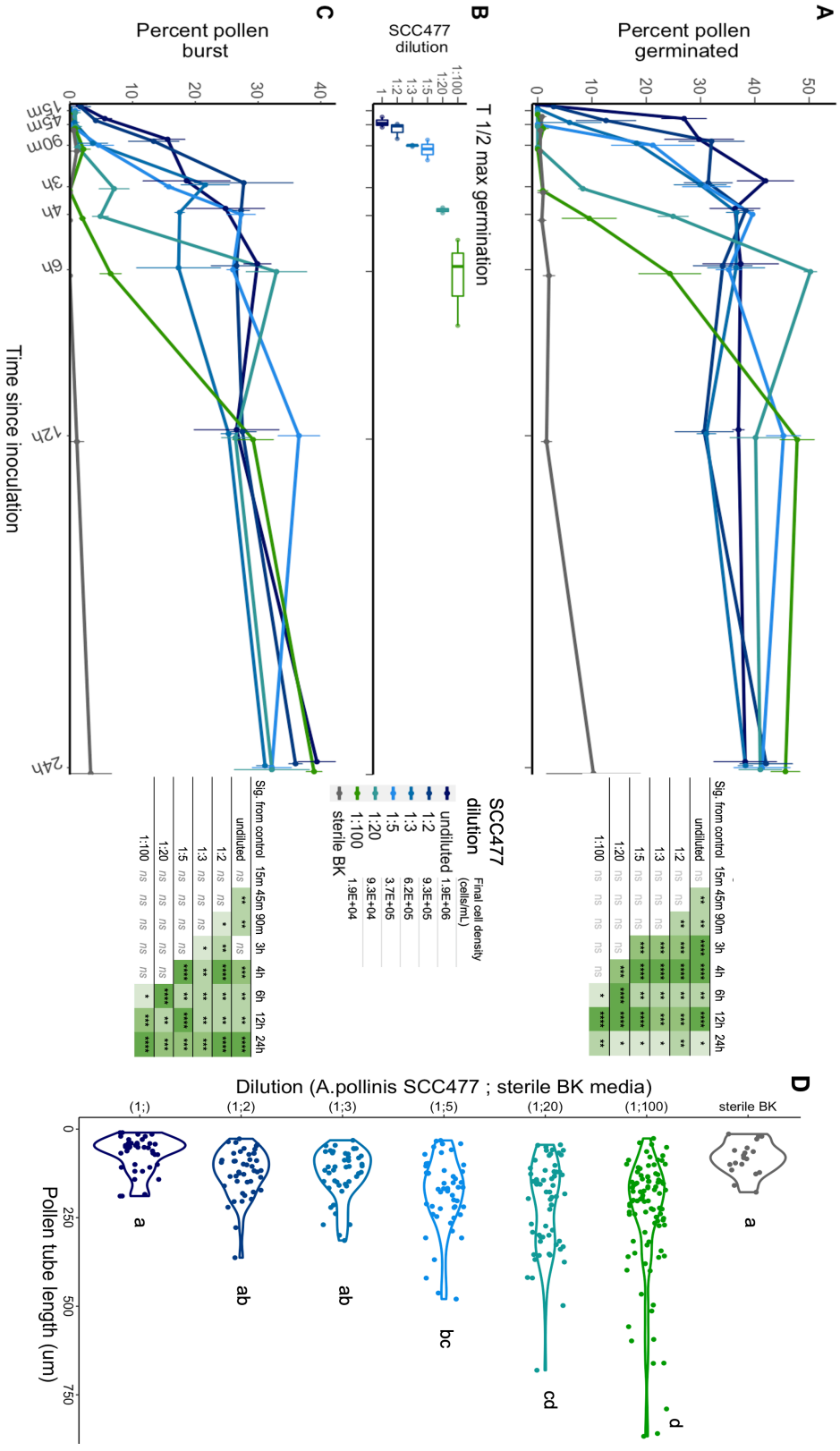
A
Percent pollen germinated
B
SCC477 dilution
T 1/2 max germination
C
Percent pollen burst
Time since inoculation
15m
45m
90m
3h
4h
6h
12h
24h
SCC477 dilution
Final cell density (cells/mL)
undiluted 1.9E-06
1:2 9.3E-05
1:3 6.2E-05
1:5 3.7E-05
1:20 9.3E-04
1:100 1.9E-04
sterile BK
Sig. from control
D
Dilution (A.pollinis SCC477 ; sterile BK media)
sterile BK
(1;100)
(1;20)
(1;5)
(1;3)
(1;2)
(1;)
Pollen tube length (um)
a
d
cd
bc
ab
ab
a

Figure S1- Response of pollen to *Acinetobacter pollinis* SCC477 is density-dependent. Related to Figure 1.2. To determine whether *Acinetobacter* density affects induction or the time until induction of germination or bursting, we assayed a range of dilutions of *A. pollinis* SCC477 on pollen phenotypes. For both pollen germination and pollen bursting, the response of pollen to solutions of *A. pollinis* SCC477 was density dependent. A and C) Points represent the mean of 3 biological replicates of each density of *A. pollinis* SCC477, from a total of 7,618 pollen grains, an average of 952 per timepoint. Standard error bars are shown. A) Germination over time for pollen inoculated with dilutions of SCC477 from 1-1:100. B) $T_{½\ max}$- time to reach half of maximum germination, as a boxplot for each dilution treatment. The $T_{1/2\ Max}$ lengthened with decreasing microbial density; the treatment with the highest density took 40 minutes to reach half of maximum germination, whereas the lowest density took over 6 hours. C) Bursting over time when inoculated with dilutions of SCC477. Undiluted indicates a OD600=0.1 solution; cells/mL for each dilution shown. All data collected at labelled timepoints- offsets are for clarity. Significance from control (sterile BK) calculated with ANOVA followed by Tukey multiple comparisons. D) All pollen tube lengths were measured in every image of the dose dependence assay; the 24h timepoint measurements are shown here. Treatment labels correspond to SCC477 dilution in sterile BK media. Letters indicate significance $p<0.05$ with ANOVA ($F= 16.02$, $df= 6$, p-value=2.9e-16), multiple comparisons with Tukey p-value adjustment. Each treatment includes three biological replicates (wells). Average 55.2 pollen tubes measured per treatment.

	A. pollinis SCC477	*P. carotovorum* (+)	*M. reukaufii* (-)	Crushed stigma	BK media only
+ pollen	No clearance (Y)	Clearance (N)	No clearance (N)	No clearance (Y)	No clearance (N)
- pollen	No clearance	Clearance	No clearance	X	X

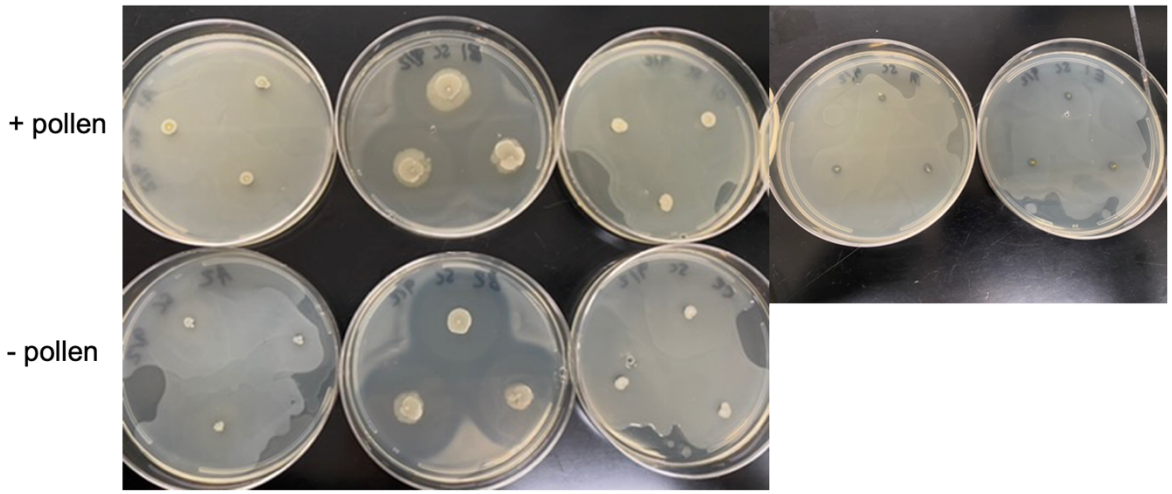

Figure S2: PGA activity not linked to germination phenotype. Related to Figure 1.2, Table S1.
Pectinase activity was tested for microbes after exposure to pollen for one hour to explore potential induction of pectinase as a mechanism for germination phenotype. Polygalacturonic acid (PGA) plates were spotted with each treatment before visualization of PGA with CTAB, which stains PGA milky white. 'Clearance' or 'No clearance' indicates activity on PGA and undetectable activity, respectively. (Y)/(N) in "+ pollen" row indicates whether the pollen was observed to be germinating (Y) or not (N) after 1h in that treatment, just before spotting onto PGA. The images below the table are in the same orientation as in the table above. The faint shadows around the spots in the 'crushed stigma' and 'BK only' plates are a result of marking the placement of the spots on the back of the plate, not clearing of CTAB. See Table S1 for PGA activity of microbes without pollen exposure

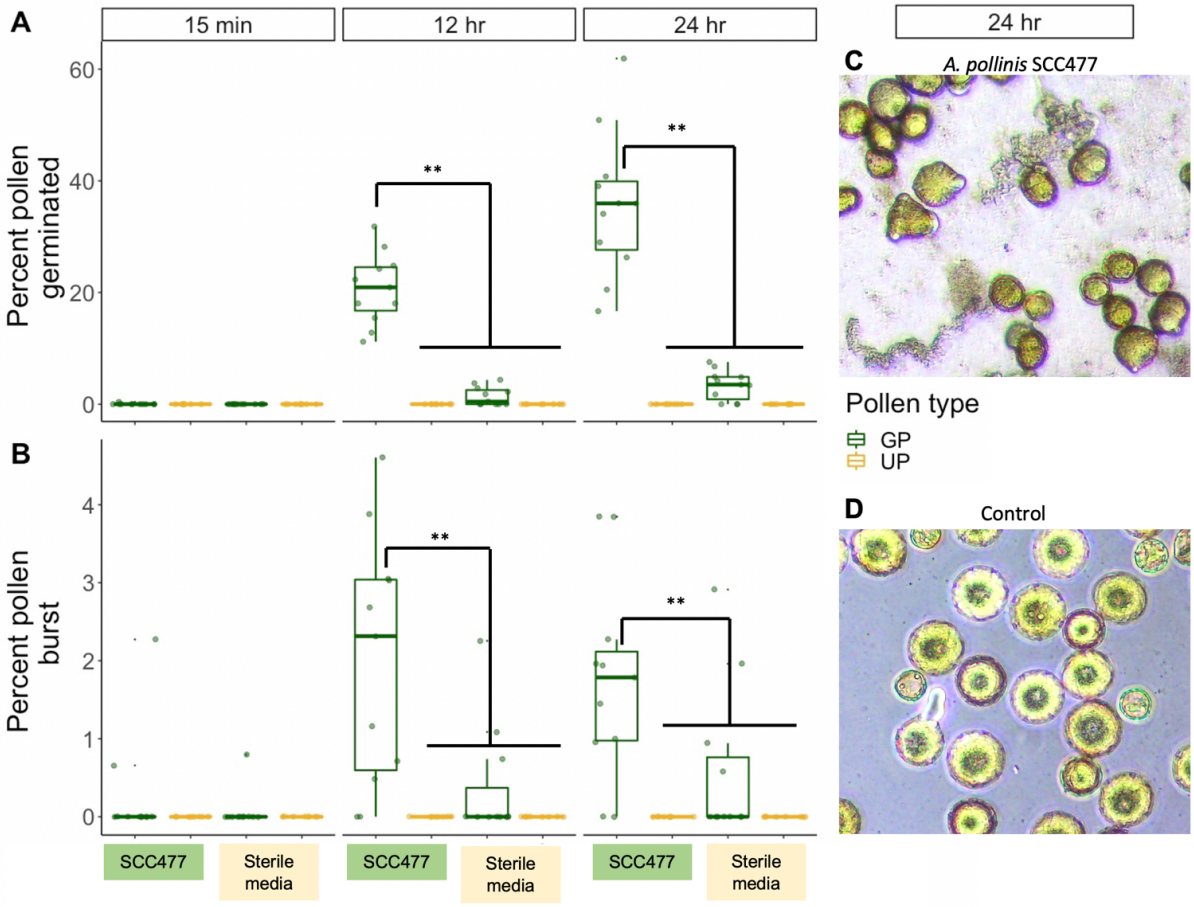

Figure S3: *A. pollinis* SCC477 induction of germination and bursting occurs in ecologically relevant conditions. Related to Figure 1.4.

In tandem with the Lowry assays (Figure 1.4 main text), we also imaged and classified pollen germination and bursting in the wells to verify that this phenotype can occur in more ecologically relevant media: supplemented artificial nectar. A) Grains that germinated with each microbe/pollen treatment. B) Grains that burst with each microbe/pollen treatment. For A and B, significance from control used Kruskal Wallis test followed by Dunn's multiple comparisons and marked by brackets. Center lines correspond to the median, boxes define interquartile range (IQR), and whiskers extend +1.5 IQR. Data represents three assays, 3-4 biological replicates of each pollen/microbe treatment combination per assay, N=9, and a total 14,544 pollen grains. Note difference in scale of y-axes. C and D) Cropped images of pollen at 24-hour timepoint show bursting and germination when inoculated with *A. pollinis* SCC477 (C), and germination in control with no microbe inoculation (D).

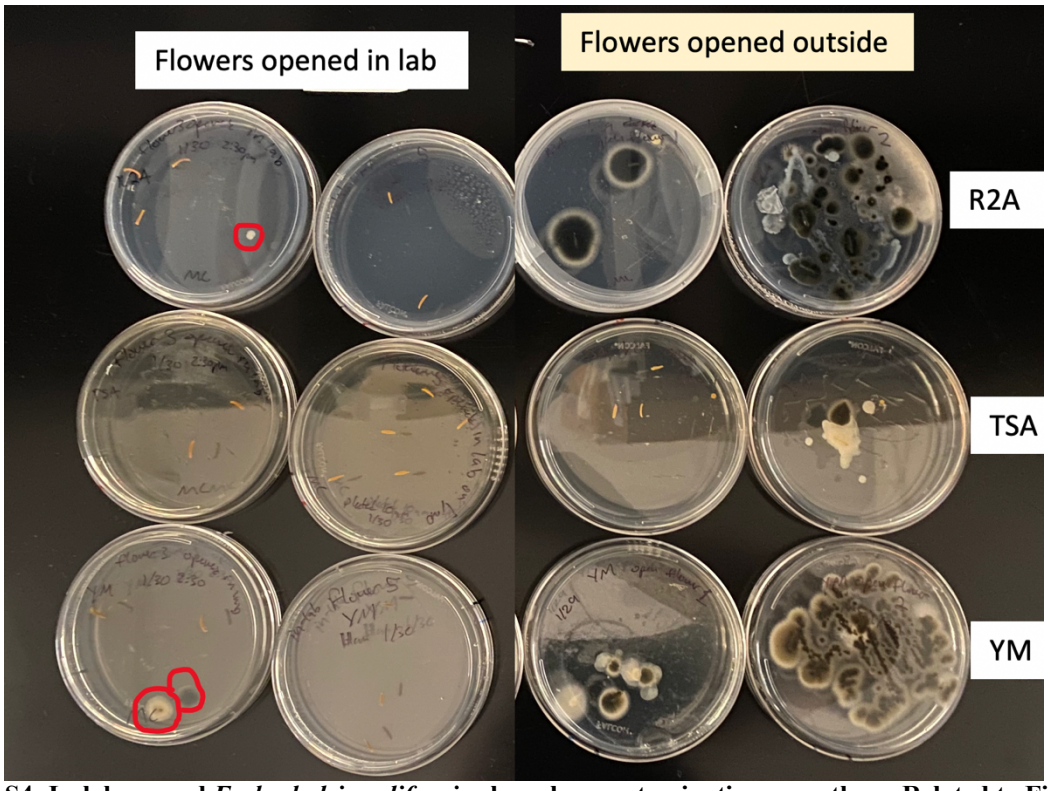

Figure S4: In-lab opened *Eschscholzia californica* have low contamination on anthers. **Related to Figures 1.2-1.4.** To verify that flowers collected prior to opening that were allowed to open naturally in lab were relatively free of contaminants, we plated the anthers (removing with sterile tweezers, rubbing across surface of plate to spread microbes and pollen) of lab-opened and outside-opened flowers onto multiple media types. Column labels indicate where flowers opened prior to anther/pollen plating. Row labels indicate media type: Reasoner's 2A agar (R2A), Tryptic soy agar (TSA), Yeast media agar (YM). Red circles indicate colonies on plates growing from in-lab flowers. We found very few colonies on the lab-opened flowers (Figure S4), which were unidentifiable (no matches) by MALDI- TOF. Some of the identifiable colonies from outside-opened flower plates were*:* *Pantoea agglomerans* (species level support), *Pseudomonas* (genus level support), *Neokomagateae* (genus level support), and *Bacillus* (genus level support). Filamentous fungi were common in outside-opened flowers but unidentifiable by MALDI-TOF.

Table S1: Polygalacturonase activity of strains used in Chapter I

Strain	Species	Clearance zone	Total reps	Reps showing clearance	Accession numbers and locus tags of *Acinetobacter* assigned pectinase genes
P. carotovorum	*P. carotovorum*	Clearance	9	9	
EC52	*M. reukaufii*	No clearance	9	0	
SCC474	*A. pollinis*	Slight	9	3	Not yet described
SCC477	*A. pollinis*	Slight	9	3	Not yet described
ANC4422	*A. boissieri*	No clearance	9	0	NZ_FMYL01000001.1, BLS38_RS01625 BLS38_RS12295
BB362 B1	*A. nectaris*	No clearance	9	0	NZ_KI530734.1, P256_RS09450; NZ_KI530712.1, P256_RS02650
A. apis	*A. apis*	ND			NZ_FZLN01000001.1 SAMN05444584_0345, NZ_FZLN01000002.1 CFY84_RS07245

Table S2: KEY RESOURCES TABLE	SOURCE	IDENTIFIER
Bacterial and virus strains		
Acinetobacter pollinis SCC474	Isolated from floral nectar	NCBI:txid2605270 ATCC: TSD-214
Acinetobacter pollinis SCC477	Isolated from floral nectar	NCBI:txid2605270
Acinetobacter boissieri ANC4422	Isolated from floral nectar	NCBI:txid1219383
Acinetobacter nectaris BB362	Isolated from floral nectar	NCBI:txid1219382
Acinetobacter apis	Isolated from *Apis mellifera*, provided by Sergio Álvarez-Pérez	NCBI:txid1229165
Metschnikowia reukaufii	Isolated from floral nectar	NCBI:txid27327
Pectobacterium carotovorum	Provided by Robert Gilbertson	NCBI:txid555
Biological samples		
Eschscholzia californica pollen	UC Davis Arboretum	N/A
Chemicals, peptides, and recombinant proteins		
cetyltrimethylammonium bromide (CTAB)	Chem-Impex	Cat. no 01781
alpha-cyano-4-hydroxycinnamic acid (HCCA)	Sigma Aldrich	Cat. no 70990
Reasoner's 2A agar (R2A)	Thermo Fisher Scientific	Cat. no DF1826171
Yeast extract Media (YM)	Teknova	Cat. no Y0750
Polygalacturonic acid (PGA)	Thermo Fisher Scientific	Cat. no AAL0420614
Tryptone	US Biotech Sources	Cat. no T01PD-500
Soytone	US Biotech Sources	Cat. no SP1PD-500
NaCl	Fisher Chemical	Cat. no 5271-500
D-Fructose	VWR Chemical	Cat. no 0226-1KG
SuperPure Agar	US Biotech Sources	Cat. no A02MG-500
Cycloheximide	ACROS	Cat. no 357420250
Chloramphenicol	Fisher Scientific	Cat. no BP904-100
Phosphate buffered saline (PBS)	Sigma LifeScience	Cat. no D8537-500ML
Sucrose	Fisher Chemical	Cat. no 5271-500
Boric acid	Fisher BioReagents	Cat. no BP168-1
Calcium nitrate	Fisher Scientific	Cat. no AC423530250
Magnesium sulfate	Alfa Aesar	Cat. no 11596
Potassium nitrate	Fisher Scientific	Cat. no AA1344322
Formic acid	Sigma Aldrich	Cat. no F0507-1L
Yeast extract	UC Biotech Sources	Cat. no Y1003-1001
Critical commercial assays		
Pierce Modified Lowry Assay Kit	Thermo Fisher Scientific	Product 23240
Deposited data		
Supplementary data: Nectar bacteria stimulate pollen germination and bursting to enhance their fitness	Dryad Data Repository	https://doi.org/10.25338/B8BS75
Supplementary code: Nectar bacteria stimulate pollen germination and bursting to enhance their fitness	Dryad Data Repository	https://doi.org/10.25338/B87045
Video S1: Nectar bacteria stimulate pollen germination and bursting to enhance their fitness	Dryad Data Repository	https://doi.org/10.25338/B83928
Software and algorithms		

ImageJ/ FIJI2 (v2.0.0)	Schindelin et al, 2012	https://imagej.nih.gov/ij
Bruker- Ultraflex III FlexControl/ FlexAnalysis (v. 3.4)	Bruker Daltonic	N/A
MALDI Biotyper Compass Explorer (v. 4.1.70)	Bruker Daltonic	N/A
RStudio 1.2.1335	RStudio Team, 2020	https://www.rstudio.com
R 3.6.2	R Core Team, 2020	https://www.r-project.org

Key Resources Citations:

Schindelin, J., Arganda-Carreras, I., Frise, E., Kaynig, V., Longair, M., Pietzsch, T., Preibisch, S., Rueden, C., Saalfeld, S., Schmid, B., et al. (2012). Fiji: An open-source platform for biological-image analysis. Nat. Methods *9*, 676–682.

RStudio Team (2020). RStudio: Integrated Development for R. Rstudio PBC.

R Core Team (2020). R: a language and environment for statistical computing.

Appendix II

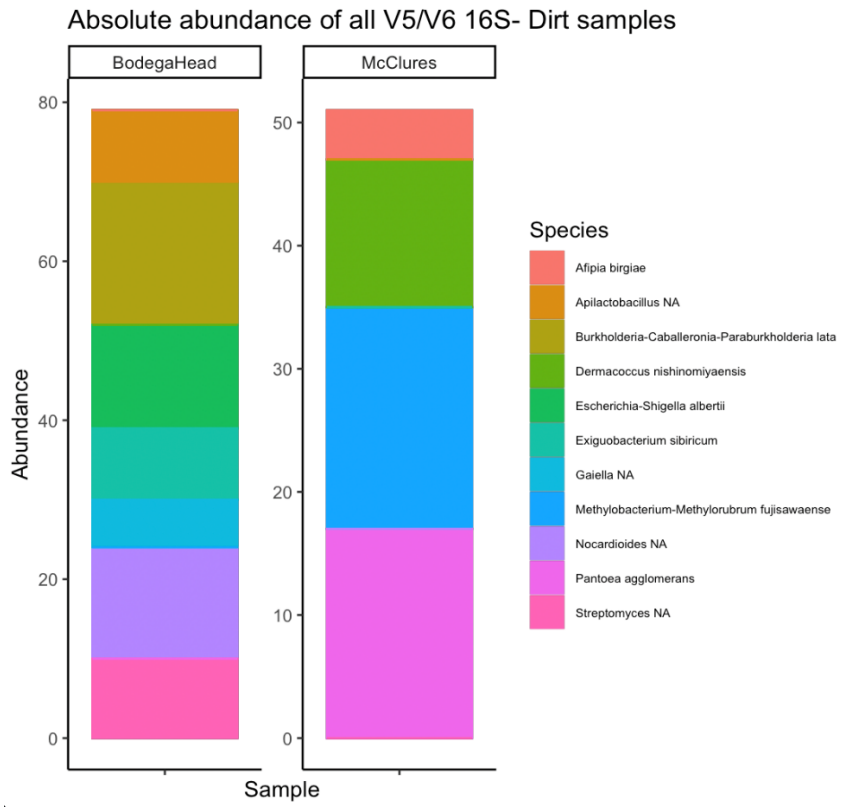

Fig. S1- Soil sample microbial composition. Soil samples were collected from each site, from ~2" beneath the surface, within the area of the nesting aggregation but not touching any nest. They were analyzed separately from the rest of the samples due to very low read count (note y axis), using a less stringent pipeline, and without using Decontam. *Nocardiodes* and *Streptomyces* (circled in key) were present in soil at Bodega Head but not found at McClure's. In separate analysis of fungal reads, no reads passed merge step: manual analysis showed there were 20 total reads in the McClure's soil sample, two of these reads were *M. spathulata* (BLAST), the rest were non-fungi.

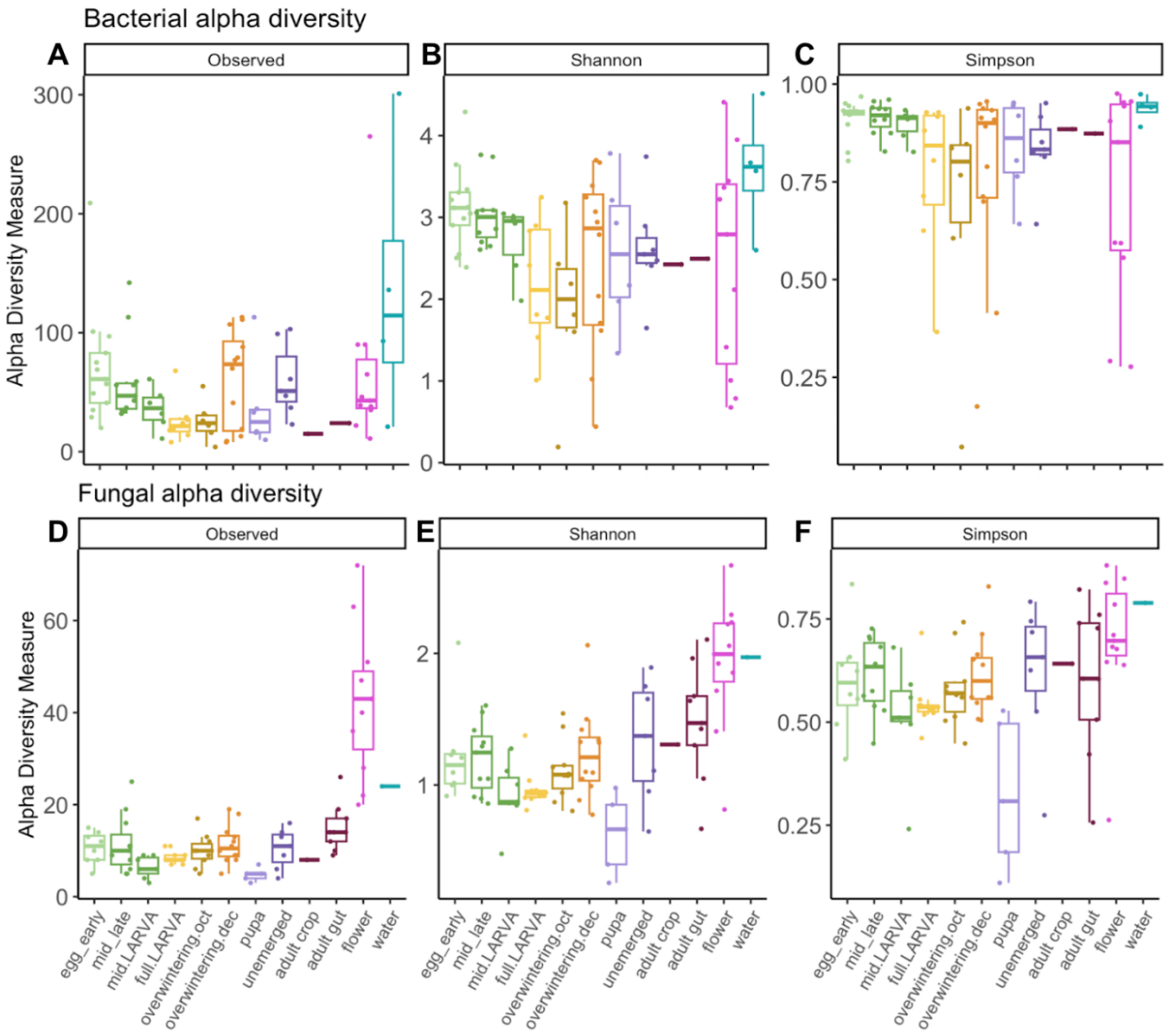

Fig. S2- Bacterial and fungal alpha diversity by developmental stage and sample type. Alpha diversity metrics (y axis) by sample type (x axis). No ASVs removed. **(A-C)** Bacterial alpha diversity: Observed alpha diversity sample type (x axis) is significant globally but no comparisons remain significant after *P* value correction. (Kruskal-Wallis χ^2= 22.838, df = 11, p= 0.01863). Shannon index does not differ globally by sample type (Kruskal-Wallis χ^2= 16.616, df = 11, *P* value > 0.05). Simpson diversity metric does not differ globally by sample type (Kruskal-Wallis χ^2 = 15.295, df = 11, *P* value > 0.05). **(D-F)** Fungal alpha diversity varies significantly by sample type in all measurements (Observed: Kruskal-Wallis χ^2= 51.8, df = 11, *P* value = 3e-7; Shannon: Kruskal-Wallis χ^2= 39.4, df = 11, *P* value =4.5e-5; Simpson: Kruskal-Wallis χ^2 = 26.9, df = 11, *P* value = 0.005).

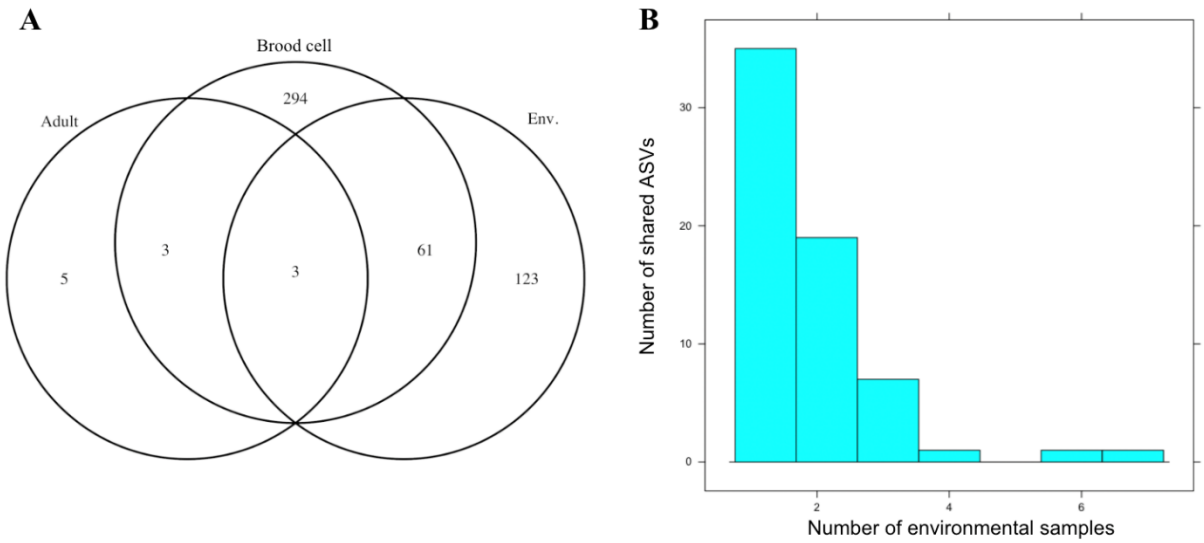

Fig. S3- Overlap of Actinobacterial ASVs with environmental ASVs does not fully explain acquisition. To assign ASV presence within a sample, we used a cutoff of 0.1% relative abundance, and filtered to only ASVs assigned to Actinobacteria. **A)** Three ASVs: ASV_29, ASV_78, ASV_471 (Assigned as *Nocardioides*, *Mycobacterium*, and order: Frankiales, respectively) were found to occur in all sample groups (eg, adult, brood cell, environment). ASV_29 was found in 53.2% of all samples, ASV_78 was found in 23.9% of all samples, ASV_471 found in 4.3% of all samples. The mean relative abundances (in samples where the ASV was found) are ASV_29 mean= 0.017 SD= 0.014; ASV_78 mean = 0.015, SD= 0.015; ASV471 mean= 0.0013 SD=0.01. In total, 64 Actinobacteria ASVs overlap between brood cell and environmental samples, which represents less than one fifth (17.7%) of the Actinobacterial ASVs found in brood cell samples. Brood cell n=69, environment n=15, adult n=2. **B)** Histogram of the 64 ASVs shared between brood and environmental samples, showing their representation in environmental samples. The vast majority (54 ASVs, 90%) of these ASVs were found in only one or two environmental samples (the first two bars on the left). The environmental samples contributing the most shared Actinobacterial ASVs were: Radish flower (15x flowers bulked) which contained 31 shared ASVs, and Sea Daisy (3x flowers bulked), which contained 27 shared ASVs.

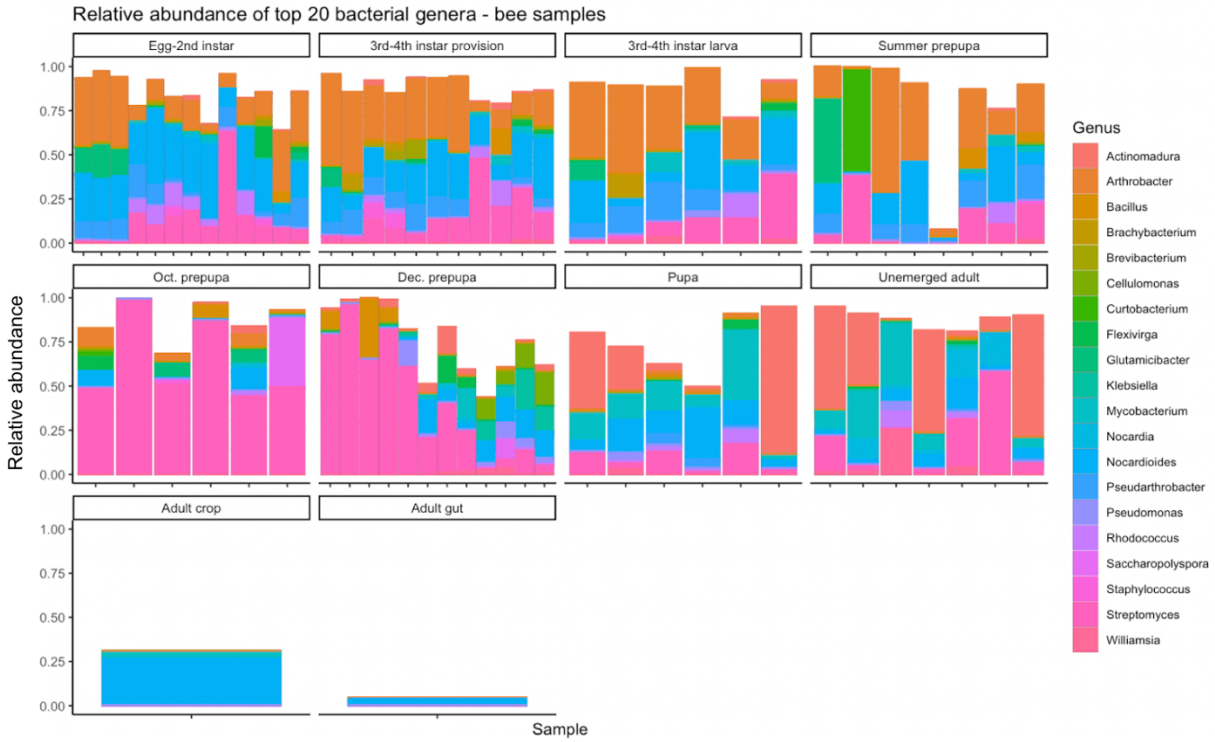

Fig. S4- Top 20 bacterial genera comprise the majority of reads in each stage, in varying abundances. Data subset to include only ASVs belonging to the 20 most abundant genera, and the white space indicates proportion of sample comprised by additional genera. ASVs are grouped and colored by genus, shown as relative abundance in sample. Each bar represents one sample, and samples are grouped by stage.

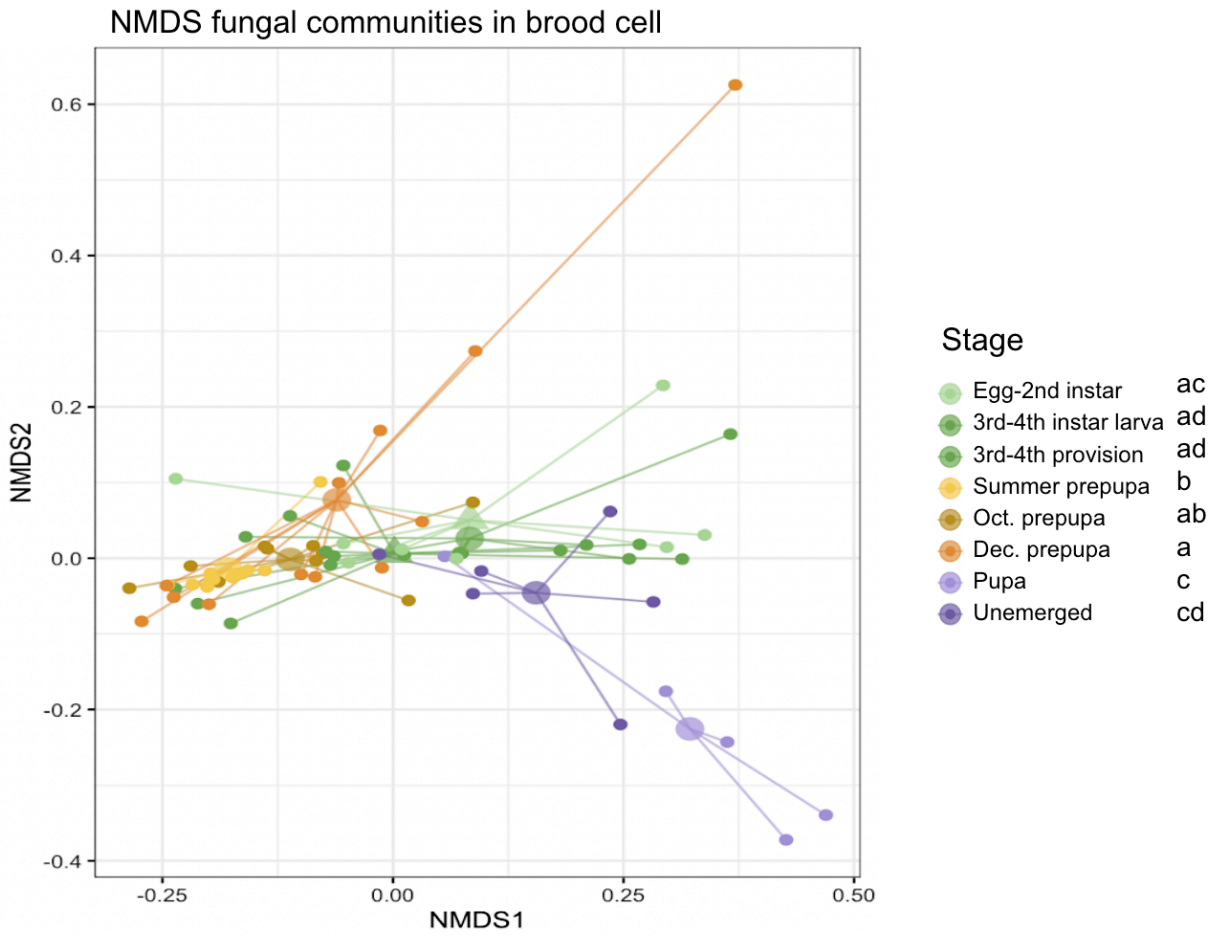

Fig. S5- Fungal communities shift with bee development. NMDS plot of Bray-Curtis distance, with color indicating stage of brood cell development. Larger semi-transparent dots indicate centroids, with lines from centroid to each point in the group. Triangular centroids indicate provision samples. Fungal- NMDS (stress=0.09) global PERMANOVA shows significant difference between stages (R^2=0.28, F=3.52, P value <0.001). Pairwise PERMANOVA of stages (P value <0.05, FDC corrected) indicated with lettering on figure key. N=71.

Fig. S6- Two ASVs of *Moniliella spathulata* comprise the majority of fungal reads in most brood cell samples and are found at both sites. Relative abundance data is shown, subset only to the top two ASVs in the fungal dataset, which are both assigned to *Moniliella spathulata*. Each bar represents one sample, samples are separated by stage or sample type and by collection site.

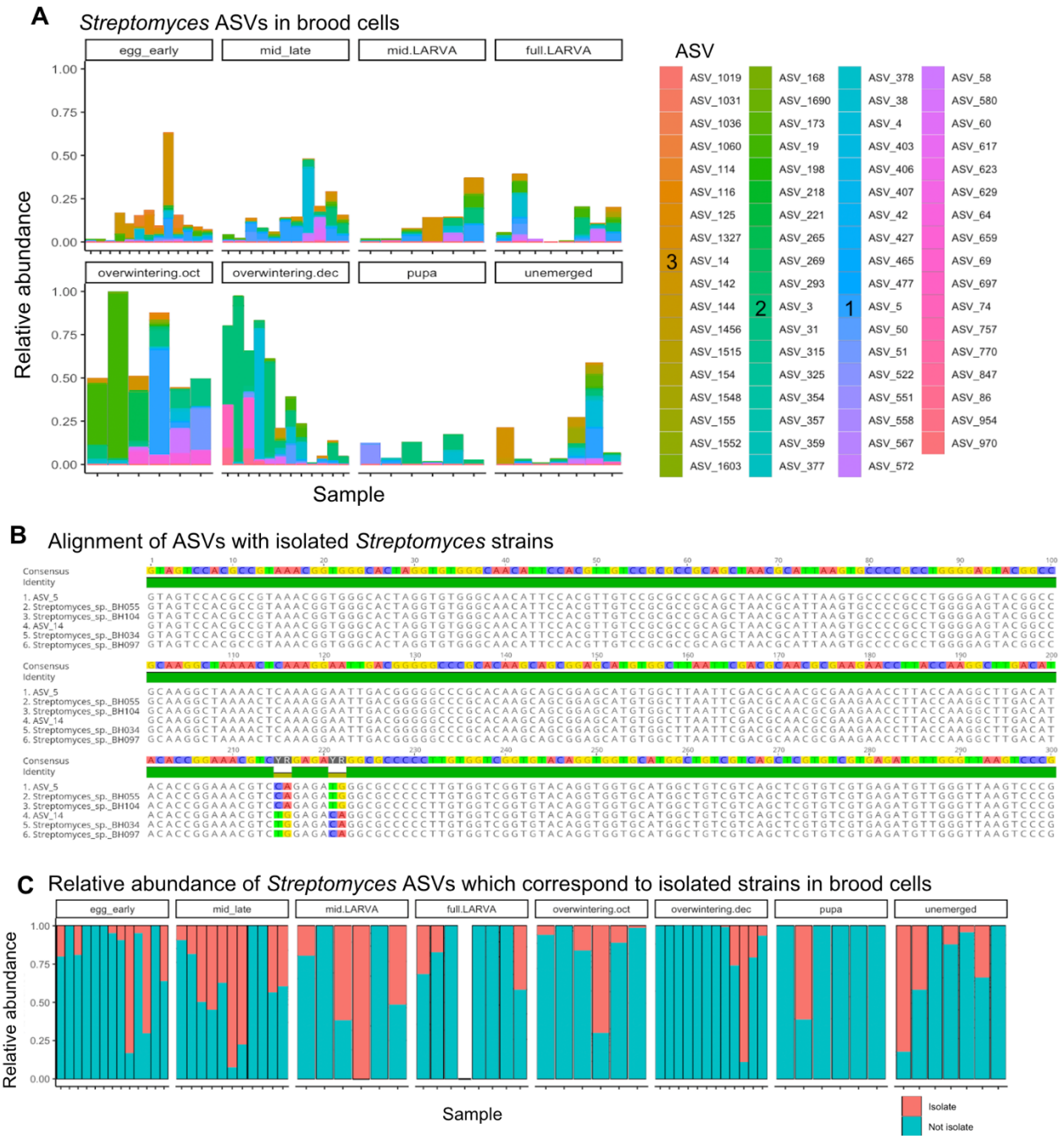

Fig. S7- *Streptomyces* ASVs are variable in brood cells, but major ASVs are likely represented by isolated strains. A) Relative abundance data is shown, subset to only show *Streptomyces* genus from the bacterial dataset. Each bar represents one sample, samples are separated by stage. Top three ASVs by total read abundance are labeled in the key (ASV_5, ASV_3, ASV_14, respectively). **B)** *Streptomyces* isolate 16S rRNA gene sequences match the sequenced region (V5/V6) of two abundant ASVs. Alignment created via MUSCLE v. 5.1. The most abundant *Streptomyces* ASV, ASV_5, matches exactly with isolates BH55 and BH104, while ASV_14, the third most abundant *Streptomyces* ASV, matches exactly with isolates BH34^{T} and BH97. **C)** Relative abundance of ASVs 5

and 14 (combined, in red), which correspond to isolated *Streptomyces* strains ("isolate"), compared to other ASVs within *Streptomyces* genus that did not align with isolated strains ("Not isolate", in blue).

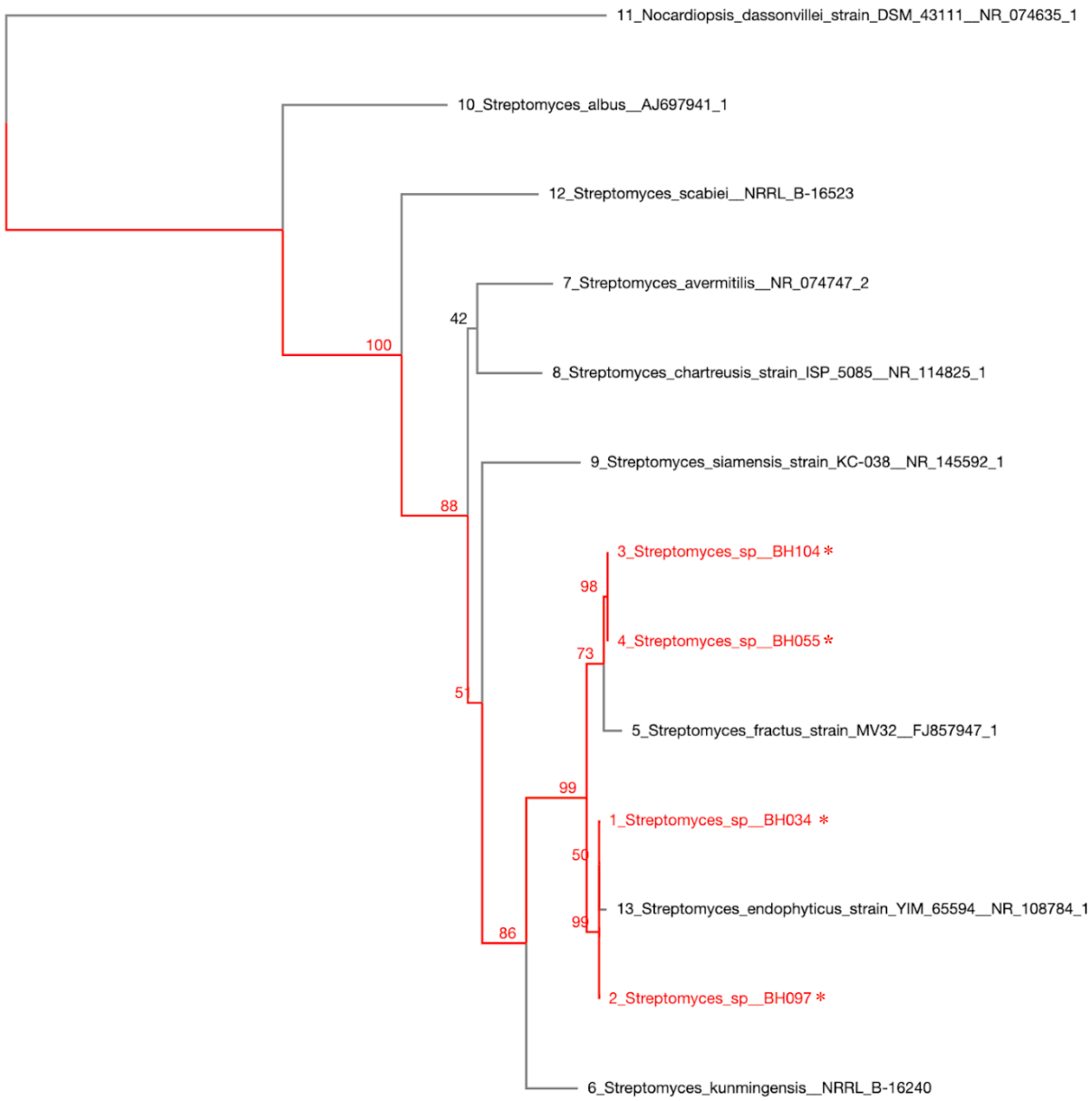

Fig. S8 – 16S rRNA gene phylogenetic tree showing the position of *Streptomyces* isolates from *A. bomboides* amongst closest phylogenetic neighbors. Alignment constructed with MAFFT using default parameters (method= L-INS-i), followed by tree construction using conserved sites (1203 sites, method= neighbor-joining, model= Jukes-Cantor, bootstrap resampling = 1000). Bootstrap support for each node is indicated as a percentage, calculated from 1,000 randomly re-sampled datasets. Isolates from this study were sequenced with Sanger using 27F/1492R primers, they are shown in red and are labeled with an asterisk (See Ch.2 Methods for Accession Numbers). Other sequences were obtained from NCBI, accession numbers follow double underscore after isolate name.

Appendix III

R Code for Figure 3.3

```
#packages
library(rJava)
library(UpSetR)
library(tidyverse)
library(grid)

rawSets1<- read.csv("~/Strep_isolates_BGCs.csv",
header = TRUE, sep = ",", stringsAsFactors = FALSE)

#Fig. 3.3#

quartz()
upset(rawSets1,
  nsets = 9, point.size = 3.5, line.size = 1.5,
  mainbar.y.label = "Number of BGCs", sets.x.label = "Total BGCs",
  intersections =
list(list("BH106","S.fractus","S.endophyticus","BH034","BH097","BH055","BH104","BH105","S.kunmingen
sis"),
                    list("BH106","S.fractus"),
                    list("BH034","BH097"),
                    list("BH055","BH104","BH105"),
                    list("BH055","BH105"),
                    list("BH104"),
                    list("S.fractus"),
                    list("S.endophyticus"),
                    list("BH034","BH097","BH055","BH104","BH105"),
                    list("BH055")))
#Fig. S1#
quartz()
upset(rawSets1,
  nsets = 9, point.size = 3.5, line.size = 1.5,
  mainbar.y.label = "Number of BGCs", sets.x.label = "Total BGCs")
```

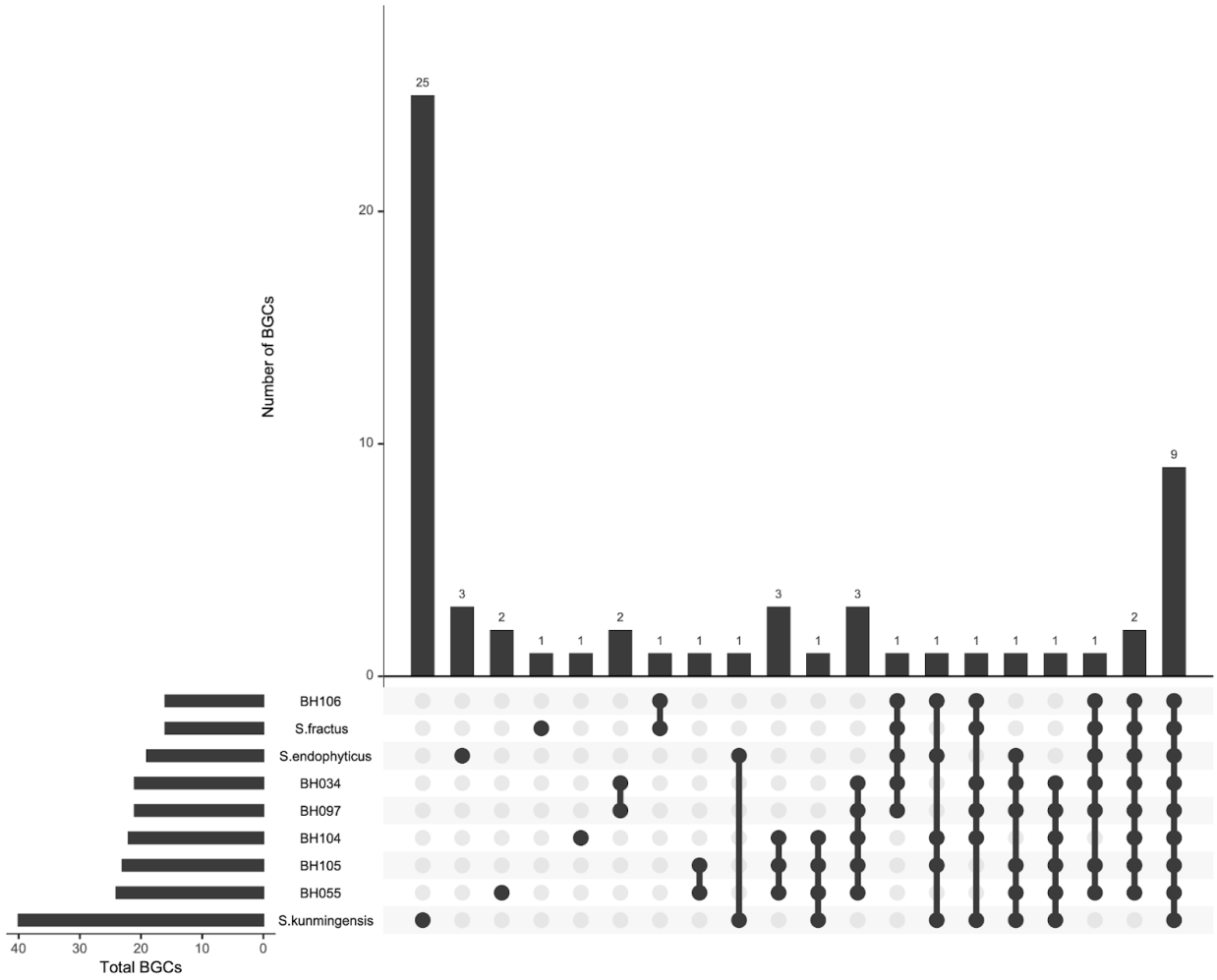

Figure S1- Upset plot showing biosynthetic gene cluster overlap between bee isolates (*S. solapis* sp. nov., two clades, *S. nidicoloris* sp. nov., *S. endophyticus*, and *S. fractus*). Total number of BGCs in each species or group indicated on far left as black horizontal bars. Filled in dots indicate individuals or groups, with the bar directly above the dots indicating the number of unique BGCs in that individual or group. Made with UpsetR package. Related to Figure 3.3.

Query	Subject	d0	C.I.do	Diff. G+C Percent
BH034	BH097	99.8	[99.6 99.9]	0,02
BH034	Streptomyces endophyticus YIM	65.9	[62.1 69.6]	0.24
BH034	Streptomyces kunmingensis DSM	32.5	[29.1 36.1]	0.31
BH034	Streptomyces xanthii CRXT-Y-14	32.6	[29.3 36.2]	1.1
BH055	BH104	86.4	[82.8 89.4]	0.07
BH055	BH097	78.4	[74.4 81.9]	0,08
BH055	BH034	78.8	[74.9 82.3]	0.1
BH055	Streptomyces endophyticus YIM	64	[60.2 67.6]	0.14
BH055	Streptomyces kunmingensis DSM	32.6	[29.3 36.2	0.21
BH055	Streptomyces xanthii CRXT-Y-14	32.2	[28.8 35.8]	1.2
BH097	Streptomyces endophyticus YIM	65.6	[61.8 69.3]	0.22
BH097	Streptomyces kunmingensis DSM	32.4	[29.1 36.0]	0.29
BH097	Streptomyces xanthii CRXT-Y-14	32.5	[29.1 36.1]	1.13
BH104	BH034	69.6	[65.7 73.3]	0.17
BH104	BH097	69.2	[65.3 72.8]	0.15
BH104	Streptomyces endophyticus YIM	58	[54.4 61.5]	0.06
BH104	Streptomyces kunmingensis DSM	31.8	[28.5 35.4	0.14
BH104	Streptomyces xanthii CRXT-Y-14	31.9	[28.5- 35.5]	1.28
BH104	Streptomyces beihajensis GXMU	27.5	[24.1 31.1]	0.54
BH105	BH055	90.9	[87.7 93.3]	0,04
BH105	BH034	73.5	[69.5 77.1]	0.14
BH105	BH097	73.1	[69.1 - 76.7]	0.12
BH105	Streptomyces endophyticus YIM	65.4	[61.6 69.1]	0.1
BH105	Streptomyces kunmingensis DSM	32.5	[29.1 36.1]	0.17
BH105	Streptomyces xanthii CRXT-Y-14	32.1	[28.7 35.7]	1.24
BH105l	BH104	80.3	[76.4 83.7]	0.04
BH106	Streptomyces endophyticus YIM	67.7	[63.9 71.4]	0.04
BH106	BH104	60	[56.3 63.5]	0.11
BH106	BH034l	64.5	[60.7 68.2]	0.28
BH106	BH097	64.2	[60.4 67.8]	0.26
BH106	BH105	64.9	[61.1 68.6]	0.14
BH106	BH055	65.9	[62.1 69.5]	0.18
BH106	Streptomyces kunmingensis DSM	32.9	[29.5 36.5]	0.03
BH106	Streptomyces xanthii CRXT-Y-14	31.9	[28.6 35.5]	1.38
Streptomyces_fractus_ MV32.f	Streptomyces endophyticus YIM	59.2	[55.6 62.8]	0.24
Streptomyces_fractus_ MV32.f	BH106	60.3	[56.6 63.8]	0.2
Streptomyces_fractus_ MV32.f	BH104	49.8	[46.4 53.3]	0.31
Streptomyces_fractus_ MV32.f	BH034	55.9	[52.3 59.4]	0.48
Streptomyces_fractus_ MV32.f	BH097	55.6	[52.1 59.1]	0.46
Streptomyces_fractus_ MV32.f	BH105	55.6	[52.0 59.1]	0.34
Streptomyces_fractus_ MV32.f	Streptomyces kunmingensis DSM	30.9	[27.5 34.5]	0.17
Streptomyces_fractus, MV32.fa	Streptomyces xanthii CRXT-Y-14	30.1	[26.7 33.7]	1.58
Streptomyces_fractus, MV32.fa	BH055	54.8	[51.3 - 58.3]	0.38

Table S1 -dDDH

dDDH table from DSMZ server showing dDDH values between new isolates (in green) and known species (in blue). d0 values formatted to show color ranging from red (low d0, low similarity) to green (high d0, high similarity), followed by the confidence interval and the difference in GC percentage.

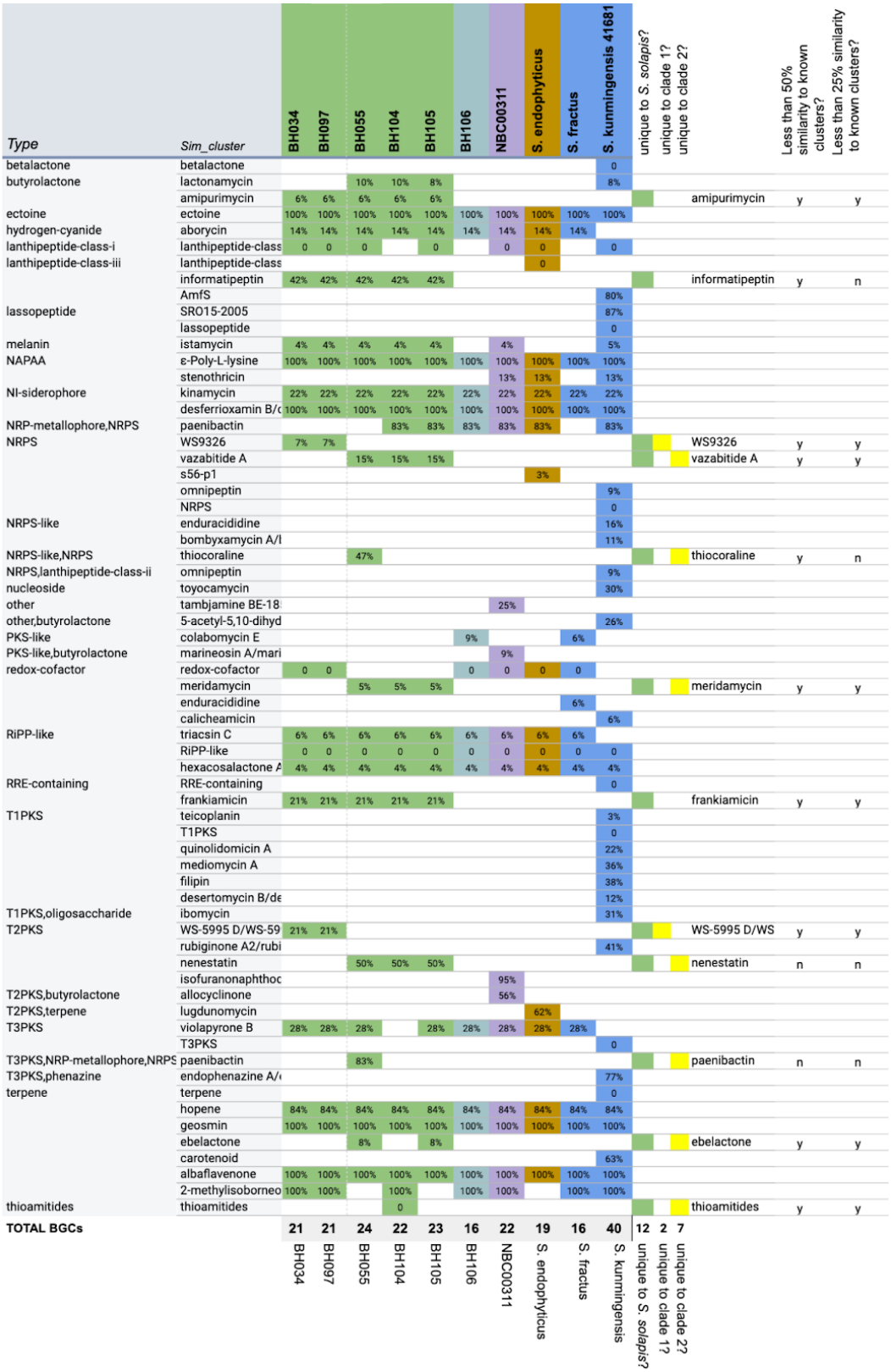

Type	Sim_cluster	BH034	BH097	BH055	BH104	BH105	BH106	NBC00311	S. endophyticus	S. fractus	S. kunmingensis 41681	unique to S. solapis?	unique to clade 1?	unique to clade 2?		Less than 50% similarity to known clusters?	Less than 25% similarity to known clusters?
betalactone	betalactone										0						
butyrolactone	lactonamycin			10%	10%	8%					8%						
	amipurimycin	6%	6%	6%	6%	6%									amipurimycin	y	y
ectoine	ectoine	100%	100%	100%	100%	100%	100%	100%	100%	100%	100%						
hydrogen-cyanide	aborycin	14%	14%	14%	14%	14%	14%	14%	14%	14%							
lanthipeptide-class-i	lanthipeptide-class	0	0	0		0		0	0		0						
lanthipeptide-class-iii	lanthipeptide-class								0								
	informatipeptin	42%	42%	42%	42%	42%									informatipeptin	y	n
	AmfS										80%						
lassopeptide	SRO15-2005										87%						
	lassopeptide										0						
melanin	istamycin	4%	4%	4%	4%	4%		4%			5%						
NAPAA	ε-Poly-L-lysine	100%	100%	100%	100%	100%	100%	100%	100%	100%	100%						
	stenothricin							13%	13%		13%						
NI-siderophore	kinamycin	22%	22%	22%	22%	22%	22%	22%	22%	22%	22%						
	desferrioxamin B/c	100%	100%	100%	100%	100%	100%	100%	100%	100%	100%						
NRP-metallophore,NRPS	paenibactin				83%	83%	83%	83%	83%		83%						
NRPS	WS9326	7%	7%												WS9326	y	y
	vazabitide A			15%	15%	15%									vazabitide A	y	y
	s56-p1								3%								
	omnipeptin										9%						
	NRPS										0						
NRPS-like	enduracididine										16%						
	bombyxamycin A/I										11%						
NRPS-like,NRPS	thiocoraline			47%											thiocoraline	y	n
NRPS,lanthipeptide-class-ii	omnipeptin										9%						
nucleoside	toyocamycin										30%						
other	tambjamine BE-18							25%									
other,butyrolactone	5-acetyl-5,10-dihyd										26%						
PKS-like	colabomycin E						9%			6%							
PKS-like,butyrolactone	marineosin A/mari							9%									
redox-cofactor	redox-cofactor	0	0				0	0	0	0							
	meridamycin			5%	5%	5%									meridamycin	y	y
	enduracididine									6%							
	calicheamicin										6%						
RiPP-like	triacsin C	6%	6%	6%	6%	6%	6%	6%	6%	6%							
	RiPP-like	0	0	0	0	0	0	0	0	0	0						
	hexacosalactone A	4%	4%	4%	4%	4%	4%	4%	4%	4%	4%						
RRE-containing	RRE-containing										0						
	frankiamicin	21%	21%	21%	21%	21%									frankiamicin	y	y
T1PKS	teicoplanin										3%						
	T1PKS										0						
	quinolidomicin A										22%						
	mediomycin A										36%						
	filipin										38%						
	desertomycin B/de										12%						
T1PKS,oligosaccharide	ibomycin										31%						
T2PKS	WS-5995 D/WS-59	21%	21%												WS-5995 D/WS	y	y
	rubiginone A2/rubi										41%						
	nenestatin			50%	50%	50%									nenestatin	n	n
	isofuranonaphthoc							95%									
T2PKS,butyrolactone	allocyclinone							56%									
T2PKS,terpene	lugdunomycin								62%								
T3PKS	violapyrone B	28%	28%	28%		28%	28%	28%	28%	28%							
	T3PKS										0						
T3PKS,NRP-metallophore,NRPS	paenibactin			83%											paenibactin	n	n
T3PKS,phenazine	endophenazine A/										77%						
terpene	terpene										0						
	hopene	84%	84%	84%	84%	84%	84%	84%	84%	84%	84%						
	geosmin	100%	100%	100%	100%	100%	100%	100%	100%	100%	100%						
	ebelactone			8%		8%									ebelactone	y	y
	carotenoid										63%						
	albaflavenone	100%	100%	100%	100%	100%	100%	100%	100%	100%	100%						
	2-methylisoborneo	100%	100%		100%		100%	100%		100%	100%						
thioamitides	thioamitides				0										thioamitides	y	y
TOTAL BGCs		**21**	**21**	**24**	**22**	**23**	**16**	**22**	**19**	**16**	**40**	**12**	**2**	**7**			

BH034 BH097 BH055 BH104 BH105 BH106 NBC00311 S. endophyticus S. fractus S. kunmingensis unique to S. solapis? unique to clade 1? unique to clade 2?

Table S2- Biosynthetic gene clusters

All biosynthetic gene clusters in the analyzed genomes listed down left side, showing antiSMASH assigned Type and most similar BGC cluster ('sim_cluster'). The following columns represent each genome (bold), with colored/filled areas indicating that the BCG in that row is present in that genome, the percentage is the assigned similarity to the closest known cluster. After the genome columns, the next three columns (13-15) indicate whether a BGC (row) is unique to *S. solapis*, and then to which clade (if it is unique to only one of the clades). These unique BCGs (their closest known cluster) is shown again in the last column.

Table S3: Media recipes:

TSA:

1000 mL DI H2O
15 g tryptone
15 g agar
5 g soytone
5 g NaCl
50g fructose
1mL cycloheximide (@ 100 mg/mL in methanol, after autoclaving)

MYM:

1000 mL DI H2O
4 g Maltose
4 g Yeast Extract Oxoid
10 g Malt Extract
15 g agar

OA:

1000 mL DI H2O
40 g pulverized oatmeal
15 g agar

YM:

1000 mL DI H20
3 g malt extract
5 g Bacto Peptone
10 g glucose
10 g agar
3 g yeast extract
500 µL chloramphenicol (@ 100 mg/mL in methanol, after autoclaving)